Stony Brook University

Cancer Invasion and Metastasis: Unraveling the Mechanism and Developing Novel Therapeutic Agents

A Dissertation Presented

By

Ashleigh Pulkoski-Gross

to

The Graduate School

in Partial Fulfillment of the

requirements

for the Degree of

Doctor of Philosophy

in

Molecular and Cellular Pharmacology

Stony Brook University

May 2015

Stony Brook University

The Graduate School

Ashleigh Pulkoski-Gross

We, the dissertation committee for the above candidate for the
Doctor of Philosophy degree, hereby recommend
acceptance of this dissertation.

Jian Cao, M.D. – Dissertation Advisor
Professor, Department of Medicine

Nicole Sampson, Ph.D. - Chairperson of Defense
Professor, Department of Chemistry

Styliani-Anna Tsirka, Ph.D. – Committee Member
Professor, Department of Molecular and Cellular Pharmacology

Stanley Zucker, M.D. – Outside Committee Member
Professor, Department of Maedicine

This dissertation is accepted by the Graduate School

_____
Charles Taber
Dean of the Graduate School

Abstract of the Dissertation
Cancer Invasion and Metastasis: Unraveling the Mechanism and Developing Novel Therapeutic Agents
By
Ashleigh Pulkoski-Gross
Doctor of Philosophy
in
Molecular and Cellular Pharmacology
Stony Brook University
2015

Cancer mortality rates remain high and the reason for this lack of progress in improving survival rates is the lack of drugs specifically targeting metastasis, which is the cause of death for 90% of cancer patients. In order to address this important aspect of cancer biology, we used a three-dimensional, high-throughput phenotypic screening approach and a target-based design to identify compounds that interfere with an early, critical stage of the metastatic process, namely cancer cell invasion. By using our phenotypic screening, we identified trifluoperazine (TFP), an FDA approved anti-psychotic, as an anti-invasive agent that interferes with migratory function with minimal cytotoxicity. TFP functions to decrease active, phosphorylated AKT (Thr^{308} and Ser^{473}) and β-cateninSer^{552}. There is a resultant decrease in β-catenin nuclear translocation and transcription of target genes, based on antibody array data. The activity of TFP on highly invasive fibrosarcoma cells results in decreased angiogenesis and invasion through the basement membrane in a chorioallantoic membrane assay. Overall, we have demonstrated that TFP is responsible for the reduced invasive behavior of these cancer cells by antagonism of a network that includes dopamine receptor D_2, AKT, and β-catenin leading to reduced cancer cell motility.

Another approach to drug discovery is a target-based approach. Considering the expression of MMP-14 contributes significantly to cancer cell invasion and is correlated with disease progression, MMP-14 is a crucial molecule to target. There are no current inhibitors for this protease and we determined the minimal region of another cell surface molecule, CD44, which is required to interact with MMP-14 for cell migration. We identified an eight amino acid region of CD44 that is crucial for MMP-14 interaction based on mutational analyses. Expression of CD44 with the minimal mutation results in decreased interaction with wild-type MMP-14 based on co-immunoprecipitation assays. Furthermore, MMP-14 mediated cell migration is reduced when co-expressed with the mutant as opposed to wild-type CD44. Furthermore, design of peptides mimicking the minimal region of CD44 reduces interaction of wild-type CD44 and MMP-14 based on a reduction in MMP-14 pulldown by CD44 and reduced MMP-14 mediated migration in the presence of the peptide. Overall, we have identified novel peptides and potential strategies for reduction of metastasis by targeting of cancer cell invasion and migration via target- and phenotype-based screening methods.

Dedication Page

This dissertation is first and foremost dedicated to my family. My extended family has been extremely supportive and encouraging of me in my pursuit of not only my Ph.D., but throughout my life. My parents and brother are deserving of special recognition for their love and encouragement of me. My father, Michael, has continuously supported me throughout my life and I cannot explain how grateful I am for that. In the big ways and the small ways, he is there for me and I am so indebted to him. My brother, Michael, has also supported and encouraged me along the way. I am so proud of him for the man and scientist he has become and there is no way to succinctly put into words the many ways in which he has helped me through my graduate studies; I can't thank him enough. Last, but not least, I am dedicating this dissertation to the memory of my mother, Debra. Although she is not here in person to witness the conclusion of my work here, I carry her with me and think of her often during my studies. She was my biggest cheerleader and encouraged me to do the best I could in everything I did. I am truly thankful for my family and I would not be who I am or have come as far as I have without them.

I would also like to dedicate this work to Tom. Over the last few years, I have been lucky enough to have him in my life as another source of love and encouragement. He has been tremendously patient with me while I work and I am so grateful.

Table of Contents

List of Figures

List of Tables

List of Abbreviations

EMT – epithelial-mesenchymal transition
MMPs – matrix metalloproteases
MT-MMPs – membrane-type MMPs
ECM – extracellular matrix
GPI-anchor – glycophosphatidylinositol anchor
Ca^{2+} - calcium ion
Zn^{2+} - zinc ion
TIMP – tissue inhibitor of MMP
PEX – hemopexin-like domain
TGF-β – transforming growth factor beta
HYA – hyaluronic acid
HA – hemagglutinin
ERM – ezrin-radixin-moesin proteins
GFP – green fluorescent protein
FITC – fluorescein isothiocyanate
CoIP – co-immunoprecipitation
EGFR – epidermal growth factor receptor
PDI – protein disulfide isomerase
TFP – trifluoperazine
VEGF – vascular endothelial growth factor
H&E – hematoxylin and eosin
CAM – chorioallantoic membrane
DRD2 – dopamine receptor D2
Erk1 + Erk2 - extracellular regulated protein-serine kinase 1 + extracellular regulated protein-serine kinase 2
NFκB p65 - NF-κ-B p65 nuclear transcription factor
Trail - tumor necrosis factor-related apoptosis-inducing ligand
PKCγ - protein-serine kinase C gamma
eIF4E - eukaryotic translation initiation factor 4 (mRNA cap binding protein)
STAT2 - signal transducer and activator of transcription 2
Smad2 - mothers against decapentaplegic homolog 2
Src - Src proto-oncogene-encoded protein-tyrosine kinase
PKCλ/ι - protein-serine kinase C lambda/iota
Jun - Jun proto-oncogene-encoded AP1 transcription factor
SOCS2 - suppressor of cytokine signaling 2
S6kb1 - ribosomal protein-serine S6 kinase beta 1
LAR - LCA antigen-related receptor tyrosine phosphatase
STAT3 - signal transducer and activator of transcription 3 (acute phase response factor)
Hsp27 - heat shock 27 kDa protein beta 1 (HspB1)
RSK1/2 - ribosomal S6 protein-serine kinase 1/2
NBS1 - Nijmegen breakage syndrome protein 1
MEK1/2 - MAPK/ERK protein-serine kinase 1/2 (MKK1/2)
CDK1 - cyclin-dependent protein-serine kinase 1
ACK1 - activated p21cdc42Hs protein-serine kinase
c-IAP1 - cellular inhibitor of apoptosis protein 1

JAK2 - Janus protein-tyrosine kinase 2
IkBb - inhibitor of NF-κ-B β (thyroid receptor interacting protein 9)
IRS1 - insulin receptor substrate 1
Cdc25C - cell division cycle 25C phosphatase
AIF - apoptosis inducing factor (programmed cell death protein 8 (PDCD8))
CDK2 - cyclin-dependent protein-serine kinase 2
CDK6 - cyclin-dependent protein-serine kinase 6
CDK1 - cyclin-dependent protein-serine kinase 1
MEK2 - MAPK/ERK protein-serine kinase 2 (MKK2)
PTEN - phosphatidylinositol-3,4,5-trisphosphate 3-phosphatase and protein phosphatase and tensin homolog deleted on chromosome 10
DDIT3 (CHOP) - DNA damage-inducible transcript 3 protein
Dab1 - disabled homolog 1
PTP1D - protein-tyrosine phosphatase 1D

Acknowledgements

I would like to thank first and foremost my mentor, Dr. Jian Cao, for being a supportive and patient mentor. I have learned not only technical skills from him, but also how to be creative and persistent in my studies. I truly appreciate all of the opportunities he has afforded me and I would be remiss if I did not acknowledge them. I am fortunate to have a mentor like Jian, as he leads us by example on how to be a productive member of the scientific community and keeps our best career interests in mind.

I would also like to thank past and present laboratory members. Kayvan Zarrabi, Dr. Antoine Dufour, Dr. Cem Kuscu, Dr. Jian Li, Dr. Hoang-Lan Nguyen, Carolina Zheng, and Deborah Kim were all supportive and helpful to me in one way or another during my time in the Cao Lab. I would especially like to thank Dr. Nikki Evensen for her advice and contributions during my graduate work. Current laboratory members, including Jillian Cathcart, Yiyi Li, Anna Banach, Vincent Alford, and Qian Zhang have also offered their help and suggestions along the way.

Thanks also to the Pharmacology department, particularly the administrative staff and my classmates. They have made my time here at Stony Brook University exponentially better.
Finally, thanks to my committee members, Dr. Nicole Sampson, Dr. Stella Tsirka, and Dr. Stanley Zucker for their insights into my project and feedback on my professional development and manuscripts.

Prologue: Introduction

Overall cancer death rates have been decreasing slowly in the United States since the early 1990s [1]. These decreases have been associated with a combination of early detection and treatment, along with education about and reduction of certain risk factors [1]. Despite these improvements, patients diagnosed with distant metastases are more likely to die of their disease as opposed to any other co-morbidity [1]. Even patients that do not exhibit gross metastasis at the time of initial diagnosis may develop distant metastasis and their death is more often than not associated with cancer dissemination and not the primary tumor [2]. Based on estimates of cancer cell doubling time and tumor formation, it is likely that most patients at the time of diagnosis carry micrometastases, which are not yet making a clinical impact on the patient [3]. Because most patients harbor micro- or macro- metastases, it is crucial to develop novel cancer treatments that target this process in order to improve treatment outcome by reducing cancer spread.

The term metastasis was coined by Joseph Claude Anthelme Recamier and in the late 1800s, Stephen Paget proposed the "seed and soil" theory, suggesting that cells of a primary tumor may only colonize hospitable organs [4]. This theory has been built upon since and our current understanding of metastasis has come to include the notion that circulatory patterns contribute to metastasis patterns and there are a subset of cells within a tumor particularly suited to the process of metastasis [4]. Metastasis is a complex, multi-step process. As neoplastic cells grow and form a larger tumor, vascularization of the tumor must occur in order for it to grow larger than 2 mm [3]. Angiogenic factors derived from both the tumor cells themselves and the stroma encourage vascular growth. In the early stages of dissemination, cells of a primary tumor that have undergone the transition from a stationary, epithelial phenotype to a motile, mesenchymal phenotype [epithelial-mesenchymal transition (EMT)] are able to breakdown the extracellular matrix (ECM) and basement membrane. These cells cleave ECM components and travel through cleared areas in order to extravasate and enter the blood stream. Those cells that are able to survive in circulation have the opportunity to intravasate from the blood stream to a secondary site. The second phase (adaptation), consists of growth of the cells at the colonization site, which constitutes development of metastasis [5]. At the secondary site, these processes can occur over again, which results in further establishment of metastatic lesions.

Although the process of metastasis is a relatively inefficient occurrence [it is likely less than 0.02% of cells in circulation will be able to form metastases [6]], it is the deadliest aspect of the disease and much remains to be determined about targeting the key players [3, 7]. Because of this, there are very limited treatment options for this cancer stage. Most currently available therapies are effective against primary tumor growth, but do little to combat cell movement, and ultimately metastasis. In addition to the complexity of the biology of metastases, there are other practical reason for a lack of anti-metastatic drugs which includes the cost of long-term clinical trials monitoring metastasis as an endpoint in early stage cancer patients and the endpoint for most current clinical trials is primarily concerned with diminution of tumor burden in a patient, which may not be relevant to anti-metastatic agents [6]. On a more fundamental level, anti-metastatic agents are currently lacking because heretofore there has not been a proper method by which to easily screen novel compounds for anti-invasive effects in a 3-dimensional milieu and there is still much work to be done in identifying unique biomarkers that can serve as prognostic factors in patients with metastases [6, 8].

Despite the National Cancer Act enactment in the 1970s, little change has been made in improving the mortality rate due to lack of metastatic control. There is an enormous gap in both understanding of the precise molecular mechanisms that influence metastasis and the lack of proper anti-metastasis therapies which are collectively detrimental to patient survival. Therefore, the overarching goals of this thesis work are two-fold: to identify and develop potential anti-metastasis agents in order to improve cancer treatment outcome and to define molecular relationships between key players in metastasis. One such group of major players in the metastatic process is the zinc-dependent endopeptidases, matrix metalloproteinases (MMPs). Matrix metalloproteinase-14 (MMP-14, MT1-MMP) is a transmembrane protease whose expression is found at high levels in cancer cells and correlates with cell migration and metastasis [EMT], and therefore reduced patient survival [9]. Thus, I endeavored to define a novel MMP-14 inhibitor in order to prevent MMP-14 mediated cell invasion and migration. Additionally, MMP-9 is a soluble MMP that also correlates with risk of cancer relapse and poor patient survival [10]. MMP-9 has been documented to dimerize and mediate cell migration [11]. In an effort to clarify MMP-9 dimerization dynamics, I analyzed the biochemical nature of MMP-9 dimerization and its effects on cancer cell migration under hypoxic conditions, as hypoxia at the site of a tumor is very common and can cause significant changes in cancer cell behavior, specifically inducing migration and invasion. Lastly, using small molecule hits from a compound library screen I have identified a novel mechanism of action of an FDA-approved antipsychotic, trifluoperazine (TFP). TFP appears to reduce β-catenin activity and ultimately results in a decrease in cancer cell invasion and migration, potentially through a network of dopamine receptor D2, AKT, and β-catenin. Collectively, this work attempts to identify strategies which might convert cancer from a fatal disease to a chronic, manageable one.

Chapter 1: Matrix Metalloproteinases

1.1 BACKGROUND

(The bulk of this background section will appear in the Frontiers in Bioscience Special Issue: Matrix Metalloproteinases and Disease)

As early as 1949, comparison of the architecture of rapidly progressing tumors and slow-growing tumors revealed stark differences [12]. These differences were postulated to be related to depolymerization of the basement membrane by soluble factors, potentially derived from stromal cells [12]. Collagen degradation in mammalian tissue was initially described by Woessner in 1962, but the field of study of extracellular matrix (ECM) remodeling proteins was pioneered by the study conducted by Gross and Lapiere, also published in 1962 [13]. The work appeared in the *Proceedings of the National Academy of Sciences* and described the ability of a single, soluble factor derived from certain tadpole tissue explants to lyse purified collagen *ex vivo* [13]. Prior to the 1962 study by Gross and Lapiere, ECM remodeling in the mammalian context was a poorly understood phenomenon and had been hypothesized to be related to lysosomal protease activity [14, 15]. The landmark discovery of a soluble collagenase led to a shift in ideology about ECM degradation and tissue remodeling. The study of these isolated proteolytic enzymes over the following decades uncovered vast amounts of information on how proteins of the extracellular space are degraded and maintained.

In the years following the publication of the work of Gross and colleagues, various collagenases and procollagenases were isolated from a variety of animal tissues [16-21]. Not only were proteases isolated from a number of tissues and cell cultures, but they were also increasingly associated with certain pathologies. Some of the earliest diseases to be associated with ECM remodeling include periodontal disease (gum resorption) and cholesteatoma [18]. Eventually, it was also found that collagenases could be derived from rheumatoid synovium and metastatic tumor explants [22-25]. As it became increasingly apparent that these isolated proteases were critical to degrading ECM and participated in both physiological and pathophysiological processes, studies to purify, characterize, and define the mode of action of these proteases were undertaken. In this section, I provide an overview of basic structure and functions of ECM remodeling proteases, specifically the matrixins, or matrix metalloproteinases (MMPs).

1.1A CLASSIFICATION OF MATRIX METALLOPROTEINASES

The MEROPS database is a large repository of information regarding families of proteases [26, 27]. MMPs are classified in the clan MA and fall into the M10 family, which is the metalloendopeptidase family. The classification of metalloendopeptidases into a group called the 'metzincins' within the endopeptidase superfamily was initially proposed in 1993 [28, 29]. The metzincin family is characterized by two major features, the requirement of a coordinated Zn^{2+} in the catalytic active site and the methionine turn (Met-turn) [28]. The sub-families that comprised the metzincin family at that time included the astacins, adamalysins, serralysins, and matrixins [28]. Each of these families could be distinguished from one another based on the residue (Z) that is found at the end of the conserved zinc-binding sequence (HEXXHXXGXXHZ) [*i.e.:* Glu (astacins), Asp (adamalysins), Ser in (matrixins), and Pro in (serralysins)]. Recently, another mechanism by which to classify metallopeptidases has been proposed [30]. Cerdá-Costa *et al.* suggest that metalloproteinases should first be divided by whether they are dimetalate (containing two catalytic metals) or mononuclear metallopeptidases.

By this system, MMPs fall into the subclass mononuclear metallopeptidases, the tribe zincins, the clan metzincins, and the family of matrixins [30]. The tribe zincins includes any peptidase that contains the motif HEXXH, with the clan metzincins including the conserved zinc binding site HEXXHXXGXXHZ and the Met-turn [30].

1.1B MATRIX METALLOPROTEINASE PROTEIN STRUCTURE

MMPs are calcium-dependent, Zn^{2+} containing endopeptidases. They can either be soluble or membrane-bound and are found in most kingdoms of life. Humans have 23 paralogs and they can be divided into groups: true collagenases, gelatinases, stromelysins, elastases, and membrane-type MMPs [31, 32]. MMPs from vertebrates are modular, containing particular elements that are similar amongst all of the family members (Figure 1). A small signaling peptide (~20 amino acids), a propeptide region (~80 amino acids), a calcium and zinc dependent catalytic domain (~165 amino acids), a linker region of varying residue length (may determine what substrates the MMP can accommodate), and a hemopexin-like domain (PEX) (~200 amino acids) [33]. Certain MMPs also contain additional domains, including fibronectin-like repeats (MMP-2, -9), immunoglobulin-like domains, and vitronectin-like repeats. Further, members of the family that are membrane bound may contain either a glycophosphatidylinositol linkage signal or transmembrane and cytoplasmic tail domains (MMP-14, MMP-17, MMP-24, and MMP-25) (Figure 1).

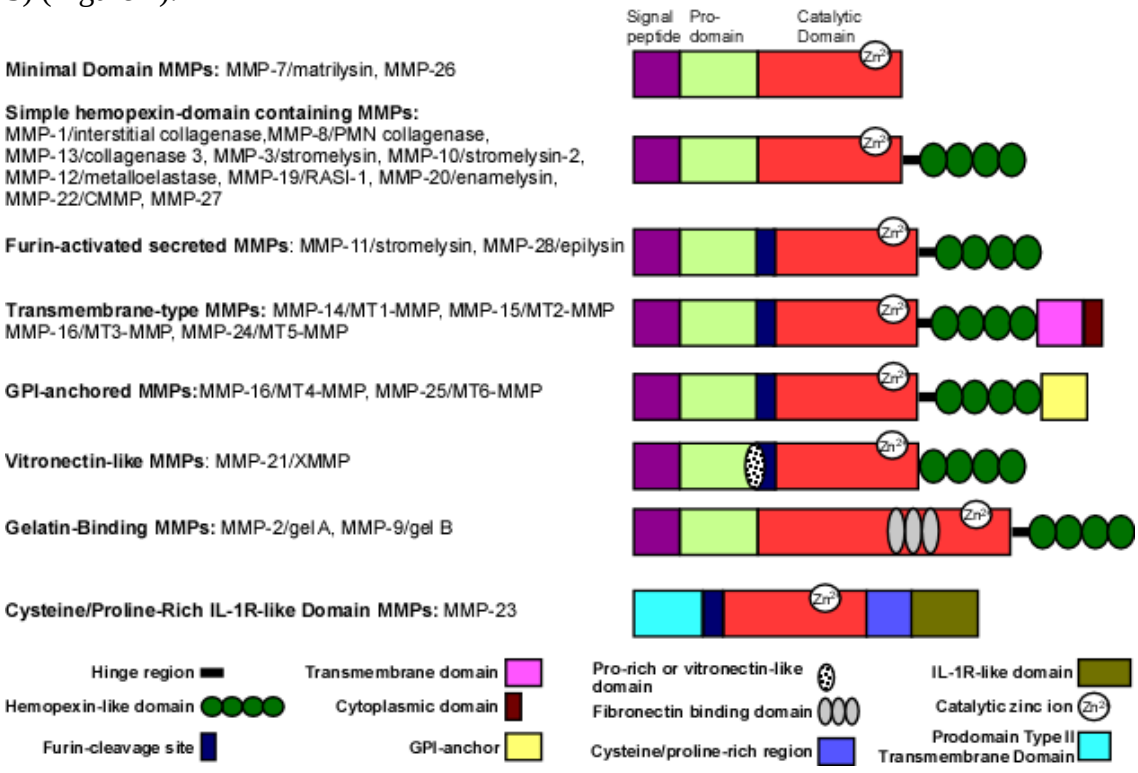

Figure 1: The MMP family. The MMP family share certain conserved domains, particularly the catalytic domain. Figure 1 demonstrates the MMPs based on structural features of the protein, which most share the hemopexin-like domain and the catalytic domain, in addition to the signal peptide and propeptide domain.

The signaling peptide region is variable amongst proteins but commonly consists of a positively charged N-terminal segment, followed by a hydrophobic section, and finally a polar C-terminal segment [34]. This peptide interacts with the signal recognition particle (SRP) and eventually the signal recognition peptide receptor at the target, *i.e.:* endoplasmic reticulum [35, 36]. This is a general phenomenon for secretory proteins and MMPs are no exception.

The propeptide domain (prodomain) is crucial to regulation of MMP activity, as it serves to block access to the catalytic domain; matrixins are usually secreted in zymogen form and require activation. The prodomain is included in even the most structurally simple of MMPs (MMP-7) and is composed of three alpha chains with flexible connecting loops [31]. It includes a highly conserved amino acid sequence that is contained within the prodomain, PRCGXPD [37, 38]. Early evidence presented by Sanchez-Lopez, *et al.*¸ indicated that mutation of the region around the autocatalytic site in rat transin increased the activation of the zymogen [39]. Later, it was determined that mutation of the cysteine residue results in a zymogen with a higher proclivity for activation [40]; modification of the sulfhydryl group also releases the cysteine switch [41]. The sulfhydryl group of the cysteine located in the highly conserved amino acid sequence of the prodomain region functions to occupy the catalytic Zn^{2+} ion and prevent the necessary water molecule from interacting with the ion, which is the so-called "cysteine-switch" [42]. Ion chelating agents such as EDTA can activate MMPs because of the removal of Zn^{2+} from the cysteine [43]; use of organomercurial agents and detergents such as sodium dodecyl sulfate results in a change in protein conformation that allows for release of the cysteine switch [43, 44].

The catalytic domain is highly conserved amongst the MMPs, nearly matching in their 3-dimensional structure [31, 33]. The spherical catalytic domain extends over a 40 angstrom diameter and the shallow active site is situated at the front surface [33]. The substrate binding groove contains a flat, unprimed side and a narrow primed side which contains the specificity pocket [45]. The catalytic domain is composed of three α-helices and a five-stranded twisted β-sheet (βI-βV) [33, 46]. The strands in the β-sheet are parallel in orientation to one another, with the exception of the βIV. The αA backing helix and the αB active site helix are in close proximity to the β-sheet; the contacts between the helices and sheets are hydrophobic and therefore form a hydrophobic core. Several of the loops connecting each β-strand extend away from the surface of the sheet and these are unique to MMPs as compared to other members of the metzincins [33]. The loops participate in coordinating the non-catalytic ions, specifically the second Zn^{2+} ion and up to three Ca^{2+} ions, which serve to provide structure to the loops [33, 46, 47]. This domain is split by the active site asymmetrically, resulting in a larger N-terminal region (average 127 residues, often termed "upper") and a smaller C-terminal region (average 37 residues, often termed "lower") [33].

The large LβVαB loop leads from strand βV to the active helix, αB. The αB helix contains the first half of the conserved zinc-binding sequence HEXXHXXGXXH, meaning it has the first two histidines required for coordinating the catalytic Zn^{2+} in addition to the glutamate that participates in catalysis and ends with a turn allowed by the glycine residue [33]. The turn is crucial for the third histidine to make contact with the zinc ion. Following the conserved Zn^{2+} binding sequence is a loop that leads to methionine, which is termed the "Met-turn" [28]. This is a highly conserved 1, 4-β-turn within the metzincins, however it has been shown not to be

necessary for proper folding and function of the enzyme [46, 48]. The loop following the Met-turn is the "specificity loop" that leads to the final helix of the catalytic domain (αC) [33, 46]. This loop is required for distinguishing substrates and imparts a level of specificity to each MMP.

The hinge (or linker) region is a stretch of amino acids that follow the catalytic domain and leads to the hemopexin domain. This region may vary from 15 to 65 residues, depending on which MMP is in question [47]. The structure of the linker plays a role in the ability of MMPs to proteolyze their substrates, as mutation of the proline rich region has been documented to reduce the ability of MMP-8 to degrade collagen [49]. The linker has been purported to make contacts with both the catalytic domain and the hemopexin-like domain and serves to stabilize their arrangement and contribute to proper enzyme function [47]. Recent evidence indicates that the linker region's flexibility is crucial to mediating the conformational change required for interaction between the catalytic and hemopexin–like domain and therefore, proper catalysis and specificity [50, 51].

The hemopexin-like (PEX) domain is a four-bladed β-propeller structure that begins with a cysteine residue and ends with another; the two cysteines form a disulfide bond to establish the propeller-like structure [47]. Mutation of these cysteines results in loss of the proper structure, and therefore function [52]. Centrally located within this region are three water molecules and three ions, including Ca^{2+}, Na^{+}, and Cl^{-} , which may be crucial to structure stabilization [47, 53, 54]. For example, use of chelating agents against the PEX domain of MMP-2 results in the loss of binding to fibronectin and heparin [52, 55]. The PEX domain has been shown to be crucial to substrate recognition and specificity (collagenases), while in other cases loss of or lack of the PEX domain does not substantially inhibit the enzymes (MMP-7, -12, and -26) [46, 52, 56]. In the case of MMP-2, deletion of the PEX domain leads to lack of collagenolytic activity but retains catalytic activity against substrates such as casein or small synthetic peptides [52]. Recently, the PEX domain has been implicated in the ability of MMPs to orient collagen for catalysis by binding two of the three strands of collagen, mediated by particular residues, allowing the third strand to be oriented into the active site [57]. Because the PEX domain of MMPs can mediate interaction with substrate, it has become a target for inhibition in recent years [58-61].

MT-MMPs are primarily responsible for pericellular degradation of ECM components and activation of soluble MMPs. They are also in a prime position to cleave other cell surface proteins. All membrane-type MMPs include an RXR/KR motif at the C-terminus of the pro-domain that serves as a proprotein convertase site and allows for cleavage of the zymogen to the active state. MT1-MMP, MT2-MMP, MT3-MMP, and MT5-MMP have all been documented to have single-pass transmembrane domains that span approximately 20 amino acids [62-67]. The transmembrane domain is followed by a small intracellular cytoplasmic tail. MT4-MMP and MT6-MMP are membrane-type MMPs that share most of the same domains as other MT-MMPs, but are membrane bound via a glycophosphatidylinositol anchor (GPI-anchor) at the C-terminus of the hydrophilic stalk region of the these proteases [65, 67-70]. The GPI-anchor allows for these proteases to be localized to lipid rafts and potentially participate in signal transduction by directly modifying components of the lipid raft [67].

The furin recognition domain is a sequence of amino acids that allows for intracellular cleavage of certain MMPs, which may result in secretion or delivery to the cell surface of active enzyme, as proprotein convertase activity can releases the pro-domain [71]. MT-MMPs, including MT1-MMP (MMP-14), MT2-MMP, MT3-MMP, and MT5-MMP contain furin recognition domains [72-74]. Interestingly, it has been suggested that cleavage of MMP-14 by a convertase is not required for its MMP-2 activating activity [72]. MT4-MMP and MT6-MMP, the GPI-anchored membrane proteases, also contain a furin recognition site and can be activated by the proprotein convertase [65, 75]. MMP-23 is also integrated into the plasma membrane (type II transmembrane protein) and includes a furin-recognition site which is sensitive to proprotein convertases [35]. MMP-11 and MMP-28 also harbor the furin-recognition site and can be proteolytically processed and activated by cleavage [71, 76]. Not only can furin act as an activator for MMP-28, but also as a chaperone for secretion, assigning a non-proteolytic role to furin for MMP modulation [77].

1.1C THE MECHANISM OF ACTION OF MATRIX METALLOPROTEINASES

As outlined by Overall, catalysis by MMPs require binding of the substrate to the active site, a compatible specificity pocket (S1') that defines the active site, the catalytic Zn^{2+} properly coordinated with the presence of the catalytic glutamate, and binding of substrates to sites outside the catalytic site (exosites) [52]. The target peptide binds to the active site by forming hydrogen bonds between the substrate and active site in an anti-parallel fashion [52]. Once properly oriented, the substrate can be hydrolyzed.

The reaction carried out by matrixins is considered an ordered, single-displacement reaction that follows Michaelis-Menten kinetics and is optimal at a neutral pH. The mechanism by which MMPs can cleave their substrates has been established based on structures gathered through the years characterizing thermolysin from *Bacillus thermoproteolyticus* and bovine carboxypeptidase A and later structures of MMPs in complex with substrates and inhibitors [30]. From available structures in 1988, Matthews stated the thermolysin active site contained a zinc ion coordinated by three amino acid residues and a solvent molecule [78]. The solvent molecule is bound by the Zn^{2+} ion and increases the nucleophilicity of the solvent. The carbonyl oxygen is polarized by the catalytic metal. Once this occurs, the scissile carbonyl carbon is available for attack by the solvent. The solvent proton then transfers to the general base, glutamate. This gem-diolate intermediate is a tetrahedral intermediate that is stabilized by surrounding amino acids. The final products are formed by bond cleavage and transfer of protons to the new amino terminus created by the enzyme's cleavage activity (Figure 2).

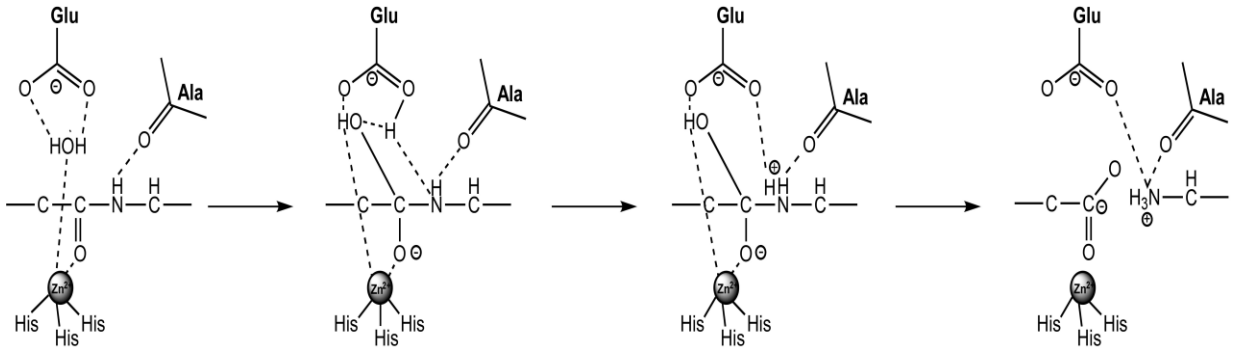

Figure 2: General catalytic mechanism of MMPs. Based on structural data, a general mechanism of action has been delineated for MMP catalytic activity.

1.1D CONTROL OF MATRIX METALLOPROTEINASES

Matrixins are classically associated with matrix degradation, but the repertoire of these proteases has expanded to include other protein substrates such as pro-proteases, clotting factors, adhesion molecules, cryptic growth factors, and cytokines, amongst others, implying that MMP activity can have a huge impact on a wide-range of processes [33]. Therefore, the function of MMPs are tightly regulated at the level of transcription, post-transcriptional modification, post-translational modification, production in the zymogen form (requiring activation), non-specific inhibition by α_2-macroglobulin, and co-expression of tissue inhibitors of metalloproteinases (TIMPs); these mechanisms collectively serve to limit the activity of the proteases [30, 33]. Frequently, these mechanisms of inhibition are dysregulated under pathological conditions, which contributes to worsening of disease [33].

Under normal conditions, most MMPs are expressed at low levels, with transcription being highly regulated. One major mechanism of control is the tissue-type restriction of MMP expression. Only certain types of MMPs are expressed in particular tissues, implying that contextual cues dictate which MMP will be expressed [79-81]. Overall, there are several transcription factors that can promote transcription of MMPs derived from a variety of signaling pathways, with each MMP having a particular combination of sites in their promoters [82].

Post-translational modification is required for MMPs in that they must release their pro-domain in order to be fully active. This often requires the action of other proteases in the extracellular space, such as fellow MMPs or serine proteases. In the case of MMP-2, MMP-14/TIMP-2 complexing is required to activate soluble MMP-2 [83, 84]. In the case of MMPs that contain furin-like recognition domains (RXK/RR), intracellular proprotein convertases activate the proteins in the Golgi as they are transported in order to get to their final destination [71].

Initially identified in human skin fibroblasts as an inhibitor of collagenase, TIMPs are naturally occurring inhibitors of MMPs that may have co-evolved with the development of connective tissue [85, 86]. Four TIMPs have been identified in humans (1-4) and are small glycoproteins that consist of two domains [87]. They include an inhibitory N-terminal domain and a C-terminal domain that are each structurally stabilized by three disulfide-bound loops [88]. TIMPs bind to MMPs in a 1:1 ratio and each have a certain specificity for each MMP and a particular expression pattern [87]. These endogenous inhibitors tend to operate by binding the PEX domain and can also bind the zymogen form of MMPs [87]. The differences in amino acid residues that exist in the PEX domain and TIMPs likely cause the differential affinities observed for the MMPs amongst the TIMPs [87].

α-2 macroglobulin also acts as an inhibitor of MMPs [89]. It is a relatively abundant serum plasma protein and is the major MMP inhibitor in circulation [80]. α-2 macroglobulin complexing with MMPs results in receptor-mediated endocytosis, indicating that α-2 macroglobulin inhibition may result in an irreversible inhibition (due to clearance) as opposed to the reversible interactions between TIMPs and MMPs [80]. Another endogenous inhibitor of the MMPs includes the C-terminal fragment of procollagen C-terminal proteinase enhancer (PCPE),

which is a protein that was originally documented to enhance the function of the procollagen C-terminal proteinase/bone morphogenic protein-1 (PCP/BMP-1) [90, 91]. Other mechanisms of control also exist for MMPs, which include pericellular segregation of the MMPs and the dependence upon substrate presence. This spatial and temporal control of MMPs limits their activity within their particular milieu [80].

1.1E MMPs UNLEASHED: MATRIX METALLOPROTEINASE'S ROLES IN DISEASE

Collectively, the family of MMPs is capable of remodeling the ECM by cleaving components such as various collagens, laminins, and fibronectin, amongst others. Additionally, MMPs have been shown to activate cryptic growth factors embedded in the ECM, for example, TGF-β. These proteases have a broad spectrum of substrates and therefore play a crucial role in development, signaling, and apoptosis [33]. Work from Woessner in 1976 and Jeffreys in 1983 demonstrated that procollagenases can be recovered from normal, postpartum uterine tissue and primary cultures of the uterine tissue [92, 93]. Shipley, *et al*., demonstrated that mice lacking macrophage metalloelastase have diminished ability to degrade ECM and have abrogated ability to invade tissues, as they normally would during wound repair [94]. In an attempt to identify the role of MMP-2 in the processing of the β-amyloid precursor protein, it was demonstrated that MMP-2 knockout mice were viable, but lagged in growth compared to wild-type from postnatal day 3 to adulthood [95]. This implicated a role for MMPs in growth. Relatedly, MMP-9-null animals survive through the embryonic stage and develop into fertile adults, but were found to have a delay in bone ossification due to a lack of proper vascularization of bone growth plates, providing more evidence that MMPs play an important role in development [96]. Even more striking is that the loss of MMP-14 expression results in viable animals with severe developmental defects, including osteopenia, arthritis, and skeletal dysplasia [97]. Not only were these animals severely deformed, they also displayed a significantly shortened lifespan [97]. Each of these pieces of evidence suggests that MMPs play important roles in a variety of non-pathogenic, physiological conditions.

Unfortunately, because of their ability to affect several crucial processes, these proteins have been associated with various pathologies such as arthritis, cancer and metastasis, and cardiovascular disease, just to name a few. Expression of MMPs has been correlated with cancer progression, relapse, and survival in multiple types of cancer, including lung carcinoma, colorectal cancer, and breast cancer [60, 98-102]. In support of the notion that MMPs contribute to tumor formation and progression, mice lacking MMP-7 expression have a reduced incidence of tumor formation of intestinal adenoma in the *Min* mouse model [103]. In 1980, Liotta, *et al.*, demonstrated that there is a correlation between metastatic behavior of cells and the overexpression of collagenases, implicating MMPs ECM disruption capacity in the aggressive behavior of transformed cells [104]. Importantly, not only have the tumor-derived MMPs been associated with primary tumor development and progression, but cells in the stroma were found to participate in tumor progression by expressing MMPs which contribute to tumor cell invasiveness [105, 106]. The impact of MMPs on tumor progression not only lies in the contribution of MMPs to tumor cell invasion, but also to angiogenesis [107]. Itoh, *et al.*, demonstrated that lack of MMP-2 can abrogate the ability of cancer cells to induce angiogenesis [108].

This brief introduction to MMP's roles in cancer makes it clear that the dysregulation of these MMPs and their endogenous inhibitors can be detrimental. Because of the ability of MMPs to affect a plethora of disease processes, including but not limited to cancer progression, MMPs became the prime target for drug development in multiple fields of disease study.

1.1F REIGNING THEM IN: EARLY SUCCESSES AND MAJOR FAILURE IN TARGETING MMPs

Evidence of the ability of MMPs to contribute to disease progression accumulated and, concomitantly, evidence that inhibiting MMPs could contribute to disease regression or delay progression also accrued. Experiments demonstrated that upregulation of the endogenous MMP inhibitor TIMP-1 in cancer cells resulted in a smaller number of metastatic lesions as compared to control cells in an experimental metastasis model [109, 110]. While TIMPs function to inhibit MMPs, the role of MMPs and TIMPs in tumor progression is complex and frequently cancer staging counterintuitively correlates with a high level of TIMP expression [111]. Therefore, TIMPs themselves are not particularly good candidates for therapeutic agents as they are small proteins and can actually perform dual functions [112].

Early synthetic inhibitors were designed such that they mimicked MMP substrates based on amino acid sequence of triple helical collagen cleavage site (MMP-1); the inhibitors mimic the collagenase cleavage site (Gly-Ile or Gly-Leu) [113]. The inhibitors should interact with the active site and inhibit MMPs by chelating the catalytically active Zn^{2+} [113]. The hydroxamic acid derivatives function to coordinate the catalytic zinc with the two oxygen atoms in its sequence and hydrogen bonding of the nitrogen of the hydroxamate and the carbonyl of the enzyme backbone help to stabilize the interaction with the inhibitor [112]. According to Whittaker, *et al.*, there are four classes that MMP inhibitors can fall into based loosely on structure, including succinyl hydroxamates, sulfonamide hydroxamates, non-hydroxamates, and natural products [113].

Hydroxamic acid derivatives, namely batimastat and marimastat, were some of the first promising peptidomimetic MMPIs [112]. Batimastat (BB-94) is a low molecular weight, reversible inhibitor of MMPs that is broad spectrum in nature and was identified in early *in vitro* studies as decreasing tumor burden in various models of cancer and significantly reducing metastatic spread, ultimately increasing survival rates of involved animals [114-116]. Inhibition of hemangioma growth was observed in an *in vitro* model, and it was postulated that angiogenesis was abrogated with MMP inhibition which is a positive effect considering tumor reliance on generating neovasculature [117]. Intrapleural injection to patients was more effective against early-stage tumors, reducing angiogenesis and tumor burden, but late-stage disease treatment elicited no benefit [118]. Batimastat is not orally available, however its relative marimastat (BB-2516) is an orally bioavailable drug [113]. While this drug did advance to clinical trials, side effects such as severe musculoskeletal pain sidelined the progress of this drug [119]. MMP inhibitors designed to target the active site were also designed to harbor carboxylate groups and thiol zinc-binding groups for the purpose of zinc chelation [113] but these inhibitors tended not to be as potent as their hydroxamate relatives. Non-peptidomimetic inhibitors were developed for the purpose of attempting to circumvent the problems observed with the peptidomimetic compounds and clinical trials with BAY 12-9566 showed some promising results regarding reduced angiogenesis and lung metastases, but the side effects included liver and kidney toxicities and anemia [118]. Bisphosphonates have been explored as MMPIs, as they are capable of inhibiting several MMPs by acting as a zinc-chelator, by reducing MMP expression, and preventing MMP activation, and breakdown [118].

Natural products have also been explored for the purpose of discovering novel MMP inhibitors. One of the most successful MMP inhibitors has been the tetracycline derivatives. Tetracycline's non-antimicrobial properties include inhibition of MMPs [120]. In order to avoid unwanted antibiotic action, chemically modified tetracyclines have been developed [121]. This family of tetracyclines inhibit MMPs as they are able to inhibit inflammatory cascades that can cause MMP overexpression [121]. In addition to this indirect method of inhibiting MMP activity, tetracyclines are capable of directly inhibiting the protease [120]. One of the most successful inhibitors of MMPs, doxycycline, is FDA-approved for use in the case of periodontal disease.

Overall, the mechanism of inhibition by synthetic MMPIs has been relatively broad spectrum and that is the primary reason for failure of these drugs in clinical trials, with the exception of a few successes. The ability of these MMPIs to inhibit multiple MMPs can result in inhibition of MMPs during normal physiological processes and, unfortunately, can also inhibit MMPs that contribute to disease prevention, *i.e.:* anti-tumoral MMPs (MMP-3, -8) [118]. Reasons for failure of Phase III clinical trials with MMPIs include dosing issues (doses for healthy volunteers as opposed to cancer patients) and study design, specifically the inclusion of only late-stage disease sufferers [122]. Despite these failures, a list of over fifty clinical trials is currently on record at clinicaltrial.gov that involve MMPIs. Furthermore, there are currently many new strategies being developed for MMP inhibition in various kinds of diseases, yet many are still in *in vitro* settings. MMPs play a large role in normal physiology, but are still considered a prime target in the context of many diseases and the race for novel inhibitors continues. Because of the lack of efficient MMP inhibitors, our laboratory has undertaken to identify MMP-specific inhibitors, including those for MMP-9 and MMP-14. We have shown that the MMP-9 PEX domain is critical to induction of cell migration and that homodimerization of the protease is required for MMP-9-mediated migration [123]. Based on this information, we developed a peptide that mimics the MMP-9 PEX domain blade IV that mediates homodimerization of the protease; this peptide effectively reduces cell migration [11]. Furthermore, we have also discovered a novel, small-molecule inhibitor of MMP-9 that selectively targets the PEX domain based on docking studies using the ZINC 2007 database [10]. The best performing hit reduced cell migration and invasion and was shown to reduce tumor growth and metastasis in an orthotopic model. Our group also identified two crucial portions of the PEX domain of MMP-14. Two of the outer blades of the PEX domain (blade I and blade IV) are responsible for interaction with CD44 (another cell surface molecule) and MMP-14. Synthetic peptides that mimic these regions of MMP-14 prevent hetero- and homo- dimerization. These peptides were effective at reducing the ability of MMP-14 expressing cells to migrate and invade, and ultimately, were able to prevent metastases in a mouse model [9].

The work presented in this chapter aims to identify additional novel mechanisms of inhibition of MMPs, particularly MMP-14 and MMP-9, both of which are associated with poor cancer prognosis and increased metastatic potential.

1.2 MATRIX-METALLOPROTEINASE-14 (MMP-14)

Although the overall incidence and mortality rates regarding cancer have steadily declined over the past fifteen years [124], cancer is still a health threat. Since the majority of those who are afflicted with cancer succumb to the disease because of the dissemination of cancer cells rather than the primary tumor itself [2], it is of utmost importance to develop methods to target invasive and migratory cancer cells.

One property of invasive cancer cells is the expression of membrane type 1-matrix metalloproteinase (MMP-14). MMP-14 is responsible for the proteolysis of ECM components, cleavage of surface molecules, and activation of soluble MMPs [125, 126]. These activities collectively contribute to metastasis of cancer cells by reducing cell-ECM contact [126].

CD44 is a cell surface molecule that is a target of MMP-14. It is an integral cell surface protein that is the primary receptor for hyaluronic acid, a major component of the ECM [127]. CD44 itself has been linked to metastasis [128] and can be found localized with MMP-14 in migratory cells, specifically at the leading edges of the cell [129]. The expression of CD44 and interaction with MMP-14 for cleavage is one requirement for motility stimulation and correlates with tumor burden [130, 131].

Because of the contribution of CD44 and MMP-14 to migration of cancer cells [130, 131], disrupting the relationship between the two is a viable method for prevention of cancer dissemination. While CD44 is a ubiquitously expressed molecule, MMP-14 is not found at the surface of normal tissues; this unique relationship can be exploited in order to develop inhibitory molecules that can prevent migration and metastasis of cancer cells away from the primary tumor.

In order to achieve this goal, I identified a crucial motif within CD44 responsible for interaction with MMP-14 and developed mimicking peptides to act as an inhibitor to the CD44/MMP-14 interaction. I scrambled regions of CD44 coding and assessed the ability of CD44 to interact with MMP-14 both biochemically and *in situ* by co-immunoprecipitation and a split-GFP system, respectively. I assessed the functional impact of the CD44 mutant interfering with the CD44/MMP-14 interaction via 2-D migration assays. Peptides mimicking CD44 were designed that imitate the region of CD44 implicated in MMP-14 interaction and the ability of the cells to migrate with or without peptide treatment was assessed by a substrate degradation assay. Overall, this work identified a region of CD44 crucial to interacting with MMP-14 and developed mimicking, inhibitory peptides against the MMP-14/CD44 interaction.

1.2A MMP-14 BACKGROUND

MMP-14 is an integral membrane protease coded for in single copy on chromosome 14 [131]. Like the rest of the MMP family, it is a Zn^{2+}-dependent endopeptidase. It shares the bulk of its structure with the other members of the MMP family (a signal peptide, propeptide domain, a catalytic domain, a PEX domain); however it also includes a furin-recognition domain, a transmembrane region, and a small intracellular domain. The furin-recognition domain allows for cleavage in the Golgi by the proprotein convertase, which serves to expose the catalytic domain [131].

One unique feature of the membrane-type MMPs is the counterintuitive function of the prodomain being implicated in the activity of the enzyme [84]. MMP-14 requires the prodomain for activation of MMP-2; loss of the prodomain does not interfere with the catalytic activity MMP-14 against gelatin substrates, but does in fact reduce the ability of MMP-2 to be activated [132]. Specifically, a conserved region of the prodomain, ^{42}YGYL^{45} contributes to the folding and function of the prodomain as an activator of MMP-2 [133].

The MMP-14 catalytic domain also has an additional eight residues forming what is known as the "MT-loop" that is found within the loop connecting β-sheets II and III (LβIIβIII) [31, 33]. The MT-loop plays a critical role in the ability of some transmembrane type MMPs, including MMP-14, to activate MMP-2 via interactions with TIMP-2 [134, 135]. Each membrane-type MMP has a slightly different MT-loop which potentially dictates the differential functions of the membrane-type MMPs, although it is currently unclear exactly which substrates would interact with the loop segment [136]. Additionally, the MT-loop of MMP-14 has been documented to affect the ability of MMP-14 to localize to cell adhesions and influence cell invasion without directly affecting the ability of the enzyme to catalyze gelatin degradation or induce cell migration [136].

The small intracellular domain of MMP-14 serves to localize MMP-14 to the appropriate places at the cell membrane. Deletion mutants of MMP-14 that span the short cytoplasmic tail on MMP-14 reveal that amino acids located in the middle portion of the tail are critical to MMP-14 localization and function [137]. Loss of these residues impairs the ability of MMP-14 to localize to invadopodia, which are crucial for cell migration, and abrogates MMP-14's capability to activate MMP-2 [137]. Another group reported that mutation of the intracellular domain of MMP-14 impedes migration, but not necessarily activation of MMP-2 [138]. The ability of MMP-14 to activate the ERK pathway confers its ability to mediate migration and the ability to activate ERK is lost upon mutation of the intracellular cytoplasmic domain [138]. The cytoplasmic tail of MMP-14 also plays a critical role in clathrin-mediated endocytosis of the peptidase from the cell surface, which may be crucial in regulating the ability of MMP-14 to participate in extracellular proteolytic events [139].

MMP-14 may also be post-translationally modified. There is evidence that the palmitoylation of Cys^{574} in the cytoplasmic tail of MMP-14 contributes greatly to the activity of this MMP by mediating internalization [140]. Furthermore, differences in glycosylation have been determined to affect protease stability; differential O-glycosylation of MMP-14 leads to slower protease turnover [141, 142]. Not only has glycosylation of this protease been linked to turnover rate, but also has been found to influence the autocatalysis of MMP-14. MMP-14 with

reduced glycosylation in the linker regions has the ability to autocatalyze, implying that glycosylation may play a crucial role in protease stability [143]. Interestingly, the glycosylation pattern of MMP-14 has been linked to a particular cytoplasmic tail motif, dileucine^{572}, which may be responsible for mediating interactions with proteins necessary for proper glycosylation [144]. O-glycosylation of MMP-14 may also be a mechanism of control, as differential glycosylation of the linker region impedes the recruitment of TIMP-2 necessary for the ternary MMP-2 activation complex without significantly affecting collagenolytic activity [142].

MMP-14 functions as an activator of soluble MMPs, but it can also directly cleave extracellular matrices. It is a cell-surface tethered collagenase and can affect a variety of extracellular matrix components. In addition to collagens I, II, and III, MMP-14 can cleave laminin-1 and -5, fibronectin, vitronectin, gelatin, casein, elastin, fibrin, and dermatan sulfate [145, 146]. Tenascin, nidogen, aggrecan, perlecan, and laminin-10 are also targets of MMP-14 [147]. The activity of MMP-14 against these various ECM components can contribute to cell motility. For example, MMP-14 can directly cleave laminin-5 and supplementation with laminin *in vitro* results in increased migration [148]. The cleavage of these matrices clears area for cells to migrate, but the fragments of matrix that are released upon cleavage can encourage cell motility by engaging growth-factor receptors [126].

The substrate repertoire of MMP-14 also includes adhesion molecules, growth factors, and chemokines [147]. MMP-14 is capable targets cell surface molecules that would normally participate in cell adhesion to the extracellular matrix. Syndecan 1 is a transmembrane heparin sulfate proteoglycan and is a target of MMP-14. It normally functions to adhere to fibronectin and collagen and MMP-14 cleavage of this molecule can contribute to cell migration [149]. CD44 is another important cell surface adhesion molecule that is a target of MMP-14 and its processing can enhance cell migration [150]. Certain integrins are also targets of MMP-14 and the effects of cleavage of these cell surface molecules can be wide ranging, contributing to cancer cell migration and adhesion. Cadherins also may be proteolyzed by MMP-14, essentially removing the ability of those proteins to function as cell-cell contacts [151]. MMP-14 activity can also convert latent growth factors to their active form, particularly TGF-β [147]. Activation of growth factors by this protease can influence cell growth, matrix deposition, and apoptosis [147, 152, 153]. Chemokines may also be activated by MMP-14, influencing inflammatory responses [154].

MMPs are frequently overexpressed in malignancies of a wide variety and MMP-14 is no exception. The variety of substrates that MMP-14 can target makes it a crucial protease that contributes to cancer progression, both in the sense it destabilizes the ECM and activates soluble proteases to amplify proteolytic activity in the extracellular environment. The use of inhibitors against MMPs has been clinically unsuccessful, primarily due to the highly conserved nature of the catalytic domain and the side effects induced by use of a broad spectrum inhibitor. Therefore, I aimed to explore the relationship between MMP-14 and CD44, a transmembrane receptor that is a reported target of MMP-14 and ultimately contributes to MMP-14 mediated cancer cell migration.

1.2B CD44

CD44 is a cell surface glycoprotein responsible for adhesion to hyaluronan (HYA), which is a glycosaminoglycan (GAG) that is a primary component of the ECM [155]. This GAG is a linear polysaccharide with repeating dissacharides composed of β1,4-D-glucuronic acid-β-1,3-N-acetyl-D-glucosamine [156]. The molecular weight of HYA easily ranges into the millions of Daltons, but the size of HYA can actually influence cellular response; for example, low molecular weight HYA (<500 kDa) can influence inflammatory responses while high molecular weight species do not [156]. HYA influences cell motility by engagement of cell surface receptors that activate changes in the cytoskeleton or certain signaling pathways related to mobility. Not only can HYA engage cells to influence motility, but it also provides physical space for cells to travel through in the ECM and proliferate [155]. Accordingly, assessment of a variety of human malignancies revealed that the level of HYA expression is correlated with tumor aggression; areas surrounding the tumor can be particularly HYA rich, which provides a mechanism by which cells can escape [155].

The primary receptor for HYA is CD44, a cell surface protein encoded on chromosome 11 [157]. The tissue distribution of CD44 is vast, being found in a variety of organs and within the central nervous system. The standard CD44 isoform is more ubiquitous than its alternatively spliced counterparts, as their expression is much more restricted. A variety of functions have been attributed to CD44 amongst the tissue types it has been found in, including cell adhesion, lymphopoiesis, and cell migration, amongst others [157, 158].

Structurally, CD44 consists of an N-terminal link-homology (HYA-binding) domain, a variant stem region, a transmembrane region, and an intracellular domain. The bulk of the extracellular region (~180 N-terminal amino acids) is conserved in mammals. Within this region, conservation of six cysteines, five N-glycosylation consensus sites, and the proteoglycan core/link homology domain occur [159, 160]. This amino acid sequence, located at the N-terminus of the protein, is sufficient for hyaluronan binding [161]. The link module shares homology with other HYA binding proteins, such as TSG-6 and cartilage-link protein [160].

Human CD44 has ten requisite exons and can include up to ten variant exons coded within a single gene; the minimal version of CD44 is generally referred to as CD44s [155, 162]. Typically, exons 1-5 and 16-17 compose the extracellular portion of the molecule while exon 18 codes for the transmembrane region and exon 20 frequently codes for the intracellular domain (as opposed to the alternatively spliced exon 19 intracellular domain) [163, 164]. This minimal version is expressed on almost all cell types and is not usually activated for HYA binding and subsequent signaling [162]. Variant exons may be inserted in a variety of combinations, for example, CD44E includes variant exon 8-10 and is primarily expressed on epithelial cells [155]. Alternative splicing and resultant various glycosylation patterns exist in pathological conditions such as cancer; the diverse population of CD44 molecules under pathological conditions results in increased tumorigenic HYA binding [162]. While alternatively spliced CD44 products are associated with tumorigenesis, the complexity of CD44 biology is exemplified by the ability of the different forms to exert differential effects dependent upon the type of malignancy they are expressed in [160]. Not only can alternative splicing result in variant exon insertions, but it is possible for this differential splicing to result in a soluble isoform of CD44; it is postulated that this CD44 solubility can influence cell-matrix binding by competing with cell surface CD44 and

therefore exert an effect on cell behavior [163]. It is not completely clear what controls alternative splicing, but cells are able to shift their pattern of expression dependent upon their need [157].

The transmembrane domain of CD44 is highly conserved, encoded by exon 8 [157, 165]. This highly conserved hydrophobic region of CD44 mediates its Triton X-100 insolubility property [165]. This particular domain is necessary for ligand binding, however it is not absolutely required, as replacement with transmembrane regions from other integral proteins also allowed for HYA binding [165, 166].

The intracellular domain is also highly conserved and encoded by one exon [165]. This distal carboxy-terminal region is responsible for interacting with the cytoskeleton of the cell [157]. It can also interact with several molecules, such as Src kinase and the ERM proteins (ezrin-radixin-moesin proteins). The cytoplasmic portion is necessary for proper dispersal of CD44 to appropriate areas of the cell membrane and may also play a role in HYA binding [157]. It has been documented that the ability of CD44 to function as a receptor for HYA is enhanced by its ability to oligomerize and this formation may be mediated by the cytoplasmic tail. Cytoplasmic tail loss decreases the ability of CD44 to bind HYA, but modifying CD44 such that a disulfide bond can be formed between transmembrane domains of the protein to force oligomerization can reverse that phenomenon [167]. Not only does the intracellular domain affect oligomerization, but perhaps more importantly, it dictates cellular localization. Swapping experiments that exchanged the transmembrane and intracellular domain for that of L-selectin adopted the cellular distribution of L-selectin and vice versa is also true [168].

The CD44 cytoplasmic tail is subject to constitutive phosphorylation at Ser^{325}; this phosphorylation is mediated by Ca^{2+}/calmodulin-dependent protein kinase II (CaMKII) and loss of this modification interferes with cell migration, but not necessarily HYA binding, suggesting that the intracellular domain is responsible for events following ligand binding [160, 169]. Phosphorylation can be influenced by protein kinase C activation, as well as protein kinase A, however total phosphorylation does not change even though the amino acid location does [170].

The standard form of CD44 has a predicted molecular weight of 37 kDa, however it has an apparent weight of 80 to 100 kDa when glycosylated. CD44 contains both N- and O-linked glycosylations and the extracellular domain may also incorporate glycosaminoglycans such as chondroitin sulfate, heparin sulfate, and/or keratin sulfate which may specifically allow for growth factor binding [162]. Glycosylation is purported to affect the function of CD44, although it has been documented that CD44 species can occur in both glycosylated and unglycosylated form, suggesting that glycosylation does not direct all functions of CD44 [157]. Evidence exists that suggests modifying the glycosylation pattern of CD44 will change HYA binding, as glycosylation site mutants (specifically N-glycosylation sites) will alter the CD44 HYA binding state [171, 172].

Keratin sulfation of CD44 results in decreased HYA adhesion, with a reduction in keratin sulfate correlating to HYA binding and a decrease in metastatic potential [173]. Oppositely, chondroitin sulfation results in an increased interaction of CD44 with HYA and this particular glycosaminoglycan modification is necessary in order for binding to other matrix substrates

[160, 174]. Since these modifications may occur on the alternatively spliced versions of CD44, the functional differences between the isoforms may be attributed in part to changes in posttranslational modifications [175].

CD44 is subject to lipid modification, specifically palmitoylation. Palmitoylation occurs on free thiols, usually those close to the transmembrane region [176]. In the CD44 amino acid sequence, two highly conserved cysteines can be palmitoylated (Cys286, Cys295) and the acylation of these residues mediate lipid raft localization and receptor/hyaluronan endocytosis [177]. Not only does palmitoylation affect membrane localization, but also influences contact with the cytoskeleton, as deacylation of CD44 can lead to reduced interaction with ankyrin (a cytoskeleton linker protein) [178]. Ultimately, the loss of palmitoylation of CD44 can result in redistribution from lipid rafts and increased cell migration and invasion [179, 180].

Binding of CD44 and HYA can lead to CD44 activation, which can result in cell signaling and cytoskeleton rearrangements. It is considered that CD44 exists in three forms, non-binding (inactive), non-binding unless activated by a stimulus (inducible), or constitutively binding (active) [162]. Signaling changes are primarily induced when HYA binds active CD44. The plethora of biological functions that CD44 can influence derives from the proteins that interact with the molecule. CD44 can interact with the ezrin-radixin-moesin proteins and merlin, as well as ankyrin [162]. Despite the ability of interacting proteins to influence CD44-HYA interactions, most evidence suggests that the structure of CD44 itself dictates ligand binding [160].

CD44 interacts with the cellular cytoskeleton [181-183] and this is a crucial observation, as the migration of cells is not only dependent on intracellular signaling, but reorganization of the cytoskeleton for cell motility. Ankyrin, actin, ERM proteins, and merlin (NF2 gene product) have been documented to make direct interactions with CD44 [160]. CD44 interacts with merlin similarly to its interaction with the ERM proteins, as CD44 co-localizes with merlin at membrane protrusions and merlin is able to interact with the actin cytoskeleton [184].

This integral membrane protein was first implicated in cancer metastasis by Gunthert *et al.*, particularly the variant isoforms of CD44; transfection of a CD44 variant to a non-metastatic cell line resulted in metastasis in a syngeneic rat model [185]. Katoh, *et al.* demonstrated that circulating, soluble CD44 was increased in a tumor-bearing mouse model, suggesting CD44 expression is associated with tumor development and CD44 is sensitive to cleavage from the cell surface [186]. Furthermore, antibodies targeting cell surface CD44 and injection or expression of soluble CD44 result in abrogation of tumor and metastasis formation [187-190]. High expression levels of CD44 variants have been associated with a number of different cancer types, including neuroblastoma, colorectal cancer, and breast cancer [191, 192]. Relatedly, circulating levels of soluble CD44 has been suggested to be an indicator of tumor burden in patients with gastric cancer and colon cancer [193].

Considering the detection of a soluble CD44 in cancer patients, CD44 proteolytic processing is critical. Early, indirect evidence suggested that CD44 cleavage was dependent upon a metalloprotease, based on the use of cation chelating agents [194]. The identification of soluble CD44 under certain pathological conditions suggest proteolytic activity, *i.e.*:

malignancies tend to overexpress proteases that can act upon CD44 which indicates that soluble CD44 detection in cancer patients is likely related to proteolytic processing of the molecule [195]. Further studies indicated that the extracellular region of CD44 can be cleaved by membrane bound proteases, including ADAMs (a disintegrin and metalloprotease) and MMPs, particularly MMP-14 [170, 195, 196]. It has been biochemically shown that CD44 can be cleaved by MMP-14 and reverse phase chromatography indicated that there are two likely sites of cleavage within CD44, one of which MMP-14 is responsible for acting upon [150]. Kajita *et al.* also demonstrated that co-expression of CD44H and MMP-14 leads to CD44 fragments being released from the cell surface [150]. CD44 cleavage by MMP-14 can lead to a more aggressive, invasive cell phenotype, as a cleavage resistant mutant of CD44 expressed with MMP-14 was unable to induce cell migration [150].

Preliminary evidence generated in our laboratory, and others, indicates that the relationship between MMP-14 and CD44 is crucial for cell migration. Knockdown of CD44 in MMP-14 expressing cells results in a significant decrease in cell migration, despite leaving MMP-14 proteolytic function intact, as evidenced by a substrate degradation assay [9]. This is indicative of the requirement of CD44 for MMP-14 mediated migration. A previous publication from our laboratory demonstrated that mutation of the MMP-14 PEX domain blade I results in a loss of interaction with CD44, based on co-immunoprecipitation (CoIP) [9]. This is in addition to the work by Kajita, *et al.* that shows MMP-14 can cleave CD44 leading to an aggressive, invasive phenotype [129, 150].

Because it appears that the CD44-MMP-14 interaction influences cell behavior that can ultimately contribute to cell migration and downstream metastasis during cancer progression, I ***hypothesize*** that the PEX domain of MMP-14 interacts specifically with the extracellular domain of CD44 to increase the migratory capacity of cancer cells and developing small peptides that mimic the minimal motif within CD44 for binding the MMP-14 PEX domain will inhibit the migration of these cells by disrupting the CD44-MMP-14 axis. The long term goal of this work is to develop a tool that can specifically target cell-surface MMP-14 and interfere with the protease's interaction with cell surface molecules.

1.2C RESULTS

In order to begin to understand how CD44 interacts with MMP-14, I rearranged the amino acid sequence of CD44 such that the extracellular regions were scrambled but maintained the cysteine residues that are responsible for mediating the proper fold of CD44 at the cell surface; there are six crucial cysteines in the extracellular region of CD44 [197, 198]. Mutations were made along the length of the extracellular region of CD44, using the smallest CD44 isoform, CD44H, as this minimal isoform still interacts with MMP-14 and inherently excludes the possibility that any variable inserts in the stem region mediate the interaction. Additionally, all mutants were designed with a hemagglutinin tag (HA) in the stem region to facilitate the co-immunoprecipitation (CoIP) process, as we employed a myc-tagged MMP-14 construct in parallel with the HA-tagged CD44 (Figure 3).

Figure 3: CD44 mutation schema. A schematic representation of planned mutations spanning the length of CD44. Cysteine residues were maintained in order to preserve CD44 protein structure. The hashed regions represent the mutated areas. TM, transmembrane and ICD, intracellular domain.

We predicted that the location of this tag would not interfere with CD44 because the region in which it is set would otherwise be where alternative splicing would result in the variable inserts such that CD44 would potentially have an extended stem structure. Addition of the HA does not interfere with CD44 expression at the cell surface as demonstrated by immunofluorescence (Figure 4). Therefore, I moved forward with testing the mutant constructs including the HA-tag by CoIP.

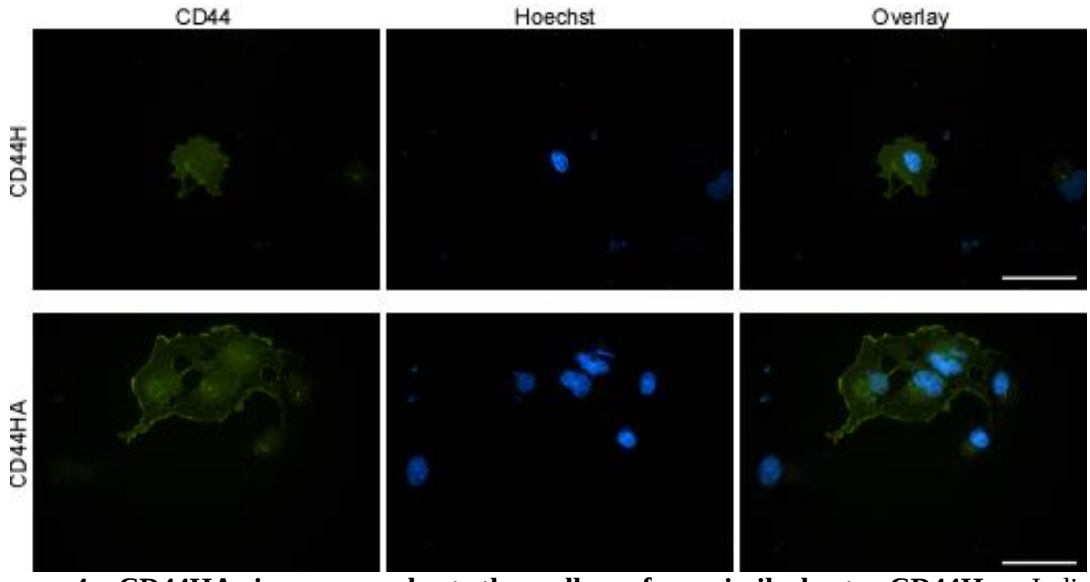

Figure 4: CD44HA is expressed at the cell surface similarly to CD44H. Indirect immunofluorescent staining for CD44 revealed insertion of the HA tag does not interfere with CD44 localization.

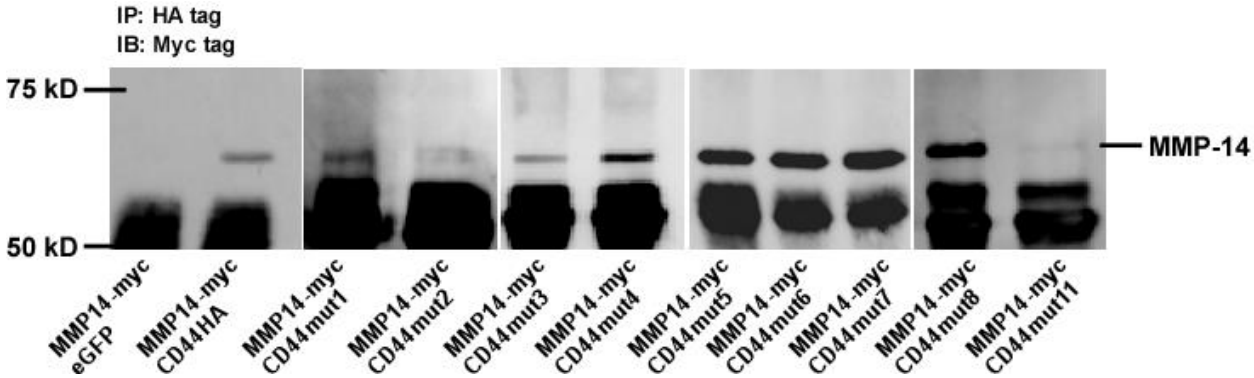

Figure 5: Co-immunoprecipitation of CD44HA mutants with MMP-14myc. Co-IP assays reveal that CD44-11 mutant had a consistently reduced interaction with MMP-14 and a representative immunoblot is presented here. IP was accomplished with an antibody targeting HA and immunoblot with an antibody targeting myc to detect MMP-14.

As expected, MMP-14 co-precipitated with wild-type CD44 in cells co-transfected with both cDNAs. Amongst the CD44 mutants generated, mutant 11 (CD44-11) had reduced interaction with MMP-14 based on CoIP assays (Figure 5). The mutation corresponds to a 24 amino acid stretch of the protein [amino acid sequence: VSSGSSSERSSTSGGYIFYTFSTV]. In an effort to monitor CD44 and MMP-14 interactions *in situ*, I established a split-green fluorescent protein (GFP) system using engineered GFP fragments derived from a bacterial system [199]. In order to achieve fluorescent signal indicative of CD44-MMP-14 interaction, the C-terminal fragment of GFP (Csp) was incorporated at the C-terminal end of CD44. Similarly, the N-terminal fragment of GFP (Nsp) was incorporated at the C-terminal portion of MMP-14. The DNA was sequenced and correct expression of these constructs was validated by Western blotting and immunofluorescence (Figures 6 and 7).

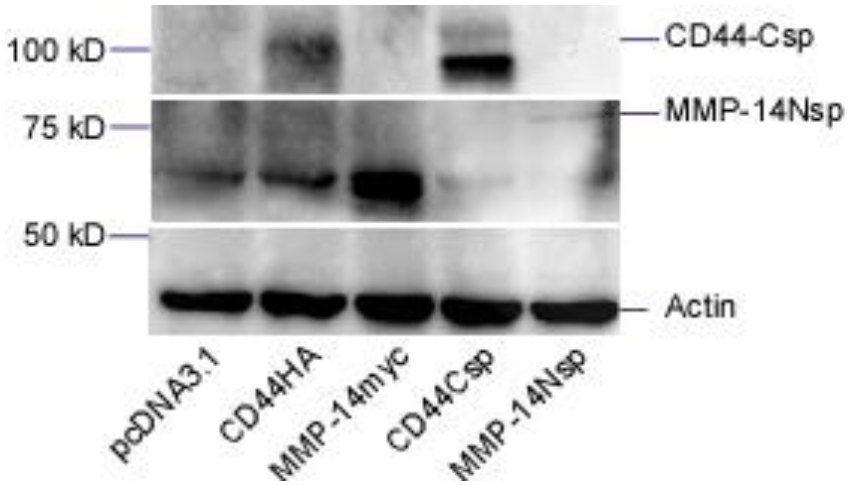

Figure 6: Western blot analysis of the split-GFP system components. COS-1 cell lysates expressing either wild-type MMP-14 or CD44 were compared to CD44-Csp and MT1-Nsp expressing lysates. Antibodies against CD44 and MMP-14 recognize the split-GFP protein products.

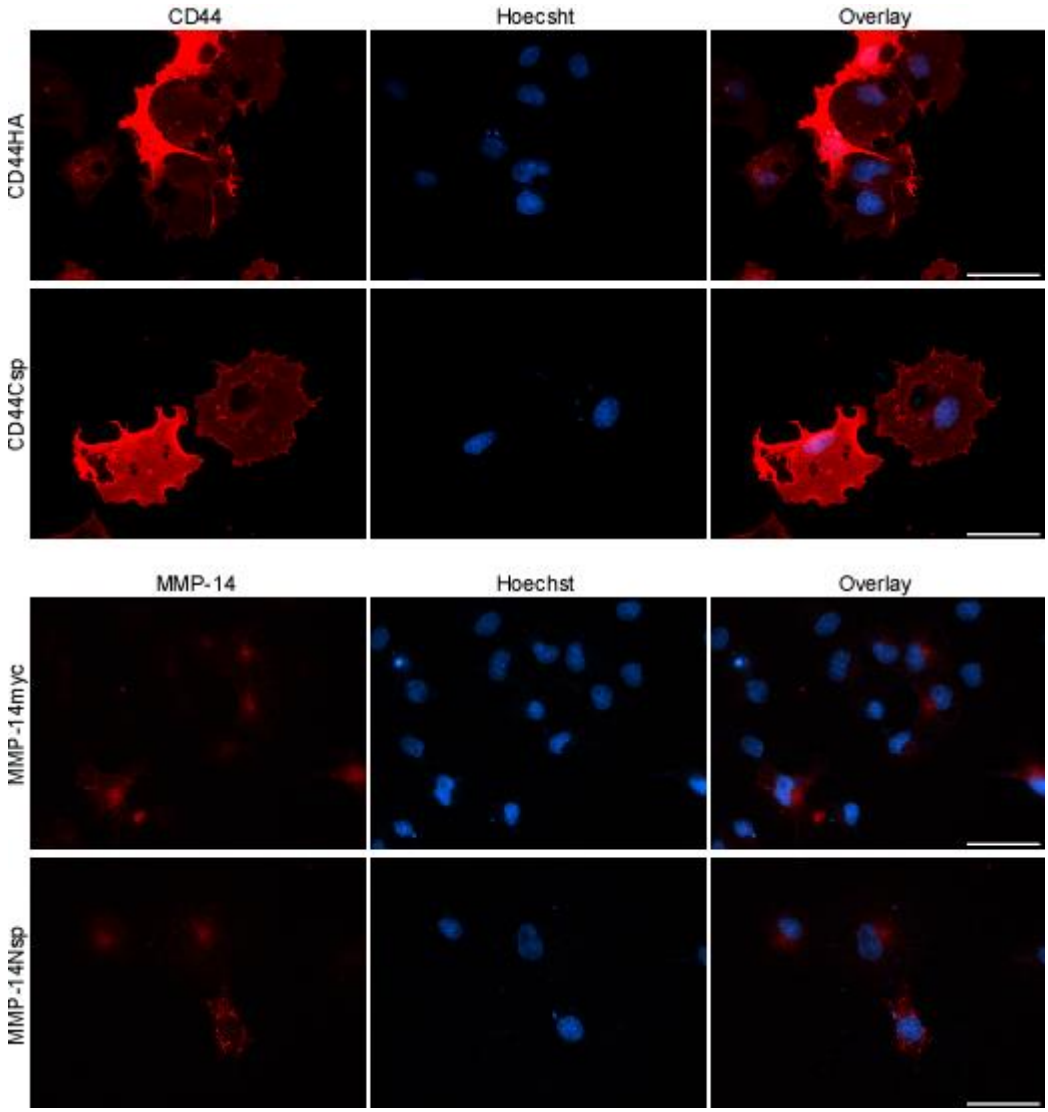

Figure 7: Indirect immunofluorescence of COS-1 cells expressing components of the split-GFP system. The top panel demonstrates a similar staining pattern between CD44HA and CD44-Csp using an anti-CD44 antibody. Similarly, MMP-14 antibodies recognize both MMP-14myc and MMP-14Nsp. White bar = 50 μm

If MMP-14 and CD44 are interacting with one another, there will be fluorescent signal. Figure 8 shows that co-expression of wild-type CD44Csp and MMP-14Nsp results in green fluorescence. Expression of CD44-11Csp with MMP-14Nsp does not result in an obvious increase in green fluorescence. Overall, the split-GFP system confirms the CoIP data, suggesting that the CD44-11 mutant area is critical for MMP-14 interaction. Flow cytometric analysis of cells co-expressing CD44Csp and MMP-14Nsp demonstrate that there is a fluorescent signal, as opposed to expression of each individual component (Figure 9). To further support our CoIP results, Csp was also incorporated to the C-terminal of mutant CD44-11. As predicted, the fluorescence signal intensity was decreased as compared to co-expression of the wild-type split-GFP constructs. Not only does this split-GFP system provide additional evidence of abrogated

CD44-MMP-14 interaction upon mutation of this 24 amino acid stretch, but it also potentially provides a downstream tool to monitor inhibitory peptide ability to interfere with the CD44-MMP-14 relationship.

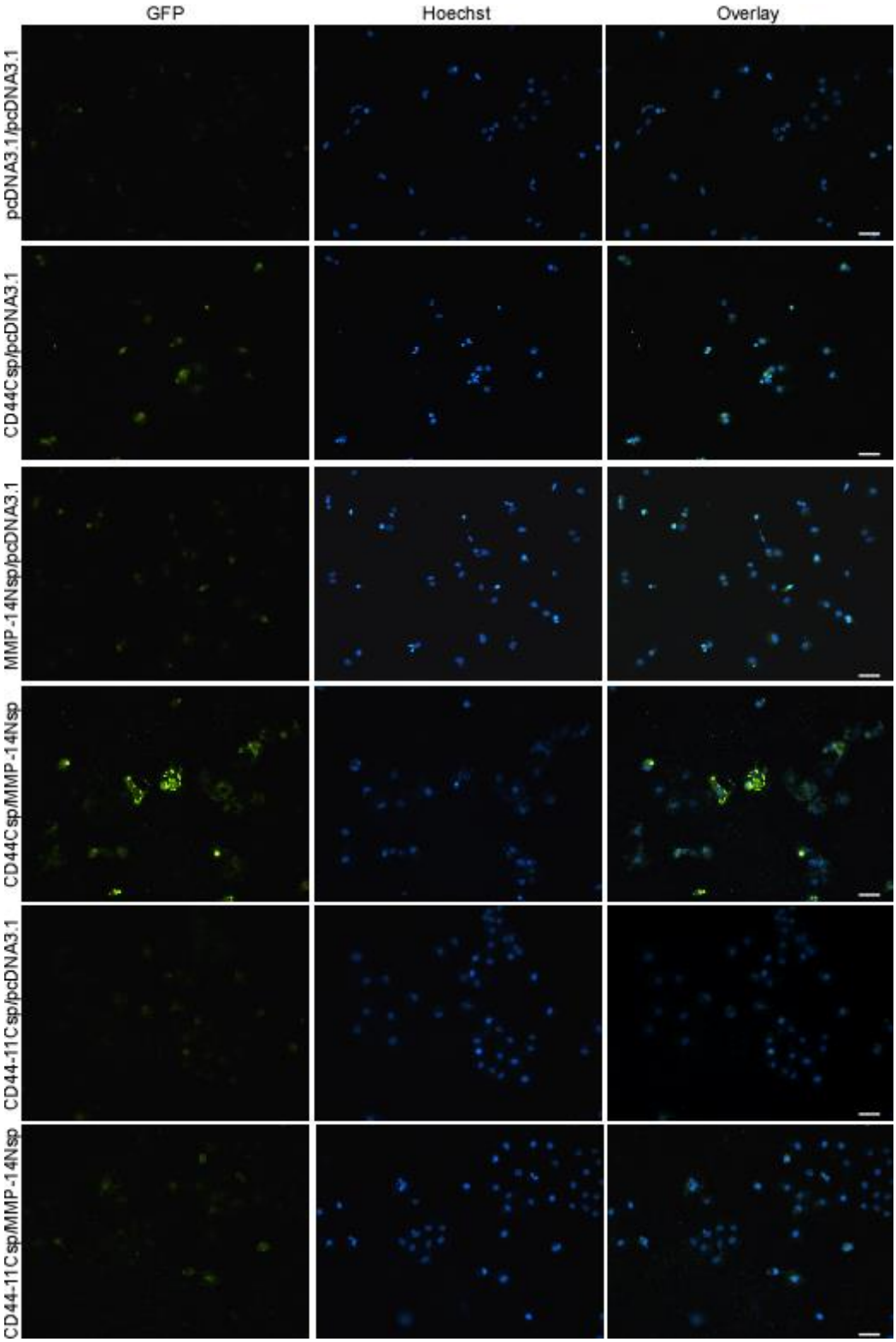

Figure 8: Split-GFP system can be used to monitor the interaction between CD44Csp and MMP-14Nsp. COS-1 cells expressing CD44Csp and MMP-14Nsp emit green fluorescence, while CD44-11Csp expression with MMP-14Nsp does not result in fluorescence. Each component expressed individually produces minimal background. White bar = 50 μm

A

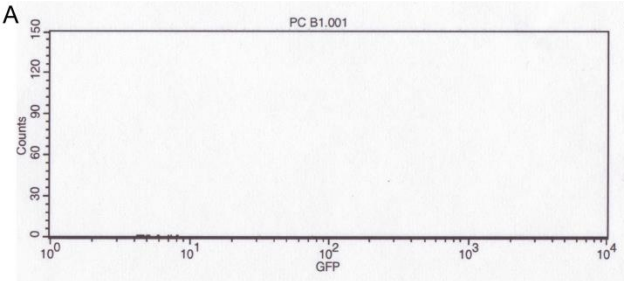

Histogram Statistics

Sample ID: PC B1
Acquisition Date: 18-Sep-14
Gate: G2
Gated Events: 39
Total Events: 20692

Marker	Events	% Gated	% Total	Mean	Geo Mean	Median
All	39	100.00	0.19	6.84	6.24	5.99

B

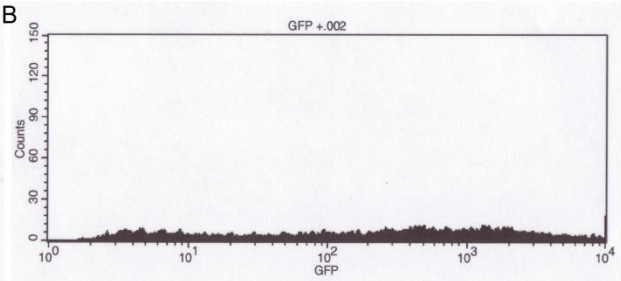

Histogram Statistics

Sample ID: GFP +
Acquisition Date: 18-Sep-14
Gate: G2
Gated Events: 4969
Total Events: 20799

Marker	Events	% Gated	% Total	Mean	Geo Mean	Median
All	4969	100.00	23.89	1047.44	177.61	268.96

C

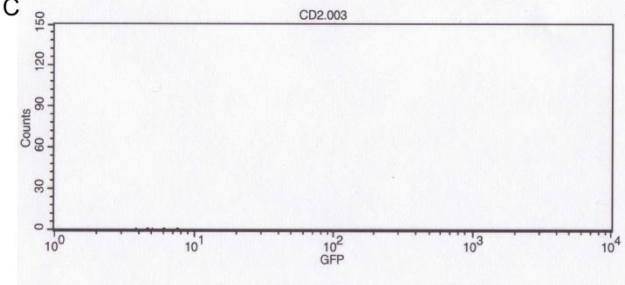

Histogram Statistics

Sample ID: CD2
Acquisition Date: 18-Sep-14
Gate: G2
Gated Events: 32
Total Events: 20823

Marker	Events	% Gated	% Total	Mean	Geo Mean	Median
All	32	100.00	0.15	74.80	7.82	5.75

D

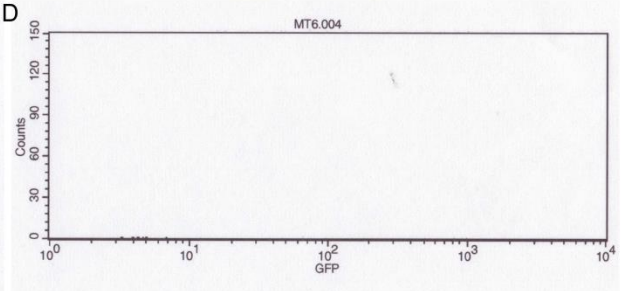

Histogram Statistics

Sample ID: MT6
Acquisition Date: 18-Sep-14
Gate: G2
Gated Events: 26
Total Events: 20839

Marker	Events	% Gated	% Total	Mean	Geo Mean	Median
All	26	100.00	0.12	7.78	5.99	4.85

E

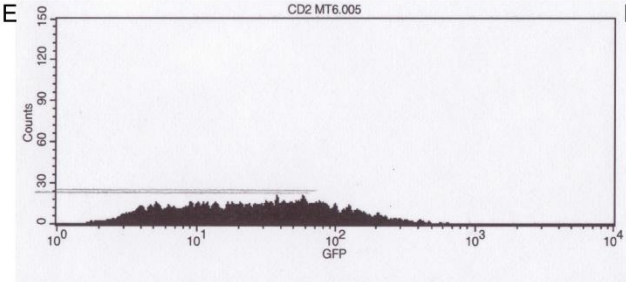

Histogram Statistics

Sample ID: CD2 MT6
Acquisition Date: 18-Sep-14
Gate: G2
Gated Events: 5923
Total Events: 20727

Marker	Events	% Gated	% Total	Mean	Geo Mean	Median
All	5923	100.00	28.58	51.82	25.28	26.66

F

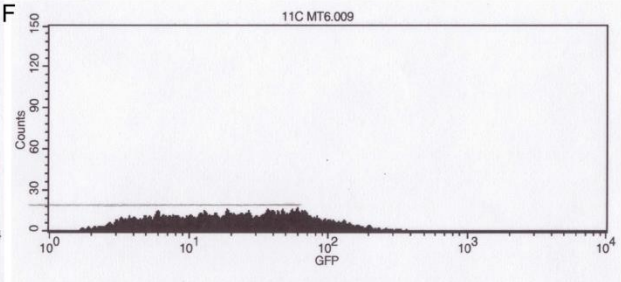

Histogram Statistics

Sample ID: 11C MT6
Acquisition Date: 18-Sep-14
Gate: G2
Gated Events: 4588
Total Events: 20764

Marker	Events	% Gated	% Total	Mean	Geo Mean	Median
All	4588	100.00	22.10	38.84	20.99	22.07

Figure 9: Cell flow cytometry illustrates that wild-type CD44Csp and MMP-14Nsp result in higher intensity fluorescence as opposed to CD44-11Csp and MMP-14Nsp co-expression. COS-1 cells transfected with CD44Csp and MMP-14Nsp display higher intensity fluorescence as opposed to co-expression of CD44-11Csp and MMP-14Nsp. Expression of each component in the system individually does not produce any significant fluorescence. (A) pcDNA transfected negative control cells (B) GFP transfected positive control cells (C) and (D) CD44Csp and MMP-14Nsp transfected cells, respectively, serve as negative controls. (E) CD44Csp and MMP-14Nsp co-transfected generate fluorescence compared to (F) CD44-11Csp and MMP-14Nsp co-transfected cells, which generate less intense fluorescence.

In order to confirm the decreased interaction of MMP-14 and CD44, I examined intact CD44 in lysates from cells co-expressing wild-type MMP-14 and either CD44 or CD44-11. Because MMP-14 can cleave the extracellular region of CD44, cells expressing wild-type CD44 and MMP-14 demonstrate a decreased signal corresponding to intact CD44, as the antibody employed recognizes an extracellular isotope that would be cleaved. Conversely, those cells expressing wild-type MMP-14 with CD44-11 maintain the signal corresponding to intact CD44 (Figure 10A). Densitometric analysis reveals a significant difference in intact CD44HA after co-expression of wild-type CD44HA with MMP-14, while CD44-11 co-expression with MMP-14 reveals no significant difference in CD44 signal (Figure 10B).

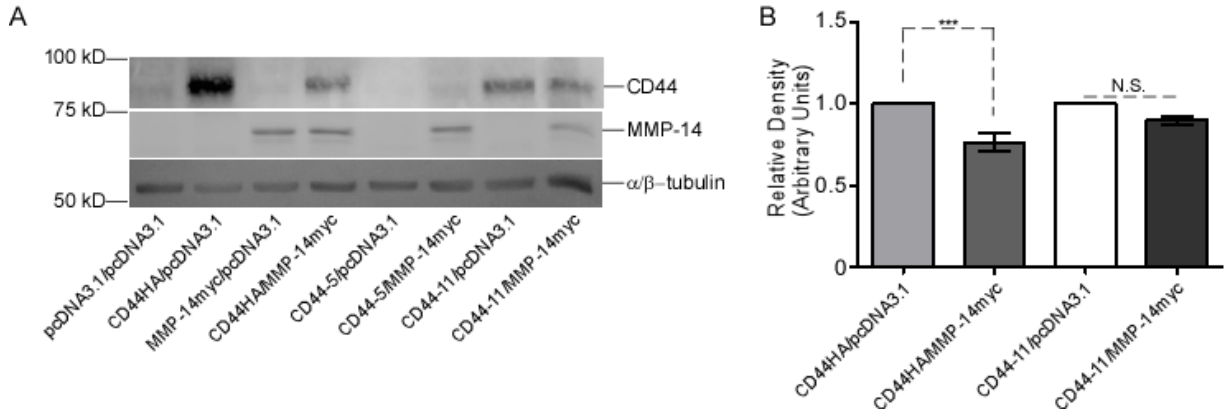

Figure 10: MMP-14 cannot cleave cell surface CD44-11. A) Western blot analysis of CD44 and MMP-14 expressing COS-1 cells demonstrates that MMP-14 is less able to cleave CD44-11 as compared in relative terms to CD44HA, implying inability to interact with MMP-14. B) Densitometric analysis of CD44 bands reveals a significant difference in intact CD44 between expression of CD44HA versus CD44HA and MMP-14 together. No such difference exists when expressing CD44-11 mutant with MMP-14.

Based on the crucial nature of the MMP-14 and CD44 interaction for cell migration, the ability of CD44-11 to mediate MMP-14 induced migration was assessed. As expected, transient co-expression of wild-type CD44 with MMP-14 results in a significant increase in cell migration. CD44-11 expression alongside MMP-14 does not allow for increased migration (Figure 11). There is a statistically significant difference between CD44 and CD44-11 mediated MMP-14 cell migration.

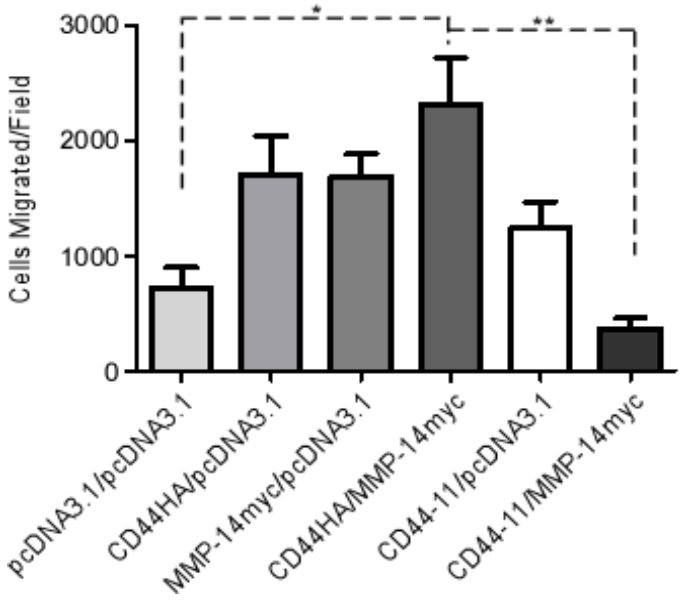

Figure 11: MMP-14 mediated migration is reduced when MMP-14 is co-expressed with the CD44-11 mutant. Expression of CD44HA with MMP-14myc results in a significant increase in migration, while expression of the CD44-11 mutant is decreased, as assessed by transwell migration assays.

My biochemical data indicates that the CD44-11 region influences the CD44-MMP-14 interaction. Attempts at synthesizing the entire region as a soluble peptide failed (amino acid sequence: VSSGSSSERSSTSGGYIFYTFSTV), therefore a series of three mutants that collectively span the entire CD44-11 mutated region was generated, but each segment mutated is only eight amino acids (CD44-111, CD44-112, CD44-113). These mutants appear to be expressed at the cell surface, similar to wild-type CD44 and the parent mutant, CD44-11 (Figure 12). Of these three mutants, CD44-112 and CD44-113 seem to be decreased in their interaction with MMP-14 based on CoIP analyses, performed in a similar manner to previously described CoIPs (Figure 13).

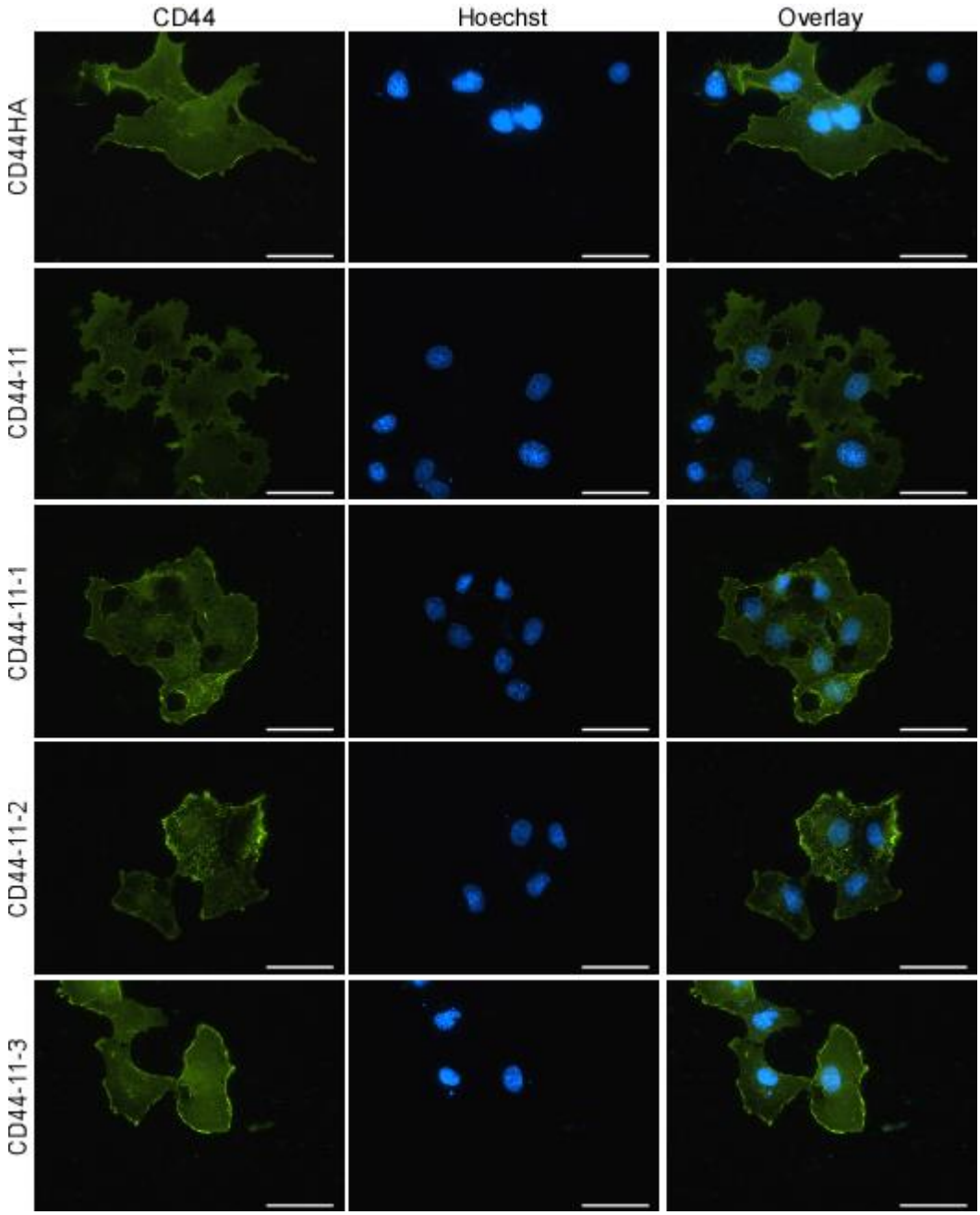

Figure 12: Indirect immunofluorescent surface staining of minimal CD44-11 mutants CD44-111, CD44-112, and CD44-113. COS-1 cells over-expressing CD44HA, CD44-11, or CD44-11 minimal mutants were stained with an anti-CD44 antibody followed by an Alexa488 conjugated secondary antibody. Each mutant appears to localize similarly to CD44HA.

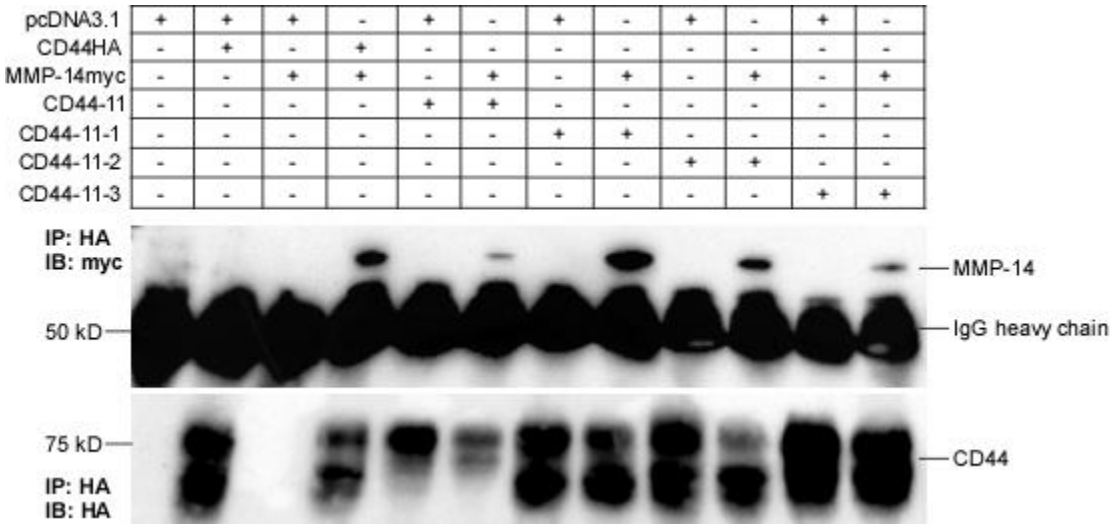

Figure 13: Co-IP of CD44 minimal mutants with MMP-14myc demonstrates that CD44-113 has a reduced interaction with the protease. Co-expression of CD44HA and MMP-14myc constructs in COS-1 cells results in efficient pulldown of MMP-14 with CD44, while CD44-113 has a reduced interaction with MMP-14. IP was accomplished with an antibody targeting the HA tag and immunoblot with an antibody targeting myc to detect MMP-14.

Region CD44-113 seems particularly important to the interaction of CD44 and MMP-14 and therefore, I attempted to determine whether these impaired interactions of MMP-14 and CD44 mutants translates to abrogated MMP-14 mediated cell migration, as CD44/MMP-14 interaction is required for MMP-14 mediated migration [9]. Co-expression of wild-type MMP-14 and CD44 leads to enhanced migration, as opposed to each individual component. Notably, CD44-113 expression with wild-type MMP-14 results in a decrease in migration (Figure 14).

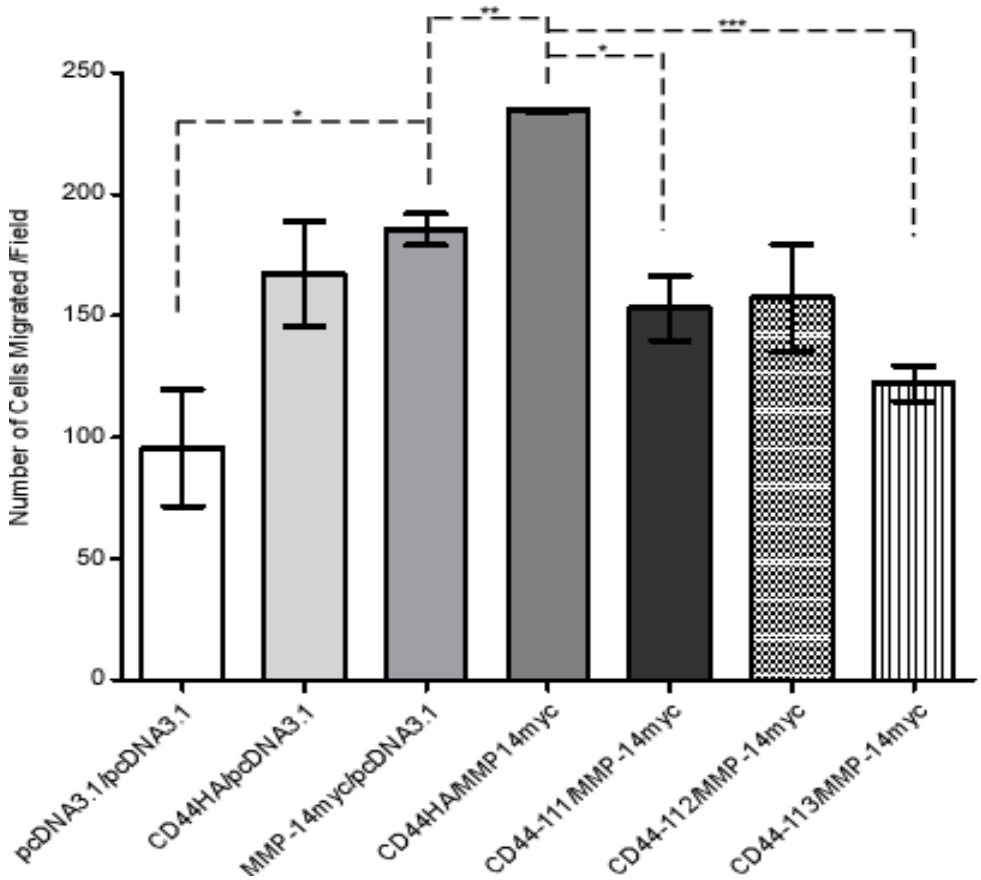

Figure 14: MMP-14 mediated migration is reduced when MMP-14 is co-expressed with the CD44-113 and CD44-111 mutant. Expression of CD44HA with MMP-14myc results in a significant increase in migration, while expression of the CD44-111 and CD44-113 mutant is decreased, as assessed by transwell migration assays.

Based on the minimal mutants, synthetic peptides were produced (EZ BioLabs) which mimics the first eight and last eight amino acids of the CD44-11 mutation (Peptide 1: VSSGSSSE and Peptide 2: IFYTFSTV). These peptides were designed unlabeled or with a fluoroscein isothiocyanate (FITC) label to allow for tracking the peptide on cells, considering these peptides theoretically bind MMP-14 at the surface and MMP-14 is endocytosed regularly [137, 139, 200]. Unlabeled peptides (Peptide 1 [CD39] and Peptide 2 [CD40]) were used to determine biochemically whether or not the MMP-14 and CD44 interaction is interrupted under peptide treatment. CoIP assays were carried out in a similar fashion to the aforementioned CoIPs, except that after transfection, cells were incubated with 100 μM of a scrambled generic peptide, 100 μM of Peptide 1, or 100 μM of Peptide 2. As seen in Figure 15, treatment with the peptides prior to immunoprecipitation results in a decrease in the ability of MMP-14 to interact with CD44. Treatment of CD44 and MMP-14 expressing cells with a scrambled generic peptide did not abrogate the pulldown of MMP-14 with CD44. Total lysates show a similar amount of CD44HA input and probing the pulldown for the HA tag demonstrates that the pulldown was similarly efficient for each group (Figure 15).

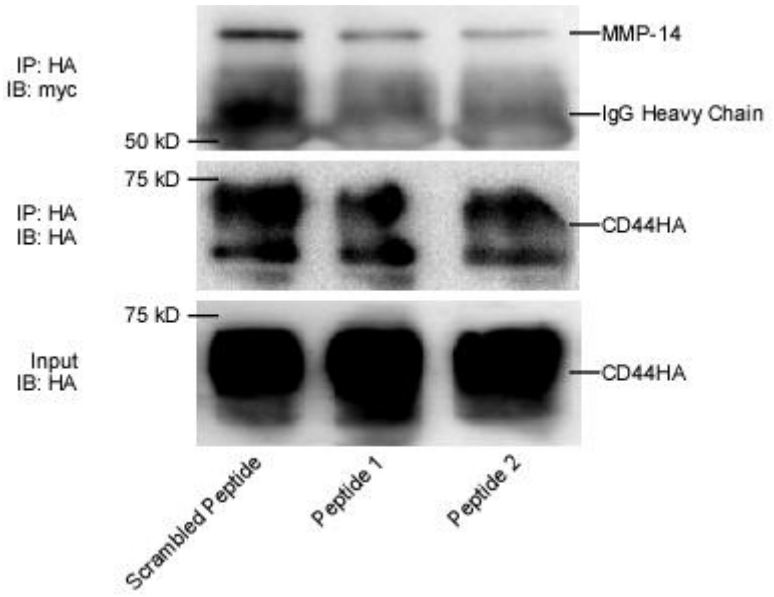

Figure 15: CoIP of CD44HA with MMP-14myc is inefficient in the presence of the CD44 mimicking peptides. COS-1 cells over-expressing CD44HA and MMP-14myc were subject to peptide treatments (100 uM) for 24 hours and subsequently lysed. Lysates were subject to CoIP using an anti-HA tag antibody. The resultant sample was probed via western blot with an anti-myc antibody, such that MMP-14 could be detected. In the presence of mimicking peptides, MMP-14 cannot efficiently interact with CD44.

Treatment of MMP-14 expressing cells with FITC-labeled peptide resulted in binding of the FITC-labeled peptide to COS-1 cells stably expressing MMP-14 (Figure 16). Furthermore, these cells endocytose the FITC-labeled peptide more intensely as opposed to stable, empty vector expressing cells (Figure 16). pQCXIP stable cells shows little evidence of binding to the cell surface by FITC labeled peptide 1.

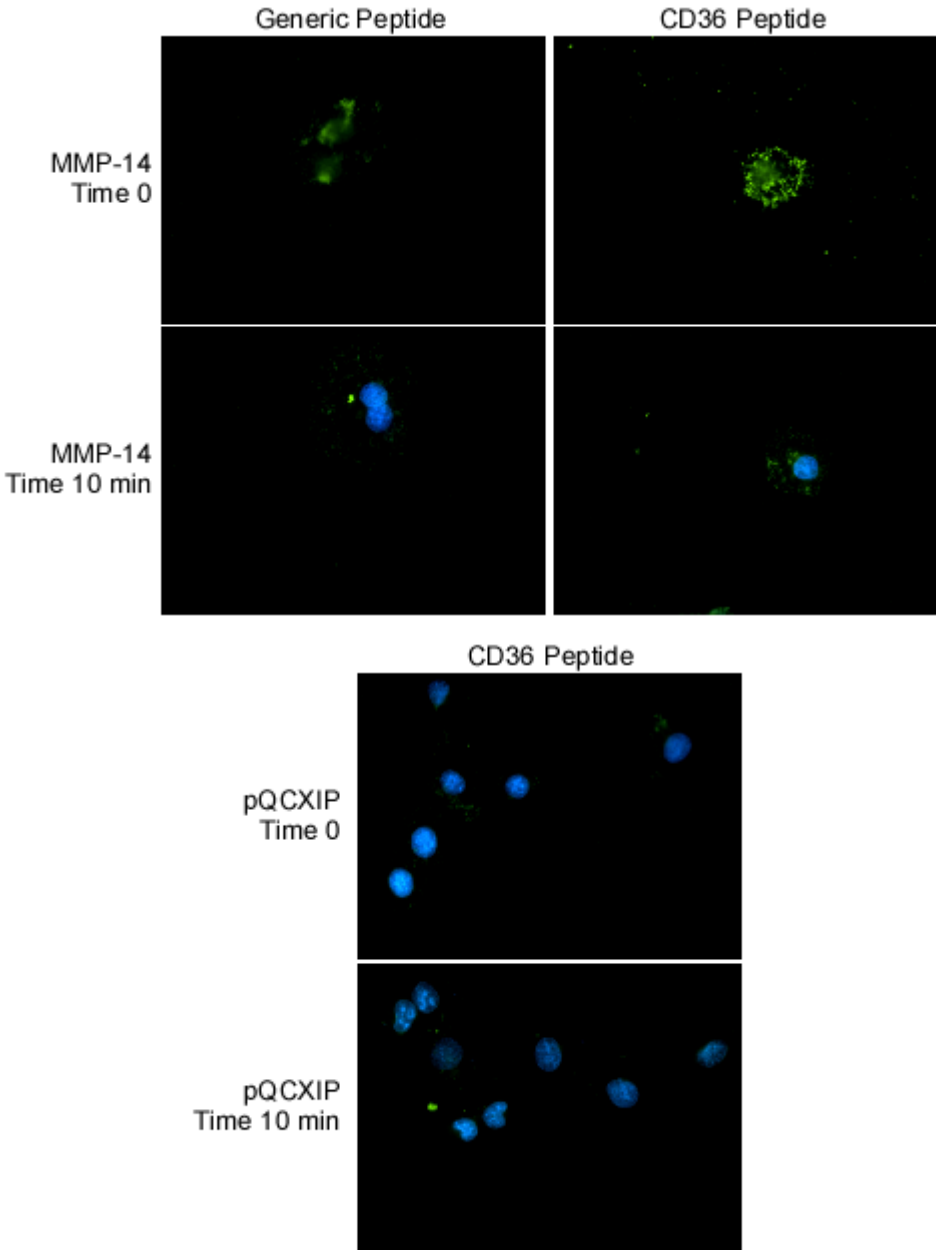

Figure 16: Endocytosis of CD36 Peptide (FITC-labeled peptide 1). Peptide designed to mimic the area of CD44 replaced by mutant CD44-111. MMP-14 stably expressing COS-1 cells were incubated with either generic peptide or CD36 peptide at 4ºC and introduced to 37ºC in order to restore endocytic activity. Empty vector expressing cells show little evidence of peptide binding.

Once the ability of our peptides to bind MMP-14 cells was established, I assessed the function of the peptide in abrogating MMP-14 mediated cell migration. In order to do this, I performed a substrate degradation migration assay. Stably expressing MMP-14 expressing COS-1 cells treated with the inhibitory peptides had diminished cell migration as compared with a control peptide treated group (Figure 17). Collectively, these data indicate that this region I have identified plays a crucial role in interacting with MMP-14 and interference with this can influence cell behavior.

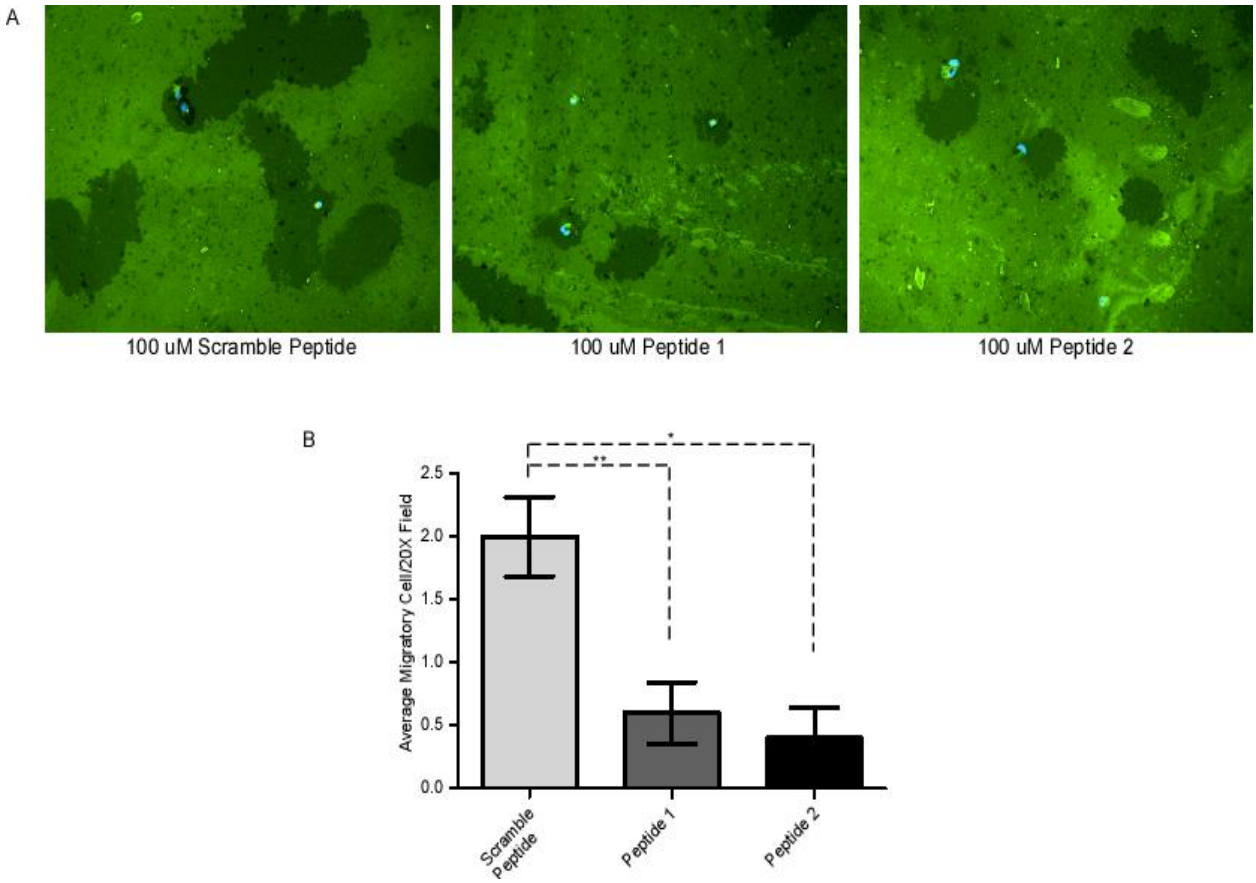

Figure 17: CD44 mimicking peptides decrease cell migration. (A) Representative images of COS-1 cells stably expressing MMP-14 and CD44 (endogenous) that were subject to a substrate degradation migration assay under treatments with a control scrambled peptide or either CD44 mimicking peptide at 100 μM. Migration is represented by a trail of cleared FITC-labeled gelatin substrate. (B) Peptide 1 and 2 treatments resulted in a significant decrease in MMP-14 mediated migration, quantified by counting five random fields and quantifying those cells with a trail of substrate degradation.

Not only does the interaction between CD44 and MMP-14 mediate migration by cleavage of CD44 from the surface, but there is also cell signaling associated with these protein interactions. Previously, we have shown that CD44-MMP-14 interactions encourage signaling through the epidermal growth factor receptor (EGFR) and Erk1/2 downstream [9]. We hypothesize that abrogating MMP-14 interaction with CD44 can modulate these signaling pathways that contribute to invasion and migration, in addition to proliferation. Co-expression of wild-type CD44 and MMP-14 results in increased phosphorylated EGFR and Erk1/2 (Figure 19). As expected, expression of CD44-11 and MMP-14 does not induce extensive pEGFR and pErk1/2 (Figure 18). Furthermore, expression of the minimal mutant CD44-113 recapitulates the effects that the full length mutant induces, displaying a similar pattern of phosphorylation as CD44-11 (Figure 19).

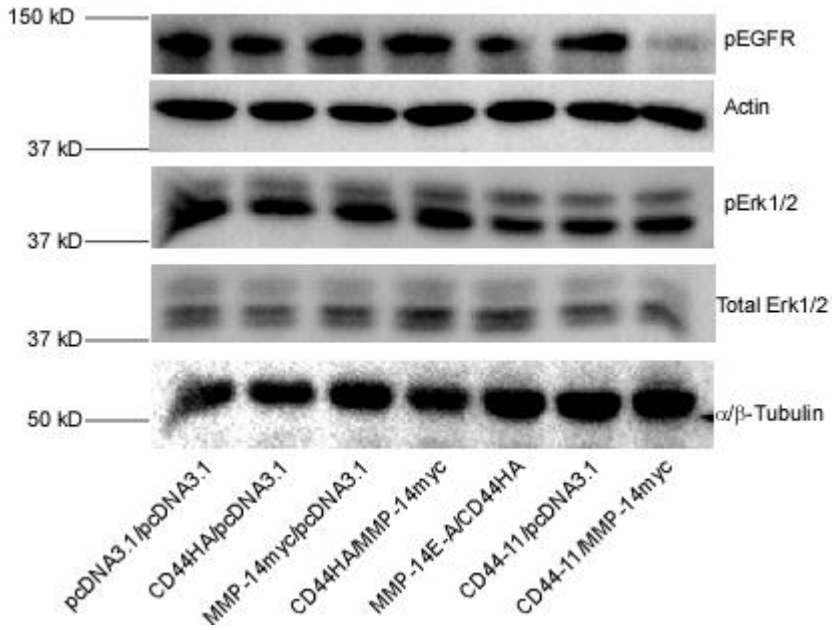

Figure 18: Expression of the CD44-11 mutant alongside MMP-14 decreases downstream signaling, including phosphorylation of the epidermal growth factor receptor (pEGFR) and Erk1/2 (pErk1/2). Co-expression of MMP-14 and the CD44 mutant CD44-11 results in reduced phosphorylation of EGFR and Erk1/2.

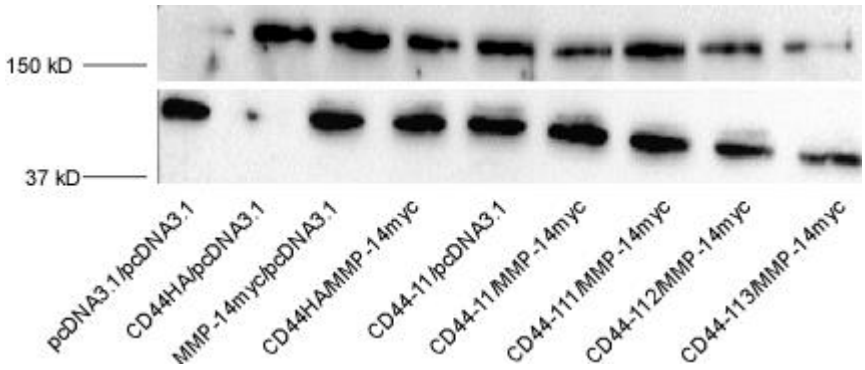

Figure 19: Expression of the CD44-113 minimal mutant with MMP-14myc demonstrates decreased phosphorylation of EGFR and Erk1/2. COS-1 cells co-expressing MMP-14myc and CD44HA show a high phosphorylation of EGFR and Erk1/2. Co-expression of CD44-113 with MMP-14myc demonstrates decreased levels of those phosphorylated proteins.

1.2D DISCUSSION

Cell migration is a critical component of cell invasion, which is an early step in the cancer metastasis cascade. The ability to abrogate cancer cell migration is a viable approach to decrease cancer metastasis. One way in which to accomplish this goal is to target key molecules that mediate cell migration. MMP-14 is an integral membrane protein responsible for pericellular proteolysis of matrices and soluble proteases and induction of cell migration. MMP-14's ability to induce migration is dependent on its relationship with the cell surface protein, CD44. CD44 has been documented to bind hyaluronic acid and act as an adhesion molecule, but it is also a substrate of MMP-14 at the cell surface [150]. We and others have demonstrated that co-expression of MMP-14 and CD44 leads to enhanced cell migration. In an effort to reduce the ability of MMP-14 and CD44 to contribute to motility, I determined a crucial motif within CD44 responsible for mediating MMP-14 interaction that when expressed with the protease reduces cell migration. Use of CD44 mimicking peptides based on this region led to reduced interaction of the two cell surface molecules and reduced cell migration in MMP-14 expressing cells.

In order to determine which region of CD44 was responsible for MMP-14, I mutated the bulk of the length of CD44 and assessed interaction by CoIP. The strategy in identifying MMP-14 interacting areas was limited to the extracellular region of CD44, as an extracellular portion of MMP-14 is required to interact with CD44 based on our previously published data [9] making it more likely that an extracellular region of CD44 was in contact with MMP-14, as opposed to the small intracellular domain. Furthermore, previous work has demonstrated that MMP-14 cleaves an amino acid motif in the extracellular CD44 portion [150]. Use of protein tags to facilitate pulldowns ensured that we were studying our CD44 proteins of interest alone, as opposed to including endogenous CD44 in the CoIP analyses, as most cells express some form of CD44. We were able to initially identify a 24 amino acid region of CD44 that consistently had reduced interaction with MMP-14 (CD44-11). Not only did that particular mutant reduce Co-IP with MMP-14, it also reduced interaction *in situ* based on fluorescence intensity of the split-GFP system, *i.e.:* wild-type constructs produced higher intensity fluorescence as opposed to expression of mutant CD44-11 with MMP-14 (Figure 8 and 9).

While not necessarily the focus of this work, it is important to note that mutations of CD44 in the N-terminal link domain led to increased interaction with wild-type MMP-14 (Figure 5). These mutants consistently had heavier bands corresponding to MMP-14 pulldown as compared to wild-type, suggesting an increased ability to bind MMP-14. It has been documented that this region of CD44 contains several N- and O-linked glycosylation sites and changes in glycosylation state of CD44 can lead to changes in the ability to bind ligands such as growth factors or hyaluronic acid [162, 171, 172]; perhaps the same is true for binding to MMP-14. It is interesting to speculate on this phenomenon, however further studies would need to be conducted in order to fully elucidate the relationship between CD44 glycosylation state and MMP-14. Site-directed mutagenesis against reported glycosylation sites followed by CoIP in addition to cell migration studies with these mutants and MMP-14 to determine the functional consequence of this apparent increase in protein-protein interaction might be undertaken.

The initial CD44 region of interest contains two previously reported MMP-14 cleavage sites on CD44, namely between Arg^{186}-Ser and Gly^{192}-Tyr. Accordingly, we determined that in comparison to wild-type CD44 co-expression with MMP-14, mutant CD44-11 remains intact based on analysis by western blotting with an antibody that recognizes the extracellular region of

CD44 (Figure 10). The loss of the interaction and/or cleavage site resulted in a significant reduction in MMP-14 mediated migration (Figure 11). Despite efforts to isolate the released fragment from conditioned media, no CD44 fragments were able to be identified when CD44 and MMP-14 were co-expressed. Attempts to validate this cleavage by detecting shed CD44 from conditioned media failed despite use of an antibody directed against CD44 directly or use of a construct designed with an HA tag inserted well above the predicted cleavage site (data not shown).

To further delineate whether the reduction in migration was due to loss of cleavage site or to reduction in MMP-14 contact with CD44, in addition to the inability to generate a 24 amino acid mimicking peptide, generation of smaller mutants was undertaken. As expected, the mutant CD44-112 that includes both cleavage sites had a reduced ability to induce migration, however it was able to pull down MMP-14 similarly to wild-type CD44 (Figure 13 and 14). Mutant CD44-113 had both a reduced ability to pull down MMP-14 and was incapable of inducing migration at a level comparable to wild-type CD44 and MMP-14 co-expression. We expected that use of the mimicking peptide based on the CD44-113 region would compete out endogenous interaction with MMP-14 and wild-type CD44. Use of these peptides reduced interaction between MMP-14 and CD44 and also served to prevent cell migration, based on substrate degradation assays (Figure 17). The peptide likely acts to interfere at the CD44/MMP-14 interface, but leaves the catalytic activity of MMP-14 unaltered (Figure 17). Unexpectedly, peptide 1 (correlating to the region of CD44 mutated in CD44-111) also displayed a similar trend of reduced interaction with MMP-14 and reduced migration of cells upon treatment (Figure 15 and 17), despite the CoIP showing significant interaction with MMP-14.

Phosphorylated EGFR at Tyr1173 and phosphorylated Erk have been documented to be increased upon co-expression of MMP-14 and CD44, which is indicative of activated receptor and effector [9]. The CD44-11 mutant and the minimal mutant CD44-113 both demonstrate decreased signaling through these particular proteins, indicative of abrogation of the relationship between MMP-14 and CD44 and their downstream signaling. These signaling pathways are important to cell motility, as EGFR and MAPK signaling both contribute to migration, either directly or by transcription of factors that contribute to migration [201, 202]. EGFR is upregulated in a variety of cancers and is associated with an invasive phenotype [203-205]. Signaling through Erk is downstream of EGFR activation [206] and this signaling pathway is crucial, as activation of Erk has been documented to directly phosphorylate paxillin (a crucial member of the focal adhesion kinase complex required for migration) [207], direct phosphorylation of focal adhesion kinase after stimulation with epidermal growth factor [208], and phosphorylation of the F-actin cross-linking protein epithelial protein lost in neoplasm (EPLIN) [209], amongst other activity. Our data demonstrating interference with the ability of MMP-14 to induce migration in the presence of CD44 may be related to downregulation of the activity of the EGFR-MAPK axis, considering the proteolytic activity of MMP-14 is not affected in our system.

Since MMP-14 and CD44 can directly play a role in cell motility, it is important to devise ways in which to impede the interaction of these two molecules. Our peptide designed to compete with the MMP-14 interacting motif of CD44 may provide a way to prevent cell motility and thus, metastasis. The early stage of metastasis, namely invasion, is dependent upon the cell's ability to both proteolyze the surrounding ECM and to migrate to the nearest vasculature.

Since selective inhibition of the proteolytic activity of MMP-14 has been notoriously unsuccessful due to a highly conserved catalytic domain, targeting exosites and exploiting protein interactions are necessary to develop effective anti-metastasis strategies. Here, I have presented a potential anti-metastasis agent by development of competitive, CD44-mimicking peptides with the function of inhibition of MMP-14 mediated migration.

Current and Future Directions:

I am currently working to further characterize the effects of our CD44 mutation and peptide treatment on MMP-14 and CD44 interaction. I am currently working to identify whether or not the minimal mutant of CD44 functions to preserve intact CD44 in a similar fashion to the CD44-11 mutant, with the intent of also confirming this phenomenon with the use of our peptide. Further documentation of cell surface binding and endocytosis of our peptides by MMP-14 expressing cells will be accomplished using labeled peptides and compared to empty vector expressing cells. Furthermore, I will determine whether our peptides will influence the same signaling pathways as co-expression of mutant CD44 with MMP-14, specifically phosphorylation of EGFR and Erk1/2. I am also attempting to employ the split-GFP system as a monitoring system by treating cells expressing the wild-type CD44 and MMP-14 constructs with the mimicking peptide and observing whether or not wild-type levels of GFP signal are generated. If the peptides are working in the predicted fashion, I expect that the fluorescence in the treatment group would be reduced.

It would also be interesting to determine whether or not the interaction between CD44 and MMP-14 exerts effects on the intracellular protein contacts that CD44 has. Not only does CD44 interact with EGFR, but it also has contact with soluble proteins intracellularly. One such protein crucial to actin cytoskeletal dynamics is merlin, the product of the NF2 gene. Loss of NF2 is associated with tumor development, so signaling through merlin is a crucial aspect of cancer biology. In an effort to understand whether or not the interaction between MMP-14 and CD44 modulates the downstream signaling through merlin, we will be assessing the status of merlin and whether or not the actin cytoskeleton undergoes any gross morphology changes in cells that express MMP-14 with wild-type CD44 versus co-expression with CD44-11.

On a more long-term scale, the CD44 mimicking peptide generated in this work has great potential. Since cancer cells usually overexpress MMP-14 in comparison to normal cells, it is possible that using a peptide that preferentially binds MMP-14 can be utilized as a drug targeting tool or imaging tool. Use of a chorioallantoic membrane assay to assess cancer cell invasion and influence on angiogenesis in the presence of the peptides should be undertaken. Perhaps most importantly, this peptide should be used in an *in vivo* model to determine its efficacy in preventing or mitigating metastases. The theoretical function of the peptide is to disrupt a protein interaction that is critical to the metastatic process, so use of this peptide in a cancer model may prove beneficial as a disease stabilizer.

1.2E MATERIALS AND METHODS

Materials

Anti-HA antibodies were acquired from Covance (Dedham, MA) and anti-myc antibodies were acquired from Roche (Indianapolis, IN). Anti-α/β-tubulin and anti-actin antibodies were attained from Cell Signaling Technologies (Davers, MA) for probing loading controls. The anti-HCAM antibody was obtained from Santa Cruz Biotechnology, Inc. (Dallas, TX). Anti-CD44 antibody was also obtained from Pharmingen. Antibodies against p-Erk1/2 and total Erk acquired from Sigma-Aldrich (St. Louis, MO). Anti-p-EGFR antibodies were obtained from Sigma. Horseradish-peroxidase (HRP) conjugated anti-mouse and anti-rabbit secondary antibodies were purchased from Rockland Immunochemicals, (Gilberstville, PA). Hoechst nuclear stain was attained from Invitrogen. Alexa Fluor 568 and Alexa Fluor 488 secondary antibodies were purchased from Molecular Probes, Life Technologies (Grand Island, NY). FITC-conjugated anti-rat secondary antibodies were acquired from Rockland Immunochemicals. FITC-labeled and unlabeled peptides were generated by EZ-Biolabs (Peptide 1: VSSGSSSE, 99% purity and Peptide 2: IFYTFSTV, 99% purity)

Cell Culture and Transfection

Cell lines were obtained from the ATCC (Manassas, VA). Cell lines including the monkey kidney fibroblast-like COS-1 and the human fibrosarcoma HT1080 were maintained in DMEM-high glucose medium (Corning, Mediatech). The human prostate cell line DU-145 was maintained in RPMI 1640 medium (Corning, Mediatech). All media were supplemented with fetal bovine serum (10%) and penicillin/streptomycin (1%) and cells were cultured under standard tissue culture conditions (37^{o}C, 5% CO_2) for the duration of experiments, unless otherwise noted.

Transfection of plasmid DNA to target cells was accomplished using polyethylenimine (PEI) (Polysciences). Briefly, plasmid DNAs and PEI were incubated at room temperature together in the appropriate volume of 150mM NaCl. The transfection mixture was then added to cells incubating in fresh, complete media. Cells were incubated for 48 hours under standard tissue culture conditions and followed by biological or biochemical assays as indicated.

DNA Construction

Primers used for CD44 mutagenesis are listed in Table 1. Mutagenesis was accomplished via a two-step PCR method [132]. Briefly, primers were used to generate fragments of CD44 that included the mutated region. Those fragments were then isolated via gel purification (Qiaex II Gel Purification Kit, Qiagen, Valencia, CA) and used for an additional PCR reaction to generate full-length CD44 coding regions that include the areas of interest mutated. These completed mutants were isolated, and along with the parent vector (pcDNA3.1/TOPO), were restriction digested with both EcoRV and HindIII (Roche). The insert was then ligated into the parent vector and the complete plasmids were transformed to DH5α *E. coli* for efficient propagation of the plasmids. Plasmid DNA isolation of each construct was accomplished using Mini or Midi prep kits from Qiagen (Valencia, CA). All constructs were verified by DNA sequencing.

Table 1: List of Primers used for CD44 Mutational Analysis

Construct	***Orientation***	***Sequence***

CD44HA	Forward	TACCCCTACGACGTGCCCGACTACGCCAGAGACCAAGACACATTC
	Reverse	GGCGTAGTCGGGCACGTCGTAGGGGTAGGTAGCAGGGATTCTGTC
CD44-1	Forward	ACCGTGTGATCCCAGTAGGACACTCACATGGGAGTC
	Reverse	CTACTGGGATCACACGGTCATTGCTGTCTGGTAGGCCGACTAGCTG CTTTAGGATTGCCACTGCGGCGTAGTCGGGCACGTC
CD44-2	Forward	GGAAGCGACTCCAAATTAAATGGCTGATCATCTTGG
	Reverse	TAATTTGGAGTCGCTTCCACGGTATACTTTGCTGGTGCTGTCGCCTG GTGTCGTCTGAGAATGGCCTGCTACCATCTGATTCAGATCCAT
CD44-3	Forward	GCAGAATTATATCGATCTGCATGCCGCTTTGCAGGTGTA
	Reverse	TGCAGATCGATATAATTCTGCCGCCAGGCTCAGCGGCAC
CD44-4	Forward	GCTAGCGGTCAGCAGGCTTCGGCTTGGCGTAGGCACAAGGTGTCAC AAGTCCTATCCGTCAGGCACTCTAGTTGCAAGGCTTTCAATAGC
	Reverse	AGCCGAAGCCTGCTGACCGCTAGCGCAGGTTATATTCAAATCGAT
CD44-5	Forward	GGTACTCGTACGGTTGAACGCAAGTTACCGACTAGAGGTCCTCGT CGCCTAGCAACACCGTACAGCCGCTGCAGGTATGGGTTCATA
	Reverse	TTCAACCGTACGAGTACCGCAGAGGTCAGCGGCCTC
CD44-6	Forward	GACGCAACCGCTCCGAGCCTCTACTATCCGGAAGTGTCTCAGAGTG AGAACGGTCGTTGTGCAGCAAACAACACA
	Reverse	GCTCGGAGCGGTTGCGTCGCAGGTCTCAAATCCGAT
CD44-7	Forward	AGCATACAACCACACGTAACGCCACGGTCGCATGCTGTACGACAT GTAACATACCTCCAATGCTTCAATGCTTCAGCT
	Reverse	TACGTGTGGTTGTATGCTACAGATGGAGTTGGGGTG
CD44-8	Forward	GATGCATTCACTTACGACCTAGCTAGCATATGTACATCAGTCACA GAC
	Reverse	TATGCTAGCTAGGTCGTAAGTGAATGCATCGCAATATGTGTCATAC CTG
CD44-9	Forward	CTGCACTATCACTTCATACGATTCACTCAATCGTCCGAGACCGTAAT CCTGCACTCCGGATGATGGAACATACGCTATGTCCAGAAAGGA
	Reverse	TATGAAGTGATAGTGCAGACAATCTTCTTCAGGTGG
CD44-10	Forward	GAACATCTGGTATTGCACAACACATCGATTCTCGACAGCATCTAGA

		CAACCGCACGGTAAGAGACAAGACCAGTGAGCAGCGGCTCCTCC
	Reverse	GTGCAATACCAGATGTTCGGTGCCATCACGGTTAAC
CD44-11	Forward	AGTCCTTCGCTAGTATTATCGCCACCTTTAGATGGCGGAAGTACGCC GACGGTACCTATAGACGTACTGTTACACCCCATCCCAGAC GAA
	Reverse	TAATACTAGCGAAGGACTGTCATCATCAGTAGGGTT
CD44-12	Forward	ACACCAGTATCAACGCCGACCGTGCTCACATCGCCGCACAACCTTC AGAGACACCACGCGTACCCCTACGACGTGCCC
	Reverse	CGTTGATACTGGTGTGATTACAGTAGAAAAGGTGTA
CD44-111	Forward	GCCACCCTGGAAGTGCGGAGGTATAGGAGCAGCACTTCAGGA
	Reverse	ATACCTCCGCACTTCCAGGGTGGCGTCATCATCAGTAGGGTT
CD44-112	Forward	GTCGATAGAGGGAGCGCCATACATATCTTTTACACCTTTTCT
	Reverse	ATGTATGGCGCTCCCTCTATCGACTTCACTGGAGGAGCCGCT
CD44-113	Forward	GACTTTACTCTCTTAATTGGTATACACCCCATCCCAGACGAA
	Reverse	TATACCAATTAAGAGAGTAAAGTCGTAACCTCCTGAAGTGCT

The split-GFP system was established by inserting either a C-terminal portion of GFP (Csp) or an N-terminal portion of GFP (Nsp) to the C-terminal ends of either CD44 or MMP-14, respectively. These GFP fragments were previously reported in a bacterial system and were engineered to have enhanced physicochemical properties to optimize the function of the split-GFP system [199]. We obtained the constructs for Csp and Nsp from Addgene (Plasmid 40729 and 40730). For use in our system however, the Csp and Nsp fragment required engineering a terminal, compatible restriction site for insertion at the 3' end of the CD44 and MMP-14 coding regions. The primers used for properly engineering the Csp fragment for placement at the 3' end of CD44 coding sequence are as follows: forward primer: 5'-GCTATGATATCATGGCAAGCGAGCAGCTGGAAAAG-3' and reverse primer: 5'-GCAACGATATCTTACTTGTAGCGTTCGTCGCG-3'. The primers used for properly engineering the Nsp fragment for placement at the 3' end of the MMP-14 coding sequence are as follows: primer: 5'-CACAAGCTTTAATGGGTCATCACCACCACCATCAC-3' and reverse primer: 5'-CGCAAGCTTTTACTGCGCCAGTTCCTTTTTCAG-3'. The inserts generated by this method were restriction digested with the appropriate restriction enzyme and ligated into their respective places following CD44 or MMP-14 coding sequences. The completed plasmid constructs were verified by DNA sequencing.

Co-immunoprecipitation and western blotting

COS-1 cells were transfected with the desired plasmids using the PEI protocol stated above. Forty-eight hours post-transfection, cells were washed twice with ice-cold PBS and

incubated for 30 minutes in RIPA buffer (Tris-HCl, pH 7.5, 150 mM NaCl, 1% Na^+ deoxycholate, 1% Triton-X100, 0.1% SDS) rocking, with agitation every 10 minutes. Lysis was completed by cell scraping and vigorous vortexing of the gathered lysate for 30 seconds. Lysates were cleared by centrifugation at 10000 rpm for 10 minutes at 4ºC. Supernatants were reserved and a small aliquot from each sample was set aside as a total input control. Supernatants were then incubated for 1 hour with anti-HA antibody (1:1200) and following that, an overnight incubation with constant rotation was allowed after addition of Protein A agarose beads. After 18 hours, the supernatant/bead mixture was centrifuged at 2000 rpm for 1 minute to isolate the Protein A agarose beads. Beads were washed three times in ice-cold PBS with a five minute incubation (rocking) and centrifugation step in between. All steps were performed at 4ºC. Finally, co-immunoprecipitation samples were isolated by boiling in SDS sample buffer supplemented with β-mercaptoethanol. All western blotting of lysates and CoIP samples were carried out according to previously published protocols and developed on a BioRad ChemiDoc [72].

Immunofluorescence and fluorescent microscopy

Immunofluorescent staining began by fixing transfected cells in 4% paraformaldehyde in PBS at 4ºC for 12 minutes. Blocking solution was composed of 3% bovine serum albumin/5% normal goat serum in PBS. After one hour blocking at room temperature, cells were exposed to anti-HCAM or anti-MMP-14 antibodies and visualized using the complimentary secondary fluorescent antibody (anti-rabbit Alexa Fluor 568 or anti-mouse Alexa Fluor 488), counterstained with Hoechst, and imaged on a Nikon Eclipse TE2000-S equipped with a Sutter Instruments SmartShutter System and a QiClick QImaging camera.

The split-GFP system was visualized 72 hours post-transfection. Cells were plated on glass coverslips, fixed in 4% PFA at 4ºC, and nuclei were stained with Hoechst. Cells were then imaged on the Nikon microscope listed above. GFP transfected cells were used as a positive imaging control and vector transfected cells were used as a negative imaging control.

Flow cytometry

In order to quantify fluorescence from the split-GFP system, cells were transfected and 72 hours post-transfection were fixed on ice for 20 minutes in 4% PFA. Cells were centrifuged at 2000 rpm for five minutes and washed once with ice-cold PBS without Ca^{2+} and Mg^{2+}. Cells were centrifuged again and then resuspended in 2% fetal bovine serum/3% normal goat serum for flow cytometric analyses at the Stony Brook University Flow Cytometry Core Facility.

Substrate Degradation Migration Assay

Briefly, glass coverslips were coated with FITC-labeled gelatin at room temperature and allowed to dry. The gelatin was then fixed with 0.05% glutaraldehyde and washed extensively with PBS at room temperature. After sterilization with ethanol and equilibration in complete media overnight at 4ºC, cells were plated at a low density and incubated for 8 hours and fixed and nuclei stained with Hoechst. The coverslips were imaged using the Nikon Eclipse TE2000-S equipped with a Sutter Instruments SmartShutter System and a QiClick QImaging camera.

1.3 MMP-9

MMP-9 has been implicated in cancer progression, both by its proteolytic and non-proteolytic functions. Previously, MMP-9 has been shown to form a dimer via the PEX domain. This dimer type was shown to be required for MMP-9 mediated migration. However, we explored the nature of the MMP-9 dimer under hypoxic conditions, as this condition tends to arise during tumor development. The high molecular weight specie MMP-9 that is evident under hypoxia is primarily composed of MMP-9, as evidenced by LC-MS/MS analysis. The dimer that forms under low oxygen tension forms intracellularly and does not depend on glycosylation state. It is reducing-agent sensitive and formation of the dimer is not reversed intracellularly by use of antioxidants under hypoxic conditions. Interestingly, MMP-9 mediated cell migration is impeded under hypoxia, suggesting the nature of the dimer may be unique compared to the high molecular weight MMP-9 that develops under normoxic conditions. Furthermore, a PEX dimer formation inhibitor, compound 1403, was unable to inhibit migration under hypoxic conditions. These data suggest that the nature of the MMP-9 dimer under hypoxia may be unique and that the milieu MMP-9 is found in may exert effects on its function.

1.3A MMP-9 BACKGROUND

(A portion of this introduction will appear in the special edition Frontiers in Biosciences: Matrix Metalloproteases)

MMP-9, a gelatinase, shares the features of the soluble MMPs (Figure 1), including signal peptide, prodomain, catalytic domain, hinge region, and PEX domain. However, it contains three fibronectin-like repeats that are oriented away from the enzyme and do not disturb the structure of the catalytic domain [33, 46]. The structure of the fibronectin-like domain with three individual repeats implies that they may be separate binding sites [46]. This domain can also be expressed on its own and has the ability to interact with basement membrane components such as collagen for degradation and proteoglycans containing heparin sulfate, implying these interactions can contribute to extracellular localization [210]. Gelatin binding capacity is also conferred to MMP-9 via these fibronectin-like repeats [211].

Another unique feature of MMP-9 is the OG domain. Approximately 85% of the glycosylation found on MMP-9 is of an O-linked nature [212, 213]. The heavily O-linked glycosylation domain of the hinge region (OG domain), in addition to the cysteine residue found in this area, is critical in mediating interactions with TIMP-1 and MMP-9's cargo receptors LRP-1 and megalin [213]. These interactions are crucial as they can limit the availability of activated MMP-9. Furthermore, this unique domain is vital to the proper function of MMP-9, as deletion of that region significantly reduces the ability of the enzyme to induce cell migration and bind its substrates [123, 214]. The OG domain is purported to offer flexibility to the MMP-9 molecule, which may influence the interaction of the enzyme with its substrates [215, 216]. The pro- form of MMP-9 also has N-glycosylation sites and this carbohydrate modification is purported to serve as protection from autocatalysis, similarly to O-glycosylation [217].

Outside of its role in normal biological processes, MMP-9 has specifically been linked to tumor progression, in addition to a plethora of other diseases, including autoimmune, inflammatory, and vascular diseases [218]. MMP-9 contributes to ECM degradation and growth factor activation, either as a soluble protease or in the pericellular region by its interaction with cell surface receptors such as CD44 [11, 219, 220]. The range of substrates that are sensitive to MMP-9 activity is wide; not only can MMP-9 cleave gelatins and other matrix molecules, but also growth factors, cytokines, some membrane-bound proteins, and intracellular proteins [218]. MMP-9 can effectively induce angiogenesis, cell migration, and tumor growth [218]. The proteolytic activity of MMP-9 can make a contribution to tumor progression and angiogenesis, but our laboratory has previously described a non-proteolytic role of MMP-9 in tumor cell migration [123]. Dufour, *et al.*, showed that proMMP-9 (proteolytically inactive enzyme) can increase cell migration and this migration is mediated by the PEX domain [123]. Furthermore, development of inhibitory peptides and compounds directed against MMP-9's PEX domain abrogate homodimer formation and lead to a decrease in MMP-9-mediated migration [11]. In the following section, I outline preliminary data regarding the accumulation of MMP-9 dimers under hypoxic conditions, as hypoxia frequently occurs during tumor progression [221] and may exert pressure on MMP-9 expression and behavior.

1.3B RESULTS

Since MMP-9 dimers are known to contribute to cell migration, we investigated the possibility that MMP-9 dimers are affected by hypoxic conditions, as tumors are frequently under similar conditions. Under conditions of 1% oxygen, MMP-9 derived from stably expressing COS-1 cells appeared to form more higher molecular weight species as opposed to those under normal oxygen conditions (normoxia) based on gelatin zymography (Figure 20). In addition, cells exposed to hypoxia mimicking agents such as $CoCl_2$, were able to produce high molecular weight MMP-9 species. Not only is this phenomenon true for COS-1 stably expressing MMP-9, but also MDA-MB-231 cells (Figure 20).

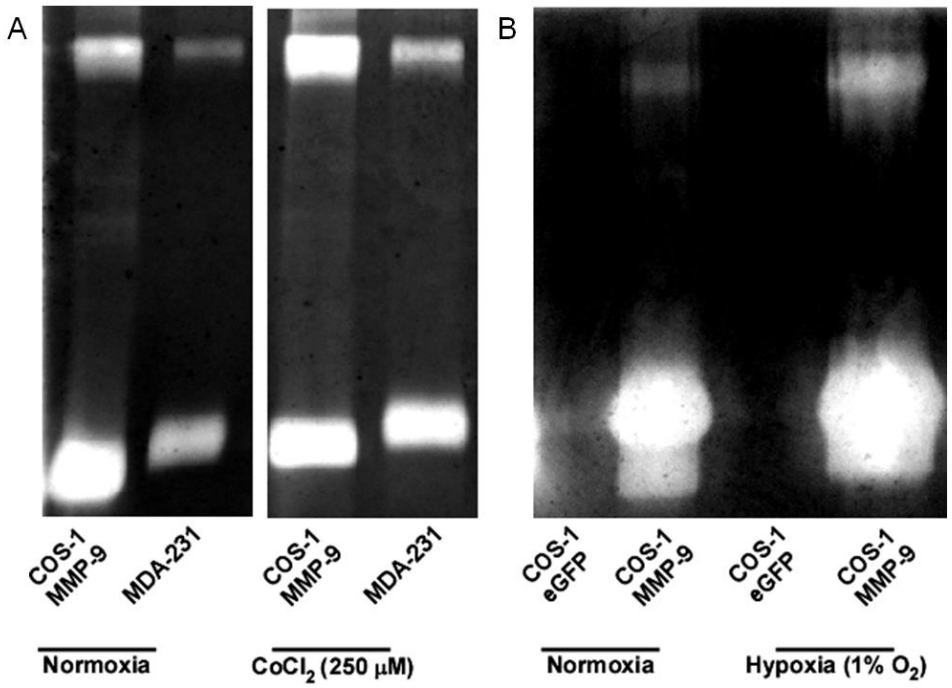

Figure 20: Hypoxia and hypoxia-mimicking conditions result in increased high molecular weight MMP-9. A) Gelatin zymography of conditioned media from either MMP-9 expressing COS-1 cells or MDA-231 breast cancer cells which express MMP-9 under hypoxia-mimicking conditions ($CoCl_2$) demonstrates there is increased high-molecular weight species of MMP-9 generated under hypoxia based on gelatin clearance. B) COS-1 cells stably expressing MMP-9 also generate high molecular weight species when exposed to hypoxic environment (1% O_2).

In order to determine whether these high molecular weight forms of MMP-9 were homodimeric or heterodimeric, as MMP-9 has been documented to bind to other soluble proteins [222-224], we collected MMP-9 samples from conditioned media of stably expressing COS-1 cells exposed to hypoxia. Conditioned media samples were exposed to gelatin-Sepharose beads and MMP-9 samples were isolated from the beads and electrophoresed through a polyacrylamide gel. After silver staining, the high molecular weight protein was isolated and LC-MS/MS (liquid chromatography-mass spectrometry/mass spectrometry) proteomic analysis was undertaken (Figure 21). Figure 21 lists the most abundant proteins, with MMP-9 appearing as the top hit, leading us to conclude that the high molecular weight species observed under hypoxia is likely an MMP-9 dimer.

Accession Number	Bio View:Identified Proteins (11)	Molecular	high band	low band
sp|P14780|MMP9_HUMAN	Matrix metalloproteinase-9 MMP9	78 kDa	98	68
SW_TRYP_PIG	SW_TRYP_PIG	24 kDa	37	46
sp|P04264|K2C1_HUMAN	Keratin, type II cytoskeletal 1 KRT1	66 kDa	43	41

Figure 21: Silver staining of isolated MMP-9 from conditioned media of hypoxia treated cells demonstrated high molecular weight species and the isolated high molecular weight band was identified as MMP-9 based on LC/MS-MS analysis.

Proteins mature as they travel through the endoplasmic reticulum (ER) and Golgi apparatus as part of the secretory pathway. In order to discern whether the high-molecular weight MMP-9 specie was forming intracellularly or extracellularly, we chose to use brefeldin A (BFA) to collapse the ER-Golgi transition [225]. BFA treatment of MMP-9 expressing cells under normoxia led to a decrease in secreted protein, as the secretory pathway was disrupted (Figure 22). A similar result was observed for cells under hypoxia mimicking conditions (Figure 22). Interestingly, cell lysates from those cells treated with BFA under hypoxia mimicking conditions demonstrated higher amounts MMP-9 dimer, even with disruption of the ER, suggesting that the dimerization of MMP-9 occurs in the ER (Figure 23).

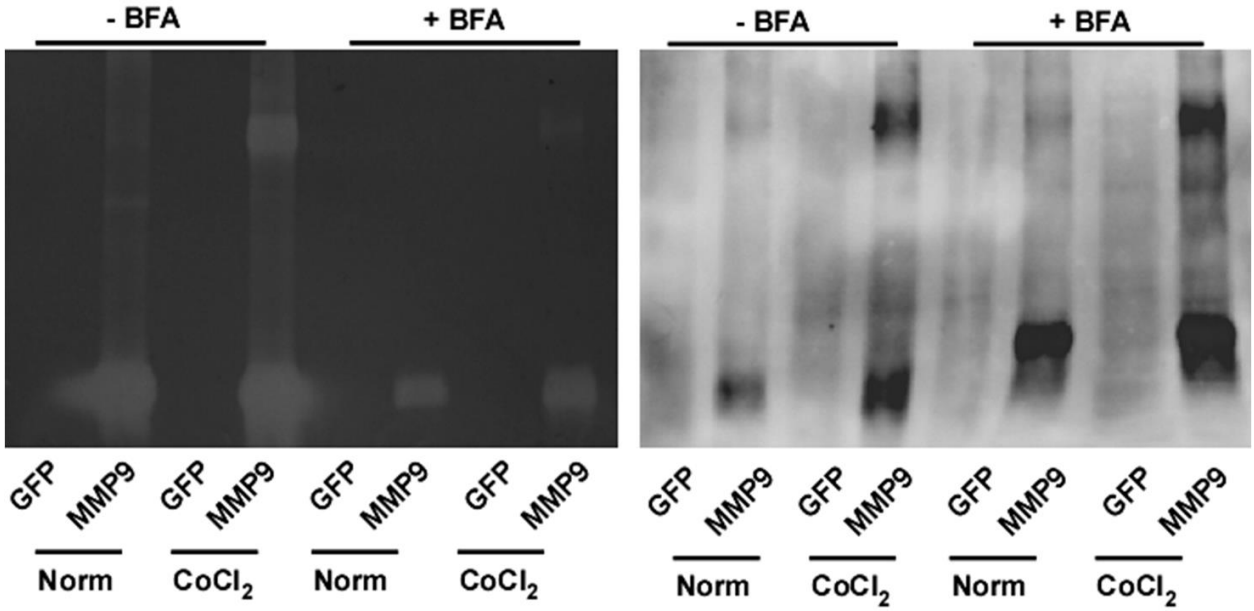

Figure 22: MMP-9 homodimers forming under hypoxia likely form within the endoplasmic reticulum. Collapse of the ER by use of BFA does not allow for secretion of MMP-9 and analysis of lysates on a non-reducing Western blot from $CoCl_2$, BFA-treated cells reveals high molecular weight MMP-9 species, suggesting MMP-9 dimers are forming under hypoxia within the ER.

In order to better define the nature of the MMP-9 dimer, we also compared the ability of MMP-9 expressing COS-1 to maintain MMP-9 multimers under denaturing conditions, as samples under gelatin zymography are not exposed to a denaturing agent. Cell lysates prepared in the presence of β-mercaptoethanol lose high molecular weight MMP-9, suggesting that the dimer is mediated via a disulfide link under hypoxic conditions (Figure 23), although there are conflicting reports on the nature of the dimerization of MMP-9 [226-228].

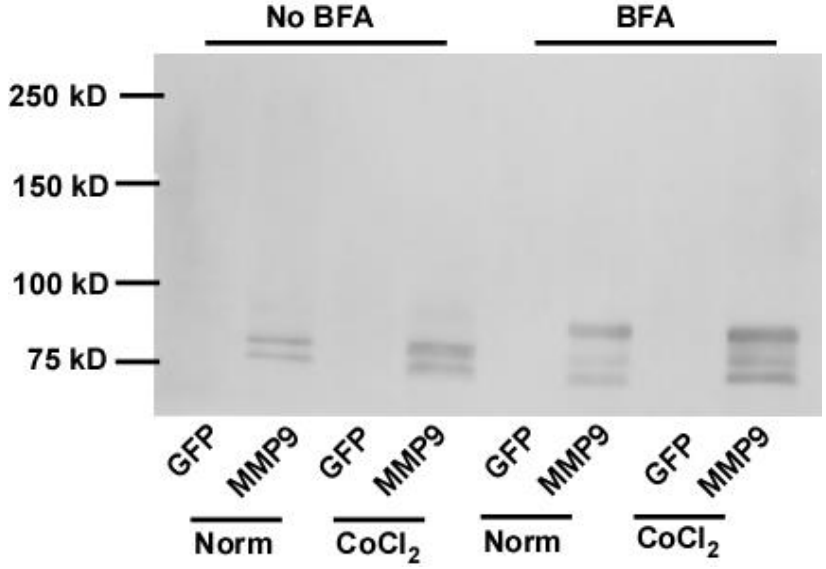

Figure 23: MMP-9 dimer formation under hypoxia is potentially mediated via a disulfide bond. Analysis of lysates from cells under normal and hypoxia-mimicking conditions under reducing, denaturing conditions results in loss of the high-molecular weight specie observed in non-reducing

conditions, suggesting that MMP-9 high molecular weight species are disulfide bonded MMP-9 molecules.

Since MMP-9 is an N- and O-linked glycosylated protein, we sought to determine whether or not protein glycosylation affects MMP-9 dimer formation under hypoxia, as it was previously reported that dimerization does not require glycosylation [227]. Exposure of MMP-9 expressing cells to an N-glycosylation inhibitor (tunicamycin) [229-231] still allows for MMP-9 dimer formation, as demonstrated by Figure 24.

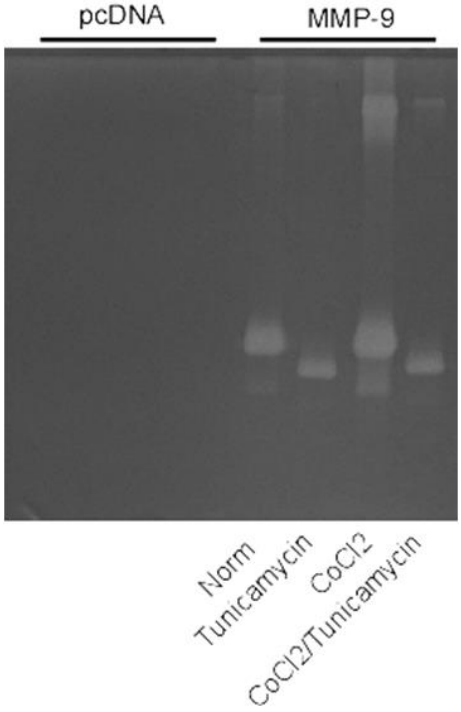

Figure 24: Treatment of MMP-9 expressing cells treated with tunicamycin to inhibit N-linked glycosylation still demonstrate formation of high molecular weight MMP-9 species under hypoxia-mimicking conditions. Gelatin zymography of conditioned media derived from COS-1 stably expressing MMP-9 demonstrates that lack of N-linked glycosylation may not play a role in mediating MMP-9 dimerization.

Unsuccessful attempts at using O-linked glycosylation inhibitors led us to explore whether or not domain mutants of MMP-9 were still capable of forming MMP-9_D under hypoxic conditions. Wild-type COS-1 cells were transfected with various MMP-9 mutants, including MMP-9ΔPEX and MMP-9ΔOG, since the PEX domain has been implicated in MMP-9 dimer formation previously [11, 123]. We used the MMP-ΔOG mutant in order to partially circumvent the use of a chemical inhibitor of O-linked glycosylation of MMP-9. Mutants of the O-glycosylation region (MMP-9ΔOG) had a reduced ability to form a high molecular weight species of MMP-9 (Figure 25).

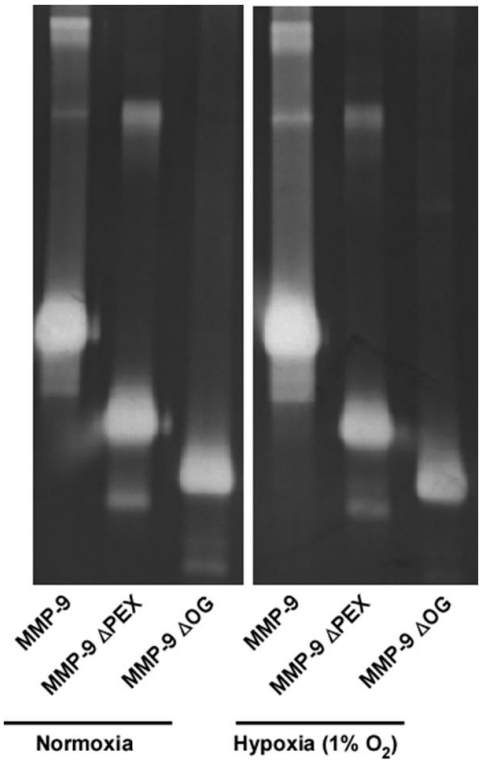

Figure 25: MMP-9 dimerization under hypoxic conditions may be mediated by the O-glycosylation domain. COS-1 cells overexpressing mutants of MMP-9, including the MMP-9ΔPEX and the MMP-9ΔOG, were exposed to normal or hypoxic conditions. Based on gelatin zymography, the MMP-9ΔOG mutant can no longer form high molecular weight species under hypoxia.

In order to determine any other influence on MMP-9 dimerization, we explored the ability of antioxidants to reverse MMP-9 dimer formation. Hypoxia and hypoxia-mimicking conditions result in intracellular changes in redox potentials. Radical species are copious under hypoxia and the change in redox and radical specie formation may be affected. This can physically damage proteins and interfere with proper disulfide bond formation; we postulated that there was potential that MMP-9_D forms because of an aberrant redox condition. Treatment of MMP-9 expressing cells with N-acetyl cysteine, an antioxidant, did not significantly affect MMP-9_D formation under hypoxia (Figure 26).

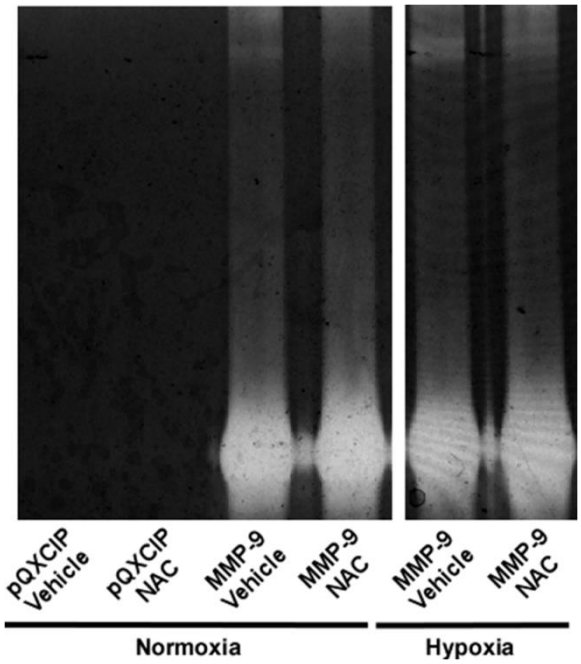

Figure 26: MMP-9 high molecular weight species can still form under N-acetyl cysteine treatment. Treatment with antioxidants to alleviate oxidative stress induced by hypoxic conditions did not serve to alter MMP-9 homodimerization. Gelatin zymography analysis indicates that high molecular weight MMP-9 is still produced in the presence of the antioxidant.

Relatedly, the possibility that protein disulfide isomerase (PDI) was playing a role in MMP-9 dimer formation was explored since PDI has been documented to mediate disulfide bonds, be upregulated under hypoxia and in invasive carcinoma, associate with MMP-9 in unique secretory vesicles in macrophages, and is required for proper MMP-9 function in other models [232-235]. There was more PDI protein present under conditions of hypoxia; pulldown of PDI with MMP-9 under hypoxia was unsuccessful (data not shown).

I next questioned whether MMP-9 dimer formation under hypoxia influenced cell migration. COS-1 cells overexpressing MMP-9 under hypoxia displayed a reduced ability to migrate, as compared to MMP-9 expressing cells under normoxia (Figure 27).

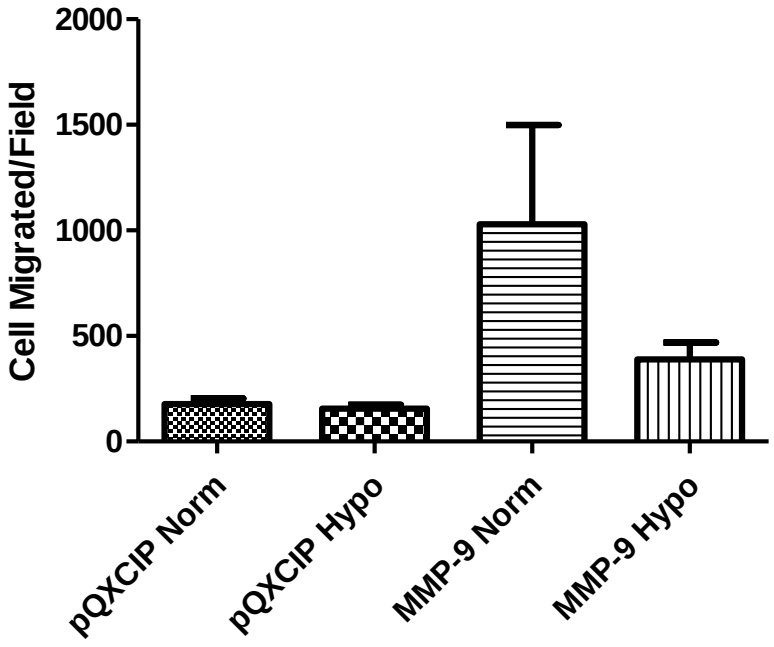

Figure 27: COS-1 expressing MMP-9 under hypoxia demonstrate reduced migration. Transwell migration assays reveal that stably expressing MMP-9 cells have reduced migration under hypoxic conditions as opposed to normoxia. Empty vector control cells demonstrate little migration.

Supporting the hypothesis that MMP-9_D formation under hypoxia is different than that under normoxia, we exposed HT1080 cells to either normoxia or hypoxia and used an MMP-9 PEX dimerization inhibitor (compound 2) [10]. HT1080 subject to a scratch wound assay demonstrated that compound 2 does not impede HT1080 migration under hypoxia (Figure 28). This suggests that the nature of MMP-9_D that forms under hypoxia may be chemically different than that of the dimer under normoxia, as HT1080 also generate MMP-9_D under hypoxia (data not shown).

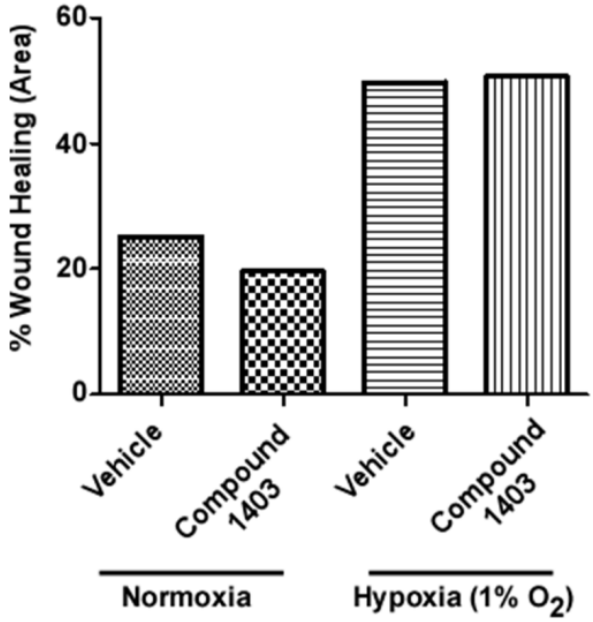

Figure 28: HT1080 cells exposed to hypoxia do not respond to treatment with compound 1403, a known PEX-mediated MMP-9 dimerization inhibitor. HT1080 ccell migration was assessed using a scratch wound assay under both normoxic and hypoxic conditions. Traetment with compound 1403 does not exert an inhibitor effect under hypoxia.

1.3C DISCUSSION

MMP-9 dimer formation has been shown to be crucial to migration, despite the proteolytic activity of MMP-9 traditionally being considered the impetus for MMP-9-mediated migration [11]. Formation of a homodimer of MMP-9 via the PEX domain contributes to cell migration [11], which is a crucial part of cancer cell invasion during various stages of metastasis. Accordingly, MMP-9 is associated with cancer progression and metastasis [236]. Here, I have shown that MMP-9 dimerization is increased under hypoxia. The dimer is reduction-agent sensitive, implying a disulfide bond mediates the interaction of the monomer components. Furthermore, the dimer forms intracellularly, specifically within the ER, without dependence upon glycosylation status. The dimer is not reversed under hypoxic conditions by use of an antioxidant and according to analysis of MMP-9 mutants, the OG domain is required for dimer formation under hypoxia. However, migration of MMP-9 expressing cells under hypoxia is dramatically reduced.

Olson, *et al.*, reported the dimerization of MMP-9 to occur intracellularly and independent of glycosylation [227], and our results are in agreement regarding the timing and nature of the dimer, even under hypoxia. The formation of dimer within the cell after collapse of the ER-Golgi transition using BFA implies that O-glycosylation is not required and dimer formation after use of tunicamycin excludes N-glycosylation as a pre-requisite.

It is interesting to consider that the nature of the dimer under hypoxia may be different than that of the dimer under normoxia. Previous data indicates the MMP-9 dimer that forms under hypoxia is mediated by the PEX domain and is required to enhance cell migration. In data presented herein, I have shown that the PEX domain mutant of MMP-9 can still form dimers, but the OG domain mutant has abrogated capacity to form dimers under both normoxia and hypoxia. This implies that the OG domain is responsible for dimer formation under hypoxia and supporting this idea, Collier *et al.*, identified a specific residue, Cys468, that is responsible for dimer formation and is located within the OG domain [237]. These authors demonstrate that a point mutation at this site prevents the ability of MMP-9 to form dimer, but suggest that this specie of dimer is related to misfolding of the enzyme [237]. Another piece of supporting data that the PEX domain may not be responsible for the MMP-9 dimer formation under hypoxia is that compound 1403 does not abrogate migration under hypoxia. Compound 1403 is an MMP-9 PEX domain specific inhibitor and has been investigated a cell migration inhibitor, as it can disrupt dimer formation [10].

Even more intriguing is the behavior of MMP-9 overexpressing cells under hypoxia. Lack of migration of MMP-9 expressing cells under hypoxia is counterintuitive; previous results indicate dimer formation is critical for MMP-9 mediated migration [11] and hypoxia is documented to induce cell migration [238]. It is possible that cell migration under hypoxia induced primarily by MMP-9, as in the case of COS-1 cells and MCF-7, is actually impeded. If the nature of the hypoxia-induced MMP-9 dimer is the disulfide-linked OG domain form, it is possible this dimer form would not induce efficient migration. It has been documented that there is differential activity of MMP-9 in the dimer form as compared to the monomer form. Collier *et al.* have shown that MMP-9 dimers are immobile on the surface of collagen fibrils and cannot interact as efficiently with the matrix molecule as compared to the monomer [237]. The authors suggest that the dimeric MMP-9 is immobile because of a higher affinity to the collagen due to

the engagement of both fibronectin-like domains simultaneously and lack the normal flexibility of MMP-9 when in the dimeric form [237].

Overall, many questions remain about the MMP-9 dimer formation under hypoxia. Hypoxia is a naturally occurring phenomenon in the tumor microenvironment. It exerts pressure on tumor cells and those cells respond accordingly. It may be important to consider that the hypoxic conditions may alter the behavior of not only the cells, but individual proteins. MMP-9 dimer formation appears to be affected by hypoxic conditions, with increased dimer formation potentially mediated through the OG domain as opposed to the PEX domain.

Future Directions

Considering available literature indicates that affinity for substrates by MMP-9 changes dependent upon dimer formation, it is of interest to assess whether or not MMP-9 generated by cells under hypoxic conditions can still cleave their substrates. MMP-9 can be isolated from conditioned media using Gelatin-sepharose beads and the MMP-9 activity against fluorescent substrates may be assessed, comparing the activity to that of normoxia isolated MMP-9. Additionally, in order to ensure that the Cys468 residue is mediating MMP-9 dimer formation under hypoxia, I have prepared primers to generate a Cys468 → Ala MMP-9 construct. Overexpressing this construct under normoxia and hypoxia would confirm whether this is the mechanism for MMP-9 dimer formation under hypoxia if there is a loss of enhanced dimer formation with this altered MMP-9. Furthermore, it is reasonable to use tagged MMP-9 constructs (HA-tagged and myc-tagged) to do a co-immunoprecipitation from hypoxia treated cells with and without compound 1403 to further confirm and define the nature of MMP-9 dimers under hypoxia.

1.3D MATERIALS AND METHODS

Materials

Brefeldin A, $CoCl_2$, N-acetyl cysteine, gelatin from bovine skin (type III), and tunicamycin were sourced from Sigma-Aldrich. Polyacrylamide was purchased from Roche and Coomassie blue was manufactured by Amresco. The hypoxia chamber is a Proox Model C21 from Biospherix (Lacona, NY). Compound 1403 and 6440 were obtained from Enamine, Ltd. The Chemicon anti-MMP-9 antibody was purchased from EMD Millipore.

Cell culture and treatment

COS-1, MDA-MB-231, MCF-7, and HT1080 were obtained from the ATCC (Manassas, VA). These cell lines were maintained in DMEM/high glucose medium supplemented with 10% FBS and 1% penicillin/streptomycin in a 37^{o}C, humidified incubator with 5% CO_2. Cells under hypoxic conditions were cultured in the same media, however they were incubated in a 37^{o}C, humidified incubator with 5% CO_2 and 1% O_2. $CoCl_2$ treated cells were incubated under normoxic conditions with 250 μM $CoCl_2$.

DNA Construction, transfection, and stable infection

MMP-9ΔPEX and MMP-9ΔOG plasmids have been reported previously [123]. Plasmid DNA was delivered to target cells using sodium chloride and polyethylenimine (PEI, Polysciences). In the case of stable infections, GP2-293 cells were transfected with either pQCXIP (vector control) or MMP-9/pQCXIP. In both cases, pVSVG was co-transfected with the target DNA for the purpose of viral infection of target cells. Titered media from GP2-293 was collected 48 hours after transfection and delivered to COS-1. After two subsequent infections and use of polybrene to enhance infection, positive cells were selected using puromycin treatment.

Gelatin zymography

Gelatin zymography was carried out as previously published [239]. Briefly, serum-free conditioned media samples were prepared with sodium dodecyl sulfate (SDS) loading buffer without a denaturing agent and run through a 10% PAG with 0.1% gelatin. The polyacrylamide/gelatin gel was then incubated at room temperature in 2.5% Triton X-100 to replace the SDS. The gel was then incubated at room temperature in a Tris-based incubation buffer (50 mM Tris-HCl, pH 7.5, 50 mM NaCl, 50 mM $CaCl_2$, 0.2% NaN_3) prior to an overnight incubation in fresh incubation buffer at 37^{o}C. Post-incubation staining of the gel was accomplished using Coomassie blue stain followed by destaining. Gelatinolytic activity corresponds to cleared areas in the gelatin.

Immunoblotting and silver staining

Protein lysates were prepared with loading buffer containing β-mercaptoethanol and boiled prior to electrophoresis in the case of reducing, denaturing western blots. For non-reducing conditions, β-mercaptoethanol was omitted from the loading buffer. Electrophoresis, transfer, and immunoblotting were performed as previously described [72] and all blots were developed using the BioRad ChemiDoc. Silver staining of MMP-9 samples was accomplished using the SilverQuest kit (Life Technologies, Grand Island, NY) according to manufacturer's instruction. Silver stained MMP-9 species were then analyzed by LC-MS/MS at the Stony Brook University Core Proteomics Facility.

Scratch wound assay

Cells were grown to confluence in the wells of a 12-well dish and serum starved to synchronize cell cycle with or without compound 1403 under hypoxic or normoxic conditions. A scratch wound was made following an overnight incubation in the serum free media. Cells were washed with PBS twice and complete media was placed on the cells with or without compound 1403. Cells were returned to their hypoxic or normoxic conditions overnight after taking time 0 bright field images using a Nikon Eclipse TE2000-S outfitted with a Sutter Instruments SmartShutter System and QiClick QImaging camera. Bright field images were also taken after 18 hours and the area calculations were made using the Nikon Elements Basic Research Software analysis tool. Time 0 and Time 18 areas were compared and percent change was calculated to determine the extent of cell migration.

Transwell migration

Transwell migration assays were performed as described [123], except nuclei were stained with Hoecst/PBS (1:2000) for at least 20 minutes and imaged using the microscope and analysis tools listed. Migrated cells on the membrane were counted using the Nikon Elements Basic Research Software.

Chapter 2: Repurposing the anti-psychotic trifluoperazine as an anti-metastasis agent

(This chapter will appear in Molecular Pharmacology for publication (03/2015) including co-authors: Jian Li, Carolina Zheng, Yiyi Li, Nengtai Ouyang, Basil Rigas, Stanley Zucker, and Jian Cao)

Since cancer cell invasion is a critical determinant of metastasis, targeting invasion is a viable approach to prevent metastasis. Utilizing a novel three-dimensional high throughput invasion assay, we screened a National Cancer Institute compound library and discovered compounds demonstrating inhibitory effects on cancer cell invasion. One hit, trifluoperazine, suppresses invasion of human cancer cell lines while displaying a limited cytotoxicity profile. This inhibition is due to the interference with cancer cell migratory ability, but not proteolytic activity. Treatment of cancer cells with trifluoperazine significantly reduces angiogenesis and prevents cancer cell invasion through a chorioallantoic basement membrane. Mechanistically, treatment results in decreased phosphorylated AKT (Ser^{473} and Thr^{308}) and β-catenin (Ser^{552}). Lack of phosphorylation of Ser^{552} of β-catenin prevents β-catenin nuclear relocation resulting in decreased expression of vascular endothelial growth factor, likely mediated through dopamine receptor D2. Taken together, we have demonstrated that trifluoperazine is responsible for reducing the angiogenic and invasive potential of aggressive cancer cells through dopamine receptor D2 to modulate the β-catenin pathway and propose that trifluoperazine may be used as an anti-metastasis chemotherapeutic.

2.1 BACKGROUND:

A. Target-based drug screening vs. phenotype-based drug screening

Target-based drug screening is based on information about disease mechanism and current treatments, but focuses only on particular molecules involved in the disease, disregarding the complex context in which the disease would manifest [240]. Compound libraries are screened only after a battery of tests are designed to examine the ability of the potential drugs to affect a chosen target that has been implicated in whichever disease is under investigation [240]. While the advent of the knowledge from the Human Genome Project and improvement in molecular technologies was predicted to propel the ability of researchers to successfully employ target-based drug screening, in reality the 'highly superior' work process of target-based screening did not deliver as expected [240]. Target selection is generally relegated to a certain class of molecules and the compounds chosen to pursue are only targeted to one member of the family; however, there are several diseases for which it is evident single-molecule targeting is not effective [240].

Phenotype-based drug screening, specifically regarding cancer, has the potential to circumvent limitations of targeted drug design. Unlike target-specific screening approaches, phenotypic screening involves the unbiased testing of compounds in cells or systems without knowing their targets and assaying for the desired cellular/systems effect [240]. These screening assays represent a practical approach to systems biology for drug discovery, because they directly measure disease-relevant cellular responses without the need for complex *in silico* models whose application to predicting human cell responses has been disappointing to date [240]. Two recent studies highlight reduced productivity by the pharmaceutical industry related to taking up a target-based drug screening mechanism for drug discovery; it has been reported that the majority of the first-in-class drugs approved by the FDA during the time period from 1999-2008 were identified via phenotypic screening and the attrition rate of drugs in the Phase I-III have been highest since the target-based drug discovery methods began to be utilized (early 1990s) [240-242]. However, while the end-result of phenotypic screening may be an increase in drugs making it to patients, phenotype-based screening is plagued by the challenge of characterizing the mechanism of action of drugs which are responsible for their pharmacological activity. This can be a time-consuming and arduous process.

B. Lack of drugs targeting cancer metastasis

Patients that present with metastatic cancers are largely considered incurable and those that have no evidence of dissemination will frequently relapse later [243], as they often harbor micrometastases that are not apparent at the time of diagnosis [3]. Local therapies designed to target primary tumors have improved, but are insufficient mechanisms by which to treat disseminated cancers [244]. This leaves a large gap in clinical treatments for cancer and there is a definite need to rapidly identify agents capable of inhibiting cancer metastasis. A strategy to combat metastasis includes pursuing drug development for compounds that can attenuate cell invasion and migration, as they are critical steps in the complex metastatic cascade [245]. The metastatic process was long considered a unidirectional event, with cells leaving the primary tumor at later stages of disease and colonizing distant organs. The course of metastasis has been redefined to include not only the distribution of cancer cells to secondary organs, but also the re-seeding and perpetuation of the established tumors by circulating cancer cells [244, 246]. Because a tumor can shed members of its cell population that can eventually replenish primary

and even secondary tumors, isolating novel compounds capable of inhibiting cell invasion will be an effective strategy for all stages of the disease.

Oncology is one of the largest areas of pharmaceutical research, making up a large portion of research and development. The complexity of cancer as a disease presents the major challenge to developing effective therapeutics, *i.e.*: those that kill or modulate those malignant cells while leaving normal cells unharmed [247]. While metastasis is often the reason for treatment failure, it is generally not an endpoint that is taken into consideration when evaluating potential anti-cancer drugs. Cancer drug development has traditionally focused on anti-mitotic effects of compounds, not anti-metastatic ones, but anti-mitotic drugs are only part of the mechanism by which to combat cancer. In order to address the lack of effective drugs targeting invasion and metastasis, we employed our three-dimensional (3-D) high throughput screen (HTS) to identify novel treatment agents. Screening drugs against cancer cells is generally done in a two-dimensional (2-D) format, assaying for cell proliferation and/or cytotoxicity on a flat surface. While this is an accepted method, it has become apparent that promising compounds identified via this strategy are not always as effective *in vivo* as would be predicted [248]. In order to increase the possibility for isolating drugs that will be efficacious in the clinic, use of a 3-D model is beneficial. A 3-D HTS format allows for monitoring of invasive behavior, not just 2-D migratory ability, and this format allows rapid screening of drugs in an *in vitro* setting that partially recapitulates *in vivo* matrix conditions and therefore *in vivo* cancer cell phenotypes, potentially increasing the likelihood of finding clinically efficient anti-invasive agents.

C. Drug Repurposing

Another potential mechanism by which to alleviate a lack of effective cancer drugs, in addition to rethinking the current drug discovery paradigm, is drug repurposing or repositioning. This term refers to the idea that currently known entities that are either on the market for another purpose or have otherwise made it through safety trials can be assessed for anti-cancer properties, effectively cutting down on the time and money it takes to get effective anti-cancer drugs to a patient [249]. These known molecular entities already have targets associated with their action and mechanisms for assessing biomarkers related to drug activity already exist [249]. Furthermore, absorption, distribution, metabolism, excretion, and toxicity (ADMET) data are usually already known, potentially all the way through Phase IV (post-market surveillance) safety data [250]. If one considers the normal drug discovery pipeline, drug approval can take up to 17 years with nine years devoted to initial steps such as target discovery and validation, screening design, and ascertaining ADMET properties alone [250]. Since repositioning of a chemical entity that has failed a clinical trial or is already FDA approved would have required these steps to be taken already, drug repositioning can reduce the process to less than ten years.

Taking into account that 95% of oncology drugs that make it to Phase I clinical trials fail to gain approval by the FDA, it may be wise to contemplate known drugs and compounds as novel tools in cancer treatment [249]. To make this point more clearly, "blockbuster drugs" from the early 1990s frequently have secondary indications unrelated to their primary indication and there is an assumption that secondary uses for any particular drug will increase in the future due to discovery of additional side-effects or mechanisms of action in separate disease classes [251]. It is estimated that repurposing drugs can improve Phase II success to 25% from 10% and Phase III success to 65% from 50% [252]. A host of drugs that are not currently indicated for

cancer treatment, in fact have anti-cancer properties. These drugs derive from vastly different classes of medications, including sedatives, non-steroidal anti-inflammatory drugs (NSAIDs), statins, immunosuppressants, anti-human immunodeficiency virus (HIV) drugs , and anti-microbial drugs [249, 250].

This particular idea has caught the attention of medicinal chemists and pharmacologists alike, but perhaps more importantly, the National Institutes of Health have taken up this strategy in an attempt to make the drug discovery process more successful and eventually improve current standards of care in various disease models [253]. After round-table meetings amongst those in both academia and industry, the NIH National Center for Advancing Translational Sciences (NCATS) introduced a program entitled "Discovering New Therapeutic Uses for Existing Molecules" (New Therapeutic Uses) in 2012 [254]. This program encourages partnerships between the pharmaceutical industry and academia, but its main goal is to take currently available drugs that have already undergone extensive development and screen them for potential roles in a host of diseases outside of their original purpose (NCATS Pharmaceutical Collection [NPC]). The main idea would be to have a molecule that is better studied than a totally new chemical entity and determine whether it has potential in alternate disease treatment and develop it from there. In this way, there is less likelihood that clinical trials designed for the disease of interest would fail early in the pipeline, as it already has been assessed for ADMET and safety. For this reason, it was of great interest to assess the ability of some of the known drugs in our compound library for action against the invasive behavior of cancer cells.

In this work, we set out to identify novel anti-invasion compounds by using our high-throughput, three-dimensional invasion assay. We screened the NCI-DTP compound library Diversity Set II and identified over 50 compounds with anti-invasive capacity. We chose one compound, trifluoperazine, to examine further. We identified that trifluoperazine may exert its anti-invasive capacity by antagonizing dopamine receptor D2 (DRD2) and modulating downstream signaling through Akt and β-catenin.

2.2 RESULTS:

Identification of compounds capable of inhibiting cancer cell invasion

To identify small molecule compounds capable of inhibiting cancer cell invasion, a novel 3-D high-throughput invasion assay was utilized to screen the National Cancer Institute's Developmental Therapeutics Program (NCI-DTP) compound library (Diversity Set II) against aggressive, androgen-independent PC3 human prostate cancer cells. This particular compound library includes 1,974 compounds and covers a wide variety of chemical structures. After incubating compounds (10 μM) with PC3 cells assembled in the 3-D invasion assay with type I collagen in a 96-well plate for 24 hours, invaded cells were quantified based on the number of cells that were able to escape the original cell-matrix dot and invade through the adjacent cell-free collagen. The positive hits were defined as any compound that impeded 50% of invasion compared to the DMSO vehicle control. Of the 1974 compounds screened, 84 compounds were found to inhibit invasion. To segregate the inhibitory hits from cytotoxic compounds, we analyzed the available GI_{50} data of those positive compounds from the NCI-60 human cell line screening dataset. We defined that compounds with a half maximal inhibitory concentration (GI_{50}) of more than 1 μM to be of interest and 56 compounds that we identified fit within this parameter (Figure 29A). One of the hits, trifluoperazine (TFP), is a Food and Drug Administration (FDA) approved antipsychotic drug. Since this hit is already clinically used as a well-tolerated, first line drug for patients in the acute phase of schizophrenia [255] (suggesting low systemic toxicity) and potentially has a novel function in inhibition of cancer cell invasion, the ability of TFP to impede cancer cell invasion and the working mechanism of this drug were further evaluated.

Validating TFP as an anti-invasion drug

To evaluate the potency of TFP, the dose dependent effects of TFP on cancer cell invasion were assessed. To determine if inhibition of cancer cell invasion by TFP is not relegated to prostate cancer cells, an additional cancer cell line, human fibrosarcoma HT1080 was assessed. The cancer cells were assembled in a 3-D collagen matrix similar to the PC-3 cells and exposed to increasing doses of TFP up to 10 μM. The HT1080 cells exposed to TFP demonstrated a dose-dependent decrease in invasive behavior as compared to vehicle control cells (Figure 29B and 29C). We continued to use HT1080 for the remainder of these experiments because of their highly aggressive, invasive nature.

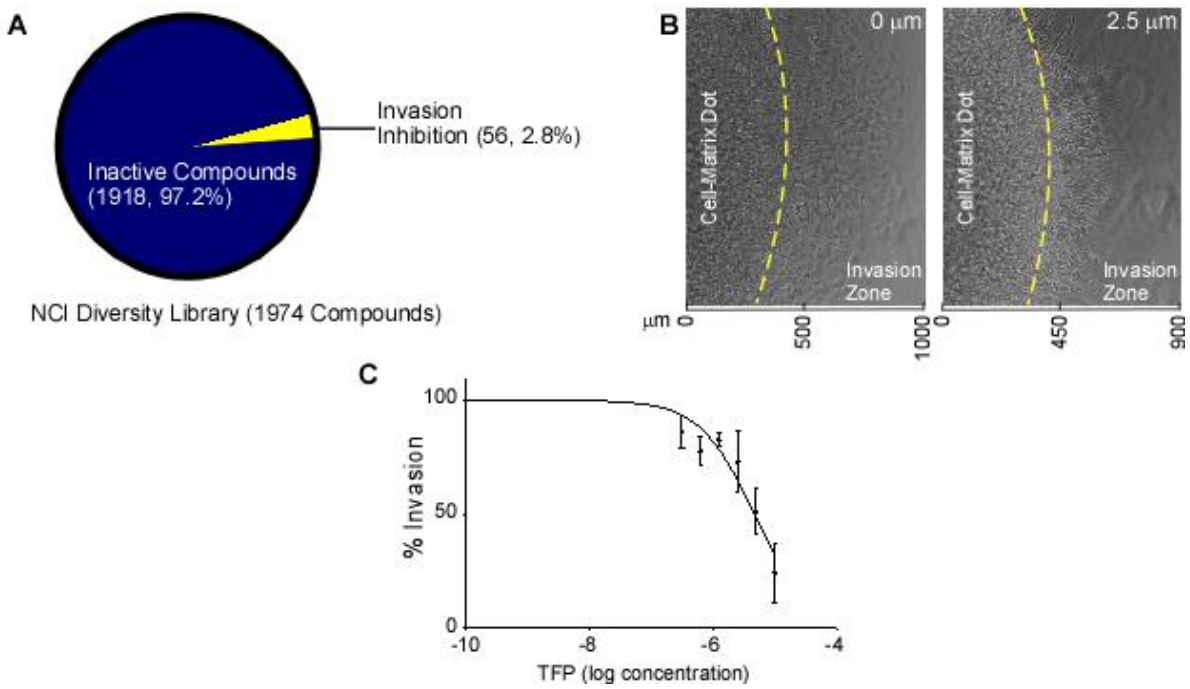

Figure 29: Identification of the new role of TFP on inhibition of cancer cell invasion. A) Classification of the compound library according to invasive ability. Of the 1974 compounds assessed, 63 of compounds were found to inhibit cancer cell invasion at 10 μM concentration, while inhibition of cancer cell invasion by another 21 compounds was due to cytotoxicity of the compounds. B) Representative bright field images of HT1080 cells in a 3-D invasion assay demonstrates TFP reduces cell invasion at 2.5 μM concentration as compared to vehicle control. Cells in the invasion zone were compared. C) Dose dependent inhibition of HT1080 cell invasion examined by the 3-D invasion assay in the presence of different doses of TFP for 18 hours.

To ensure that the inhibition of invasive behavior was not due to toxicity from TFP exposure, both normal fibroblasts (murine NIH/3T3) and HT1080 cells were analyzed for chronic (repeated exposures for 3 days) toxicity in the presence of increasing doses of TFP using an MTT viability analysis. The chronic cytotoxicity assay did not show any significant cell death (Figure 30A). Given the consideration that cells behave differently in two-dimensional (2-D) culture as opposed to 3-D culture in response to cytotoxic agents [256], cytotoxicity of TFP was also determined in the 3-D culture system in the presence or absence of TFP for 24 hours, followed by imaging-based determination of cytotoxicity using propidium iodide (PI). As negative and positive controls for cell death, cells embedded in collagen were also treated with DMSO alone or 1 μM staurosporine (STS), an apoptosis inducer, respectively. Induction of cell death by STS resulted in PI positive staining. Consistent with the 2-D MTT cytotoxicity assays, TFP did not cause cell death in the 3-D milieu (Figure 30B). Collectively these data indicate that the reduction in invasive capacity of cancer cells observed is not a result of cell death, but rather inhibition of the drivers of invasion.

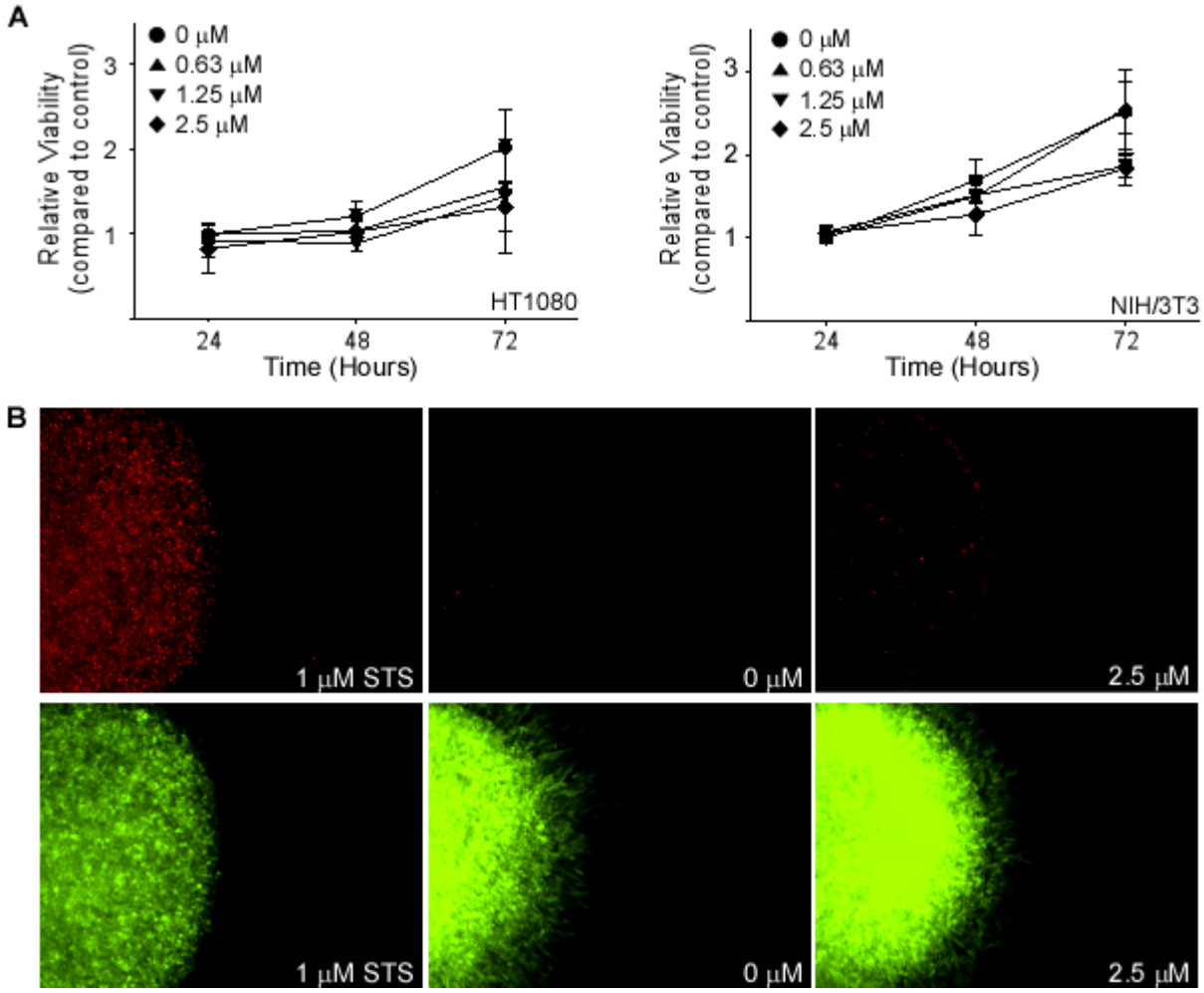

Figure 30: TFP does not induce significant cell death in either a 2-D or 3-D culture milieu. A) No significant effect by TFP on HT1080 (left panel) and NIH/3T3 (right panel) cell growth examined in a 2-D platform by MTT assay in the presence of different concentrations of TFP up to 72 hours B) TFP at 2.5 μM concentration does not cause HT1080 cell death as examined by propidium iodide staining in the 3-D invasion assay. Staurosporine (STS) serves as a positive control for cell death.

Inhibition of cancer cell migration by TFP without affecting global protease activity

Cancer cell migratory ability and proteolytic activity are two critical determinants of cancer cell invasion [257]. To determine which pathological process of cell invasion is interfered with by TFP, both cell migratory ability examined by transwell migration assays, scratch wound assays, and proteolytic activity examined by substrate degradation assays were assessed. PC3 cells and C4-2b cells are inhibited from migrating by TFP treatment based on transwell migration assay analyses (Figure 31A). HT1080 cells treated with TFP had significantly reduced migratory ability as compared to vehicle control (Figure 31B and 31C). Importantly, TFP had no effect on the migratory ability of the immortalized fibroblastic cell line NIH/3T3 (Figure 31B and 31C).

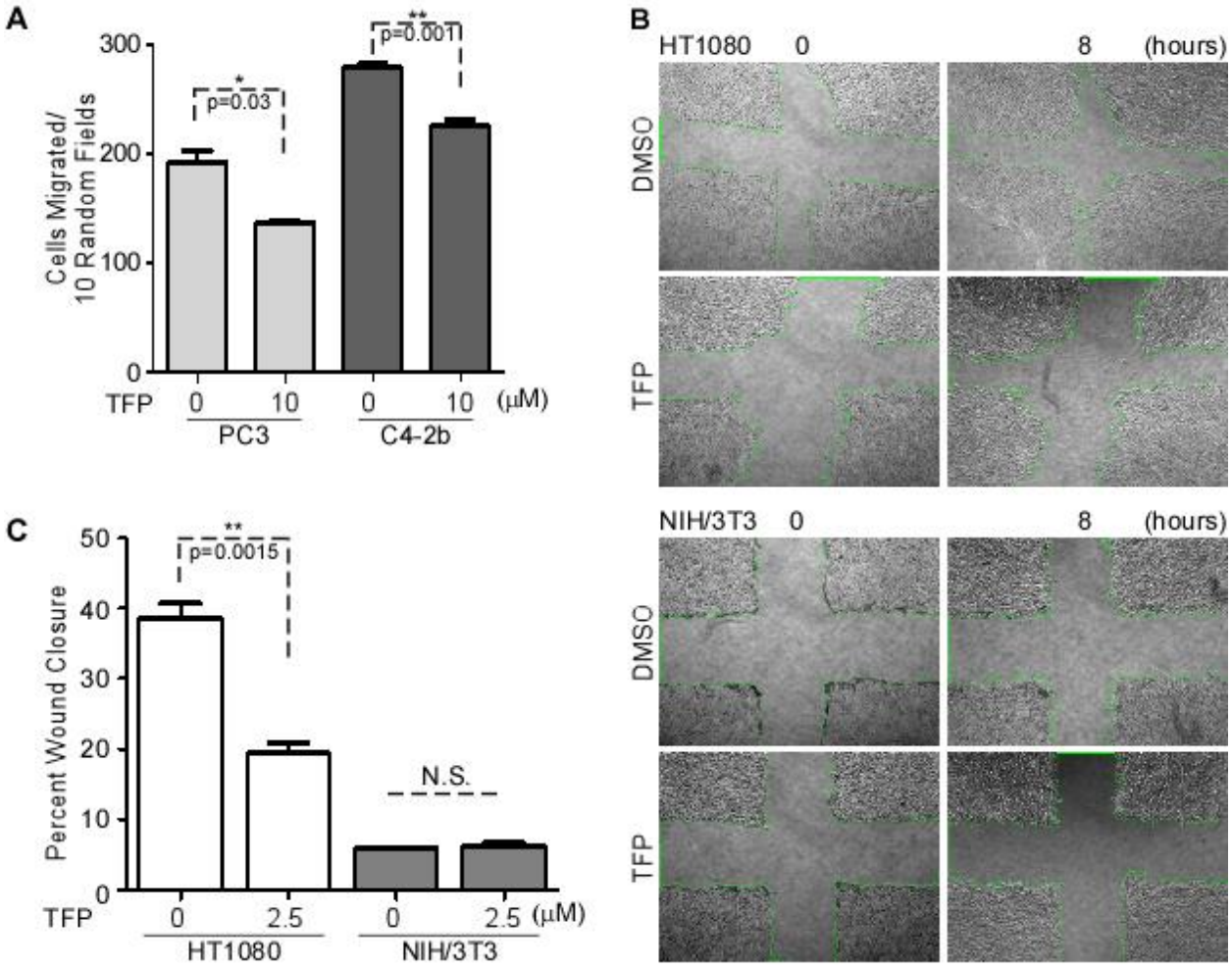

Figure 31: TFP inhibits cell migration amongst several cell lines. A) Transwell migration assays reveal inhibition of cancer cell migration among PC3 cells and C4-2b by TFP at 10 μM concentration. B and C) Treatment of HT1080 cells with TFP results in a significant decrease in cell migration based on wound healing analysis, while exhibiting no effect by TFP on NIH/3T3 wound closure. NIS-Elements imaging software was used for wound closure analysis. Representative images are shown.

In order to rule out the possibility that TFP interferes with the global proteolytic activity of the cells, a protease assay was employed to monitor enzymatic activity using a fluorescently-labeled general protease substrate. The cell lysate from HT1080 cells treated with increasing doses of TFP were incubated with fluorescently-labeled general protease substrate followed by analyzing substrate cleavage on a fluorescence spectrophotometer. Treatment of HT1080 cells with TFP had no significant effects on global protease activity at any dose as compared to DMSO control (Figure 32A). It has been demonstrated that HT1080 cells express a variety of matrix metalloproteinases, specifically MMP-2, -9, and -14, which have been correlated with migratory behavior [9, 123]. Gelatin zymography of conditioned media from HT1080 cells treated with TFP in increasing doses show no changes in MMP-2 or MMP-9 gelatinolytic activity from any group (Figure 32B). Since MMP-14 is a physiological activator of proMMP-2, our results suggest the possibility that TFP does not affect MMP-14 activity. Taken together,

these data suggest that reduction of cancer cell invasion by TFP is via inhibition of cell migratory ability, rather than protease activity.

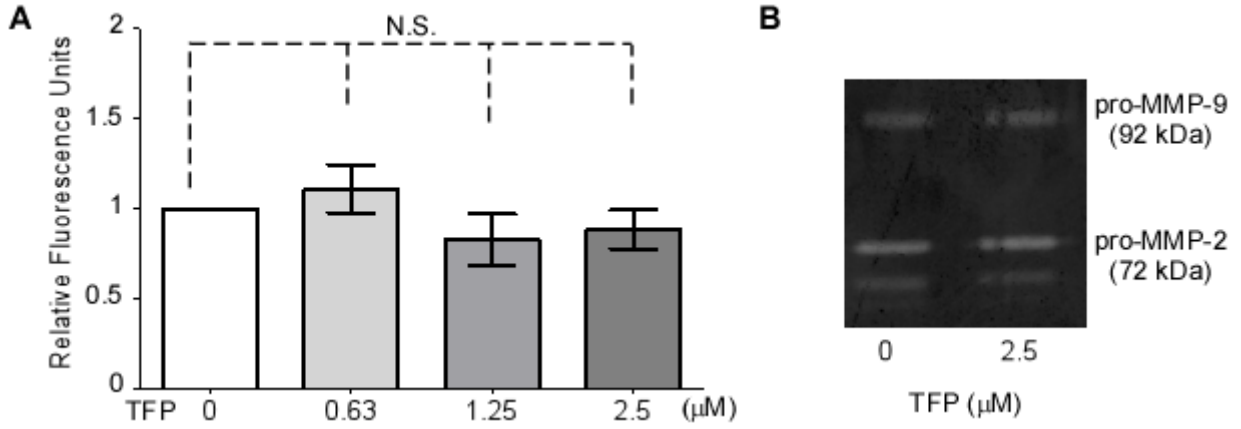

Figure 32: TFP does not cause alteration of proteolytic activity in treated HT1080 cells. A) TFP has no effect on HT1080 cell proteolytic activities as examined by a fluorescent substrate degradation assay. B) TFP treatment of HT1080 cells does not influence the expression of MMP-2 and MMP-9 and does not influence the activation of either of the gelatinases as observed in gelatin zymography.

Effects on angiogenesis and basement membrane invasion by TFP *in vivo*

Cell migration is essential to angiogenesis and invasion [258]. We next sought to determine if exposure to TFP of invasive cancer cells results in reduced angiogenesis and invasion through underlying basement membrane *in vivo*, by using the chicken chorioallantoic membrane (CAM) assay. HT1080 cells pre-treated with TFP were adsorbed to an inert sponge and implanted on the surface of CAM of chicken embryos. After a four day incubation, neovascularization induced by HT1080 cells significantly decreased in the presence of TFP as compared to DMSO controls (Figure 33A and 33B). This result is not due to TFP inhibiting endothelial cell migration, as human umbilical vein endothelial cells (HUVEC) treated with TFP had no change in network formation capacity (data not shown).

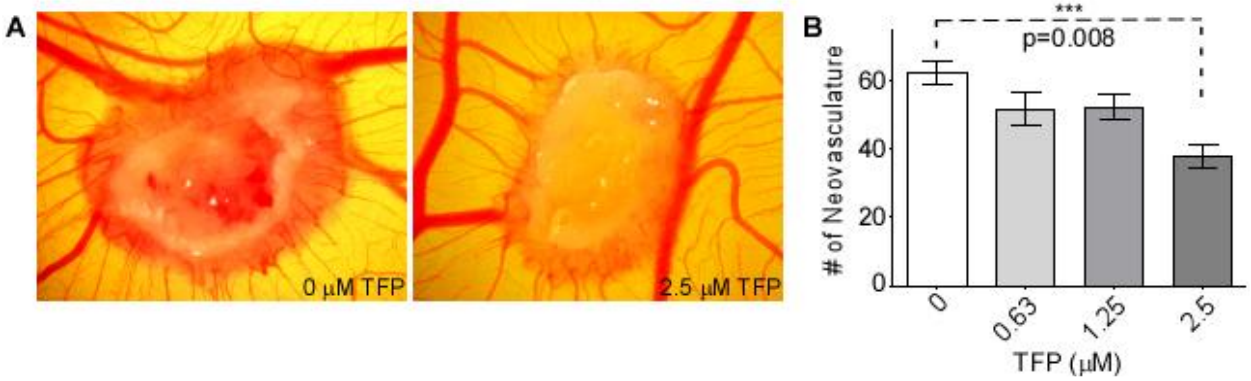

Figure 33: TFP reduces angiogenesis as examined by a chicken chorioallantoic membrane (CAM) assay. A) Representative image of a CAM assay demonstrates that treatment of HT1080 cells with TFP reduces the ability of those cells to induce angiogenesis. B) Quantification of neovasculature induced by HT1080 cells in the CAM assay. 2.5 μM treatment results in a significant decrease in angiogenesis.

In an effort to determine the mechanism of the TFP mediated reduction in angiogenesis, the effect of TFP on secretion of vascular endothelial growth factor (VEGF), a major soluble protein involved in vascular dynamics [259], was examined. Conditioned media from HT1080 cells treated with or without TFP was evaluated by enzyme-linked immunosorbent assay (ELISA) to quantify secretion of VEGF. The conditioned media collected from HT1080 cells treated with TFP demonstrated a decreased amount of soluble VEGF in a dose responsive fashion (Figure 34A). This data suggests that TFP is able to inhibit the production of VEGF, leading to a decrease in angiogenesis *in vivo*.

To directly examine if TFP is capable of inhibition of cancer cell invasion through basement membrane *in vivo*, the CAM invasion assay was employed. The CAM consists of the chorionic epithelium and underlying allantoic membrane that is primarily made of type IV collagen [260], which simulates the basement membrane of human epithelium [261]. Invasion of cancer cells through the epithelium and basement membrane of the upper CAM into connective tissue was examined by hematoxylin and eosin (H&E) staining. DMSO-treated HT1080 cells that were loaded into 2 mm diameter plastic rings over the CAM invaded into the connective tissues through the breached basement membrane. In contrast, TFP-treated HT1080 cells failed to cross through the basement membrane. Instead, the TFP-treated cells only grew on the top of the CAM (Figure 34B). This reduction in invasion, along with the decrease in angiogenesis, suggests that TFP is effective at inhibiting invasion *in vivo*.

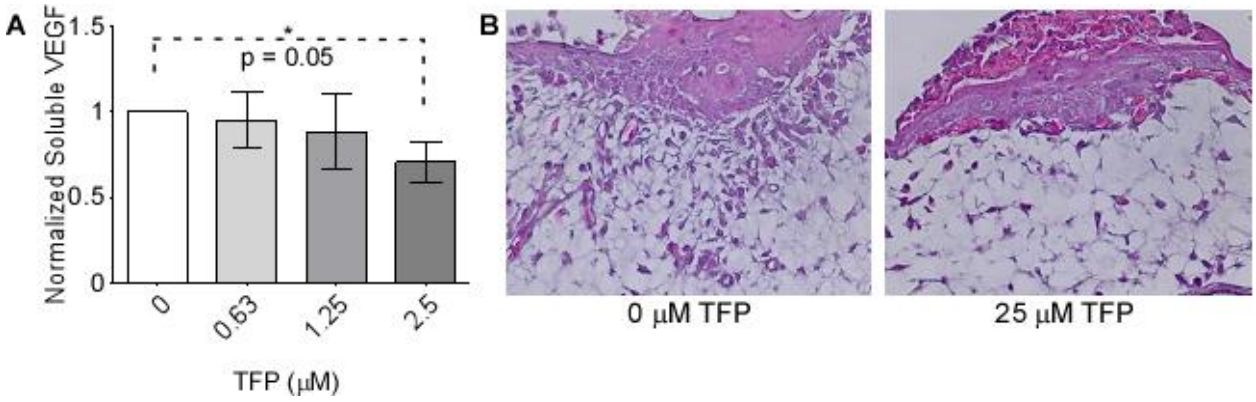

Figure 34: TFP treatment of HT1080 cells reduces VEGF secretion and invasion through basement membrane in the CAM assay. A) TFP treatment reduces soluble VEGF. HT1080 cells treated with various doses of TFP demonstrate a reduction in VEGF expression as determined by VEGF ELISA. B) H&E staining of a tissue section collected from the CAM assay shows that HT1080 cells implanted on the CAM surface can invade through the underlying membrane whereas TFP treatment reduces the ability of these cells to invade, but continue to grow.

Dissection of the mechanism of TFP-inhibited cell migration via a cascade of DRD2, Akt and β-catenin

To aid in determining the molecular mechanism by which TFP reduces cancer cell invasive ability, antibody microarrays (Kinexus) were employed using HT1080 cells treated with or without TFP. These arrays simultaneously detected the presence and relative quantities of over 500 pan-specific and over 300 phospho-site specific antibodies by comparing the relative signal from lysates derived from treated and untreated cells (Table 2).

Target Protein Name	Phospho Site (Human)	Z-ratio (HT1080TF, HT1080D)
Erk1 (MAPK3)+ Erk2 (MAPK1)	Pan-specific	2.36
NFkappaB p65	S536	1.94
Trail	Pan-specific	1.55
PKCg	T655	1.53
eIF4E	Pan-specific	1.50
STAT2	Pan-specific	1.45
Smad2	S467	1.43
Paxillin 1	Y118	1.38
PKCg	T514	1.37
Src	Pan-specific	1.36
PKCl/i	T564	1.33
Jun	Pan-specific	1.28
SOCS2	Pan-specific	1.21
S6Kb1	Pan-specific	1.17
LAR	Pan-specific	1.17
STAT3	Pan-specific	1.16
Hsp27	S82	1.08
RSK1/2	S380/S386	1.04
NBS1	S343	-1.00
MEK1/2 (MAP2K1/2)	Pan-specific	-1.01
CDK1 (CDC2)	Pan-specific	-1.01
ACK1	Pan-specific	-1.01
c-IAP1	Pan-specific	-1.02
JAK2	Pan-specific	-1.04
Erk1 (MAPK3)+ Erk2 (MAPK1)	Y204	-1.07
IkBb	Pan-specific	-1.08
Jun	S73	-1.09
IRS1	Y1179	-1.14
Cdc25C	Pan-specific	-1.14
AIF	Pan-specific	-1.17
Cofilin 2	S3	-1.23
CDK2	Pan-specific	-1.24

Catenin b1	Pan-specific	-1.25
CDK6	Pan-specific	-1.32
CDK1 (CDC2)	Pan-specific	-1.33
MEK2 (MAP2K2)	T394	-1.45
PTEN	S380+T382+S385	-1.50
DDIT3(CHOP)	Pan-specific	-1.88
Dab1	Y198	-1.93
PTP1D	Pan-specific	-2.82

Table 2: Short-list of top hits from the Kinexus Antibody Microarray comparing vehicle-treated control cells to trifluoperazine treated cells. Those proteins whose microarray intensity increased compared to control under trifluoperazine treatment are listed in pink. Those whose intensity decreased after treatment are listed in blue.

The data from the antibody array was analyzed using the DAVID bioinformatics program [262, 263]. Input of the top hits from the antibody array into the DAVID program identified potential pathways involved, including the focal adhesion kinase pathway and the β-catenin pathway. Given the ability of each of these pathways to influence cell migration, we attempted to validate each pathway to determine the mechanism of action of TFP in inhibition of cancer cell migration. Considering that glycogen synthase kinase-3 (GSK-3) plays a role in the turnover of β-catenin as part of the destruction complex for β-catenin, the phosphorylation state of GSK3-β and phosphatase and tensin homolog (PTEN) were assessed. PTEN can negatively regulate protein kinase B (Akt), which can exert effects upon GSK3-β [264]. Based on western blotting, GSK3-β undergoes no increase in phosphorylation at Ser9 (Figure 35), which is usually indicative of inactivation [264]. There is no significant changes in phosphorylation state of PTEN (Ser380) (Figure 35), which suggests that there is likely no change in PTEN stability, discounting this molecule as a key player in the changes observed upon TFP treatment.

Upon further analysis, we found that treatment with TFP reduces the phosphorylation of β-catenin at Ser^{552} in HT1080 cells, while NIH/3T3 cells, which do not respond to TFP treatment in terms of cell migratory ability, exhibit no change in p-β-$catenin^{Ser552}$ (Figure 36A). This particular phospho-site has not been documented to be acted upon by GSK3-β. Ser^{552} phosphorylation of β-catenin is associated with β-catenin stabilization and subsequent translocation to the nucleus for transcription of downstream targets, some of which are associated with invasive behavior and angiogenesis [265, 266]. Accordingly, immunofluorescent staining of HT1080 cells with anti-p-Ser^{552}-β-catenin antibody resulted in significant nuclear staining of p-β-catenin in HT1080 cells treated with DMSO control. In contrast, HT1080 cells treated with TFP displayed decreased p-Ser^{552}-β-catenin in the cytoplasm and nucleus (Figure 36D). This decreased phosphorylated β-catenin was accompanied by reduced β-catenin activity examined by a TOPflash reporter luciferase assay (Figure 36B).

Since active Akt has been reported to phosphorylate β-catenin at Ser^{552} for nuclear translocation and subsequent interaction with the T-cell factor and lymphocyte enhancer factor (TCF/LEF) transcription factors [265], Akt phosphorylation at Ser^{473} and Thr^{308} was examined by Western blotting using anti-p-Akt^{Ser473} and anti-p-Akt^{Thr308} antibodies, respectively. When

HT1080 cells were treated with TFP for 24 hours, Akt phosphorylation at both phospho- sites was decreased, suggesting that TFP suppresses activity of Akt and therefore was unable to activate β-catenin through its kinase activity (Figure 36C).

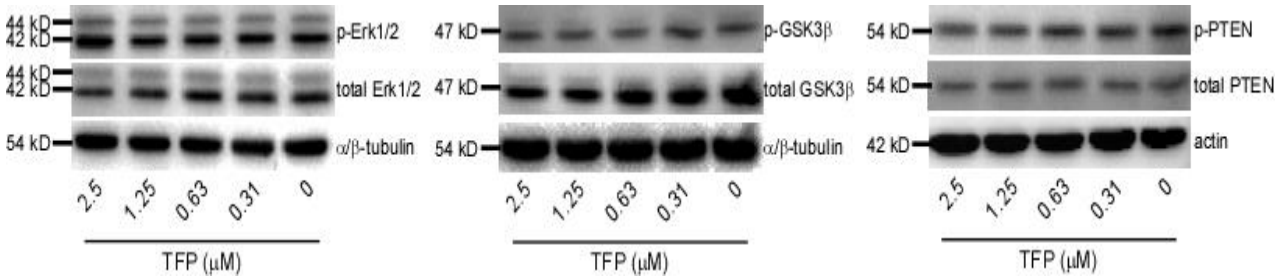

Figure 35: TFP does not modulate the phosphorylation of Erk1/2, GSK3-B, and PTEN. HT1080 lysates exposed to various doses of TFP overnight do not demonstrate any significant changes in phosphorylation of either Erk1/2, GSK3β, and PTEN.

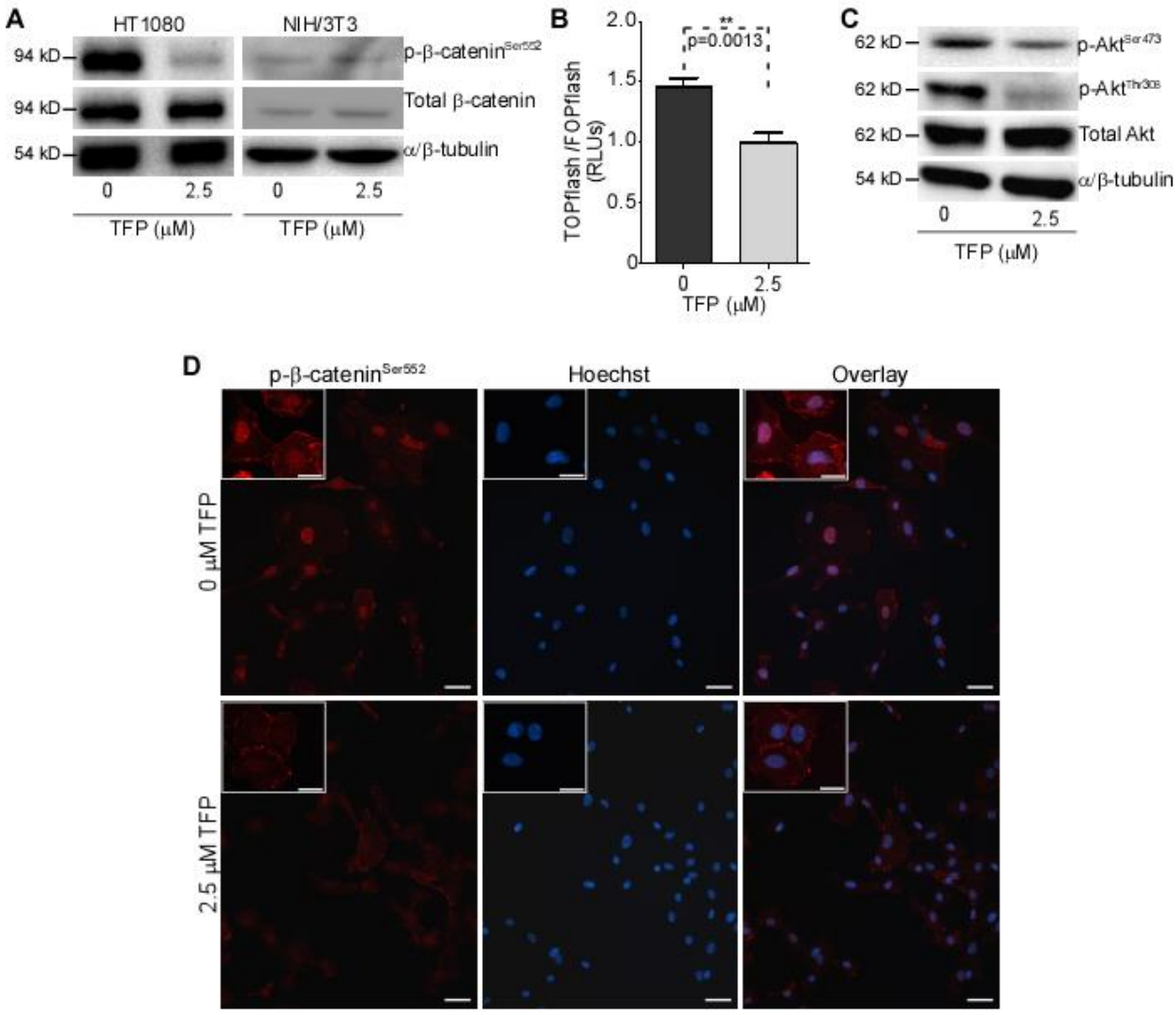

Figure 36: TFP treatment of HT1080 cells results in a decrease in phosphorylated β-catenin^{Ser552}, AKT^{Ser473}, and AKT^{Thr308}. A) Western blot analysis of HT1080 lysates show that TFP treatment results in a decrease in p-β-catenin^{Ser552}, while there are no changes in TFP-treated NIH/3T3 cells. Total β-catenin and α/β tubulin were used as controls. B) TFP treatment of HT1080 cells reduces the transcriptional activity of β-catenin as assessed by TOPflash/FOPflash luciferase activity, expressed in relative luciferase units (RLUs). C) Decreases of phosphorylated AKT in HT1080 cells treated with TFP (2.5 μM) for 18 hours examined by Western blot using anti-phospho-AKT^{Ser473} and AKT^{Thr308} antibodies, respectively. Total AKT and α/β-tubulin were used as controls. D) Immunofluorescent staining of HT1080 cells treated with TFP shows decreased nuclear p-β-catenin^{Ser552} staining as compared to vehicle control using anti-phospho-β-catenin antibody. Nuclei were stained by Hoechst. β-catenin staining and nuclear staining were superimposed (Overlay) Bar = 50 μm. Enlarged representative images are shown in the inserts. Bar = 20 μm

TFP effectiveness as an antipsychotic derives from its ability to abrogate dopamine receptor D2 (DRD2) activity [255]. To determine if TFP-reduced cell migration is working through DRD2, we first surveyed DRD2 expression in cell lines that differentially respond to TFP treatment. Employing a real-time PCR approach, we observed that HT1080 cells demonstrate higher expression of DRD2 as compared to NIH/3T3 cells (Figure 37A). Interestingly, NIH3T3 cells do not respond to TFP treatment in terms of inhibition of cell migration (Figure 31C). To further extend and determine whether inhibition of cell migration by TFP is through antagonistic effects on DRD2, we used an aiRNA interference approach to downregulate DRD2 expression in HT1080 cells. Effective downregulation of DRD2 was achieved using DRD2 aiRNA in HT1080 cells demonstrated both at the mRNA and protein levels (Figure 37B and 37C). By the functional study in terms of cell migration, silencing DRD2 in HT1080 cells results in a decrease in cell migration as compared to controls (Figure 38A). Since TFP affects protein phosphorylation status of β-catenin^{Ser552} and Akt^{Thr308} (Figure 36A and 36C), we additionally measured these protein phosphorylation status in DRD2-silenced cells. By Western blotting using corresponding antibodies, those HT1080 cells with knockdown of DRD2 demonstrate a reduced level of p-β-catenin^{Ser552} and p-Akt^{Thr308} (Figure 37D and 37E), further confirming that TFP-reduced cell migration is through antagonistic effects on DRD2.

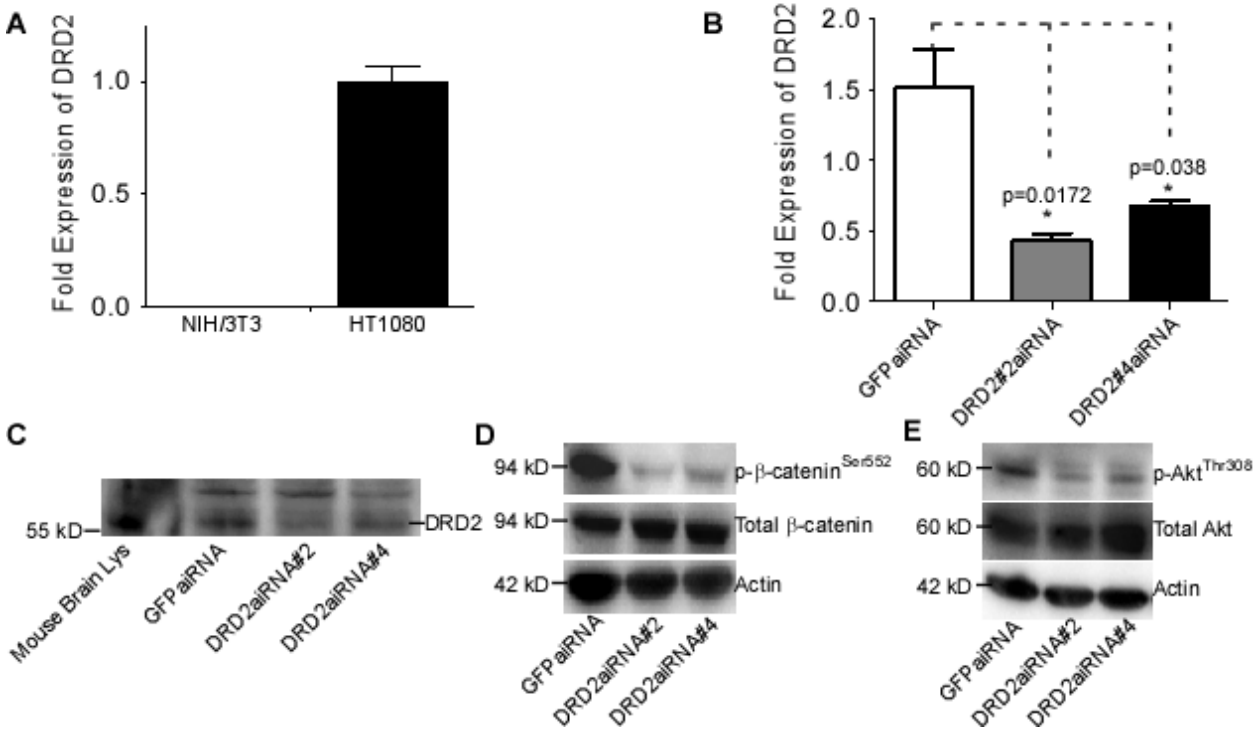

Figure 37: Knockdown of DRD2 results in decreased phosphorylated β-catenin^{Ser552} and AKT^{Ser473} A) Real-time RT-PCR analysis of NIH/3T3 and HT1080 cells reveals that HT1080 cells express a relatively high level of DRD2 mRNA as compared to NIH/3T3. The HPRT housekeeping gene was used as a normalization control. The experiment was repeated three times. B) Silencing of DRD2 by validated aiRNAs in HT1080 cells examined by real-time RT-PCR. The HPRT housekeeping gene was used as a normalization control. The experiment was repeated three times. C) aiRNA knockdown of DRD2 results in less DRD2 expression examined by western blot using an anti-DRD2 antibody. Mouse brain lysate was used as a positive control and non specific bands were used as loading control. D) Knockdown of DRD2 results in decreased p-β-catenin^{Ser552} as demonstrated by western blot analysis using an anti-p-β-catenin^{Ser552} antibody. Total β-catenin and β-actin were used as controls. E) p-AKT^{Thr308} is reduced when DRD2 is knocked down in HT1080 cells examined by western blotting using anti-p-AKT^{Thr308} antibody. Total AKT and actin were used as controls.

To further support the idea that DRD2 antagonism is the cause of these molecular changes, we treated HT1080 cells with haloperidol, another FDA approved antipsychotic known to inhibit DRD2 followed by Western blotting analysis. Consistent with TFP treatment, cells treated with haloperidol display reduced p-β-catenin^{Ser552} (Figure 38B). In addition, HT1080 cells treated with haloperidol demonstrated reduced migration when assessed via scratch wound, similar to those treated with TFP (Figure 38C and 38D). These data reinforce our conclusion that TFP-reduced cell migration is primarily through antagonistic effects on DRD2, while inhibition of alternate targets of TFP, such as calmodulin or multi-drug resistance [MDR] gene products, may not be the primary cause of a reduction in p-β-catenin^{Ser552}, p-AKT^{Thr308}, and p-AKT^{Ser473}. Collectively, our data shows that DRD2 is likely the direct target of TFP and inhibition of cell migration by TFP is via a DRD2-AKT-β-catenin network that ultimately modifies migratory behavior.

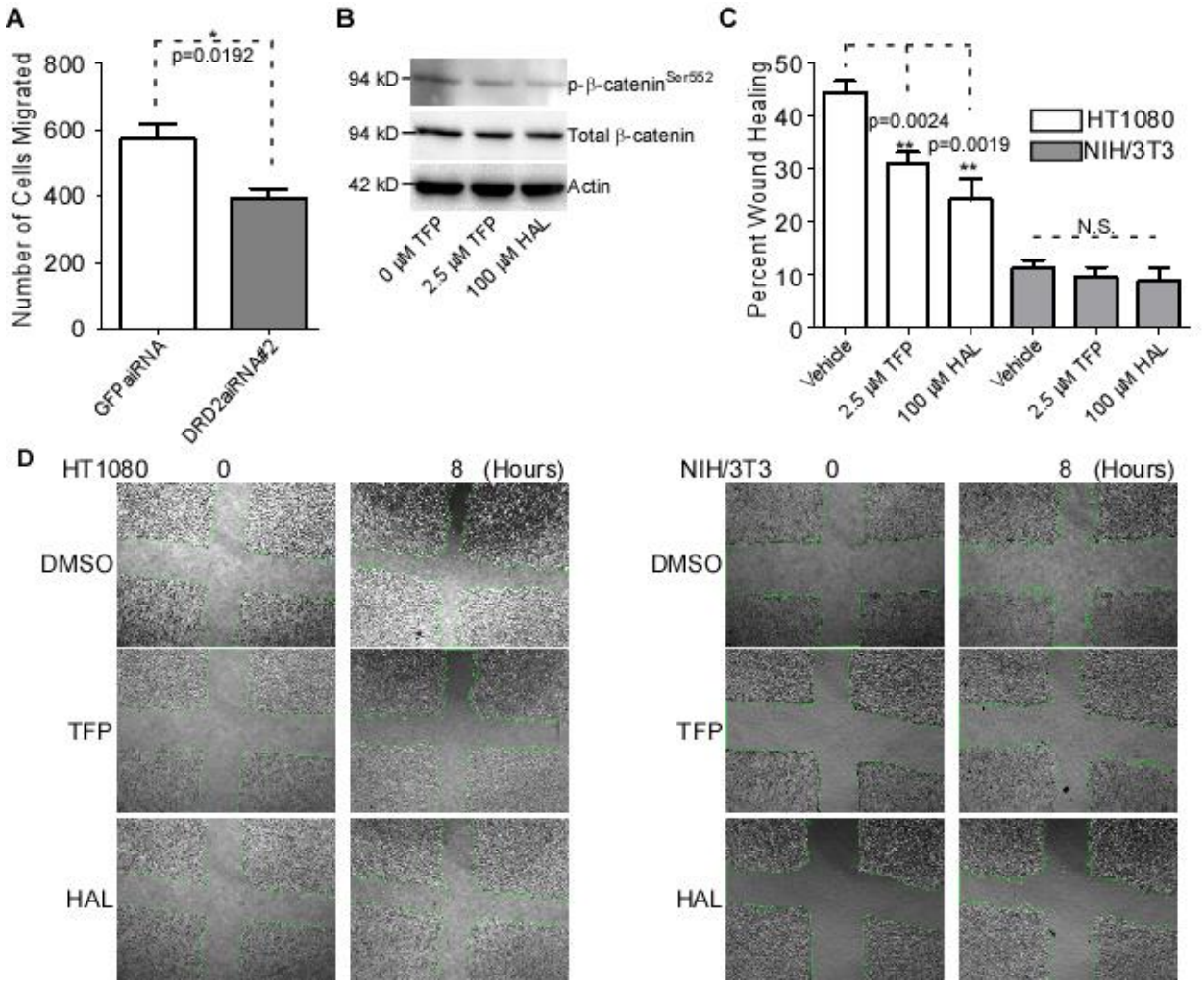

Figure 38: Knockdown of DRD2 results in decreased cancer cell migration and inhibition of DRD2 with an alternative antagonist results in decreased migration A) Knockdown of DRD2 results in reduced cancer cell migration in HT1080 cells examined by a 2-D dot cell migration assay. B) Haloperidol, as well as TFP reduced p-β-catenin^{Ser552}, examined by western blotting analysis using an anti- p-β-catenin^{Ser552} antibody. Total β-catenin and β-actin were used as controls. C) TFP and haloperidol decrease HT1080 cell migration as demonstrated by a wound healing migration assay. There are no effects on NIH/3T3 cells. The experiment was repeated three times. D) Representative images of wound healing in HT1080 and NIH/3T3 untreated, TFP-treated, and haloperidol-treated cells.

2.3 DISCUSSION

Unlike other conventional high throughput screening assays for anti-cancer invasion drug discovery that used biochemical assays for targeting proteolytic activity or various 2-D migration assays for targeting cancer cell migratory machinery, our unbiased 3-D screening platform has the capacity to mimic *in vivo* conditions of cancer invasion for identification of compounds that efficiently inhibit cancer cell invasion. Utilizing this novel 3-D high throughput invasion assay, we identified TFP, an FDA approved antipsychotic drug, which was efficient at attenuating cancer cell invasion through a DRD2-AKT-β-catenin network without causing significant cell death, as a drug for preventing cancer metastasis. Our data highlight a new potential treatment strategy by use of an old drug against cancer progression.

The cancer drug discovery process has traditionally focused on identifying cytotoxic agents in lieu of compounds that reduce the mobile phenotype of invasive cancer cells. While highly effective in some hematologic malignancies, the tumor-shrinkage paradigm is not curative for most advanced solid cancers. This important point indicates that a phenotype based screening program targeting cancer invasion has the potential to yield effective, less-toxic drugs. Utilizing the high-throughput 3-D invasion assay developed in our laboratory [8], Diversity Set II from the NCI collection was screened for compounds that target cancer cell invasion, a critical determinant of cancer metastasis. Based on our initial screening, TFP is found to be effective at reducing invasion without notable cytotoxicity, as evidenced not only by the *in vitro* data presented here, but also by its wide clinical use and tolerable side effects.

Our findings may have implications for a novel treatment strategy in patients with cancer. Not only is TFP safe when administered alone to patients, but it has been shown to be safe in combination with some traditional chemotherapies [267, 268]. Evidence exists that TFP is a potent calmodulin inhibitor and can contribute to potentiation of cytotoxic actions of traditional chemotherapeutics *in vitro* and *in vivo* [269, 270]. We currently propose that TFP is a valuable tool specifically for prevention of metastases. In support of this idea, a retrospective study indicates that cancer patients that were incidentally taking calcium channel antagonists, including TFP, for several months during their treatments had delayed disease progression and increased survival rates [271]. The work presented here suggests that TFP has great potential because of its ability to reduce cancer cell invasion and tumor angiogenesis as a single agent in some cases, not necessarily related to potentiating chemotherapeutic effects or reversal of multidrug resistance or calmodulin inhibition.

The angiogenesis data presented here demonstrate that TFP can have far-reaching effects, even in an *in vivo* context. Our use of 25 μM concentration of TFP *in vivo* is justified in that the volume that contained TFP and tumor cells was small compared to the volume of the entire chicken embryo and there is an assumption that diffusion through the fluids in the chicken embryo reduces local concentrations of TFP during a four day incubation period. Furthermore, the TFP concentration in the CAM assay shows no sign of cytotoxicity, as there is a mass of cells that grow atop the basement membrane during the length of the experiment even with higher concentration TFP exposure. Finally, there are reports that identify patient plasma levels of TFP in the range of 2-36 μM [268], placing our chosen higher concentration within a clinically relevant range.

Previous studies have demonstrated that the effect of TFP on neurological diseases is via antagonism of DRD2 [255]. We postulate based on the data herein that the reduction in phosphorylated β-catenin and Akt is a result of inhibition of DRD2. DRD2 is a seven transmembrane domain, G-protein coupled receptor that is highly expressed in certain parts of the central nervous system, particularly the striatum, and in vasculature and the retina, amongst other organs [272]. Over several years, evidence that dopamine receptors are expressed in cancerous cells outside the nervous system has been increasing. DRD2 receptor expression has been found in abnormally proliferating Jurkat cells, prostate cancer lines (LnCAP), and lung cancer stem cells [273-275].

Our data specifically indicates that TFP treatment of HT1080 cells leads to a decrease in phosphorylated β-catenin. Not only does inhibition of DRD2 results in this decrease, but knockdown of DRD2 in DRD2 expressing HT1080 cells recapitulates the molecular phenotype of TFP treatment. Further, we have demonstrated that β-catenin inhibition by TFP, potentially via inhibition of Akt, results in a decrease in β-catenin transcriptional activity and therefore a downregulation of downstream targets, specifically VEGF. The antibody array indicated that proteins such as cyclin D1, c-met, c-MYC, and connexin were downregulated, which is relevant, considering these molecules have been tied to β-catenin activity [276-279]. β-catenin is the central effector of Wnt signaling and has been associated with neoplastic progression and the genesis of cancer stem-like cells, which are notoriously resistant to treatment and contribute to disease progression [280]. While β-catenin is a crucial molecule to cancer, this protein has traditionally been considered difficult to specifically target because of the nature of its interacting site participating in several different interactions [281]. A number of recent reports have focused on identifying specific β-catenin inhibitors, with various strategies being taken to effectively and specifically disrupt β-catenin signaling.

Interfering with β-catenin activity can reduce products such as IL-10 that influence the ability of cancer cells to act in an immunosuppressive fashion [282]. Additionally, it has been reported that cancer stem-like cells (CSCs) rely on the β-catenin pathway for self-renewal [283]; since this particular cell type found in the heterogeneous milieu of tumors are thought to be responsible for cancer metastasis and relapse it would be beneficial to target the pathways on which they are reliant. A recent publication that focused on lung CSCs found that TFP treatment results in a decrease in the β-catenin pathway and loss of some stem-like phenotypes [275]. In additional support of our findings here, a screening of compounds by Sachlos *et al*. to identify anti-CSC therapies revealed that dopamine receptors are found on CSC surfaces as well as patient breast cancer cells and antipsychotic drugs may be promising avenues of treatment [284]. Therefore, there exists potential for agents such as TFP that reduce β-catenin target gene products to influence multiple aspects of cancer cell biology that contribute to disease progression, such as migration and invasion, angiogenesis, local immunosuppression, and reduction in the clonogenic CSCs that have been widely reported amongst various cancer types that perpetuate the disease. Since the Wnt/β-catenin pathway is frequently dysregulated in cancer and mediates some of the cancer stem-like properties of a subpopulation of involved cancer cells, it is desirable to inhibit this pathway [285, 286]. TFP's ability to inhibit β-catenin signaling is valuable for a broad spectrum of cancers. We have shown that cancer cell lines of various lineages have functional responses to TFP, specifically those of fibrosarcoma and prostate origin.

Our observation of this old drug as an anti-invasive agent opens up the possibility of using an FDA-approved, clinically-used drug "off-label" for patients with cancer. Since TFP is an approved drug, its pharmacological properties are well known. The FDA approval associated with TFP implies that it is a safe drug to use in large populations and has tolerable or manageable side-effects. It has been reported that only 5% of oncology drugs that reach clinical trials will succeed to approval, but there exists hope in improving these statistics by re-examining known drugs that might have secondary applications [for review, see [249]]. Repurposing known small molecules is a strategy to combat the decline in introduction of new molecular entities to the market [287]. Our work clearly identifies a relatively safe, known drug (TFP) as a potential anti-invasion cancer drug in addition to its role as an anti-psychotic. The pharmaceutical industry has been facing a decline in research and development productivity for some time and repurposing known small molecules is a strategy to combat the decline in introduction of new molecular entities to the market [287]. As mentioned, this approach has already been embraced by the National Institutes of Health (NIH), demonstrated by the launch of the program 'Discovering New Therapeutic Uses for Existing Molecules' (New Therapeutic Uses) by NCATS in 2012. The benefit to this lies in the ability to hasten development of new treatments for difficult diseases, as these molecular entities have already gone through extensive testing, up to and including human safety trials in some cases. Toxicities associated with drug treatments are the most common reason for discontinuation of drug development [288]. Using known molecules decreases the likelihood of identifying toxic agents and/or being able to circumvent toxicities by having knowledge on how to employ countermeasures against them [288]. In line with the goals of the NCATS program, our work clearly identifies a relatively safe, known drug (TFP) as a potential anti-invasion cancer drug in addition to its traditional role as an anti-psychotic.

In conclusion, we have identified TFP as a potential novel therapeutic agent for invasion and metastasis via a reduction in phosphorylation of AKT and β-catenin, reducing target gene expression and invasive behavior. This drug has potential immediate translational value, as this compound has a relatively low cost and has been used extensively in other clinical situations. We have identified the potential molecular basis for the anti-invasive activity of TFP, but based on effects on other properties of cancer cells (*e.g.* CSC, calcium channels), the clinical effectiveness of this type of drug use in cancer, remains to be determined. Future studies are needed to determine whether the cellular and molecular changes that we demonstrated in prostate cancer and fibrosarcoma cells are recapitulated in a variety of cancer cell types.

2.4 MATERIALS AND METHODS

Materials

Collagen Type I (acetic acid-extracted native type I collagen from rat tail tendon) and propidium iodide (PI) were obtained from BD Bioscience Discovery Labware. Diversity Set II compound library was obtained from the Developmental Therapeutics Program in the NCI/NIH. Hoechst nuclear stain was purchased from Invitrogen. Trifluoperazine hydrochloride and haloperidol were acquired from Sigma-Aldrich. Rabbit anti-p-PTEN, anti-PTEN (total), anti-p-Erk1/2, anti-Erk1/2 (total), anti-p-GSK3B, anti-GSK3B (total), anti-p-β-catenin^{Ser552}, anti-β-catenin (total), anti-p-AKT^{Ser473}, anti-p-AKT^{Thr308}, and anti-AKT (total) were all purchased from Cell Signaling Technology (Davers, MA). Anti-DRD2 antibody was purchased from EMD Biosciences (Billerica, MA). Mouse anti-actin and anti-α/β-tubulin antibodies were purchased from Cell Signaling Technology (Davers MA). Horseradish peroxidase [HRP] conjugated anti-rabbit and anti-mouse antibodies were obtained from Rockland Immunochemicals (Gilbertsville, PA). Alexa Fluor 568 anti-rabbit antibodies were purchased from Molecular Probes, Life Technologies (Grand Island, NY).

Cell Lines and Treatment of Cells

Cell lines were obtained from the ATCC (Manassas, VA). Cell lines utilized include human prostate cancer PC3 and human metastatic prostate cancer C4-2b, both of which were maintained in RPMI 1640 medium (Corning, Mediatech). Human fibrosarcoma HT1080 and murine fibroblasts NIH/3T3 were maintained in DMEM-high glucose medium (Corning, Mediatech); all media were supplemented with 10% FBS and 1% penicillin/streptomycin. Cells were maintained in a humidified environment at 37^{o}C and 5% CO_2 for all experiments.

3-D High-Throughput Invasion Assay

The 3-D high-throughput invasion assay was performed as previously described [8] . Briefly, cells were mixed with 3mg/mL neutralized type I collagen. The mixture was dotted into each well of a 96-well plate and allowed to solidify at 37^{o}C. The cell-matrix dot was then covered with a layer of 1.5 mg/mL neutralized type I collagen. After solidification of cover collagen at 37^{o}C, compounds from the NCI library were added at 10 μM and DMSO was used as a control in complete medium. Incubation was carried out overnight at 37^{o}C and cells were stained with PI and Hoechst.

Cell Viability Assay

HT1080 and NIH/3T3 cells were cultured in complete media with or without TFP. Media and drugs were changed daily and cell viability was monitored by MTT assay [3-(4,5-dimethylthiazol-2-yl)-2,5-diphenyltetrazolium bromide] (Promega). Each day, cells were exposed to MTT and incubated at 37^{o}C for four hours. The reaction was stopped and formazan crystals were solubilized; the resultant solution was subject to colorimetric spectrophotometry and read at a wavelength of 570 nm.

Protease Assay

Total proteolytic activity was detected by employing the Fluorescent Detection Kit (Sigma). Cell lysates were incubated overnight at 37^{o}C with a fluorescein isothiocyanate (FITC)-labeled casein substrate and subsequently precipitated with trichloroacetic acid (TCA). The supernatant was assessed for fluorescence intensity after dilution in assay buffer.

Fluorescence was measured using excitation and emission wavelengths of 485 nm and 535 nm, respectively, on a SpectraMax Gemini EM (Molecular Devices) fluorescent plate reader.

Chorioallantoic Membrane (CAM) Angiogenesis and Invasion Assay

The CAM assay was performed as previously described [289]. Fertilized white chicken eggs (SPF Premium, Charles River Laboratory) were incubated at 37°C in 70% humidity for three days. The embryos were then incubated *ex ovo* in a sterile Petri dish for seven days. Gelatin sponges adsorbed with HT1080 cells treated with or without TFP were implanted on the CAM surface [290] and neovasculature was counted on day four post-implantation. For histochemical analysis of the chorioallantoic membrane, embryos were treated as for the angiogenesis assay, except at day 10 the embryos were inoculated with pretreated HT1080 cells in a sterile 2mm ring. After a four day incubation, CAM segments containing the ring were formalin fixed and sectioned by microtome into 5 μm sections after paraffin embedding. Sections were then stained with hematoxylin and counterstained with eosin.

Enzyme-linked immunosorbent assay (ELISA) for vascular endothelial growth factor (VEGF)

Secreted VEGF was assayed using the R&D Systems Human VEGF DuoSet ELISA kit (R&D Systems,). Briefly, HT1080 cells were incubated overnight in the presence or absence of TFP in complete media and the media was then incubated in a 96-well plate that had previously been coated in the VEGF capture antibody and blocked with filtered 1% BSA and washed in phosphate buffered saline-Tween (PBS-T [0.05% Tween]). Subsequently, the samples were removed and the plate incubated with the VEGF detection antibody and streptavidin-HRP at the concentrations suggested by the manufacturer, with PBS-T washes between each buffer change. 3, 3',5,5'-tetramethylbenzidine (TMB) was utilized to develop the ELISA and the optical density was read at 450 nm with a correction wavelength of 540 nm. Concentrations were calculated based on a standard VEGF curve.

Kinex Antibody Array

Cell lysates from HT1080 cells treated with TFP or with a DMSO control were obtained according to the protocol suggested by the Kinexus Bioinformatics Corporation (KBC), which manufactures the Kinex antibody microarray. This assay contains over 700 antibodies against both phospho- and pan-specific antibodies. The detailed protocols can be found at the KBC website (www.kinexus.ca). The short list of proteins generated by Kinexus as having the most fold change (positively or negatively) under trifluoperazine treatment (Table 2) were analyzed using the DAVID bioinformatics program [262, 263].

Dual Luciferase Assay

To study β-catenin promoter activity, HT1080 cells were transiently transfected with either TOPflash or FOPflash promoter constructs (Upstate Biotechnology) along with the Renilla luciferase reporter gene using polyethylenimine (PEI, MW: 250kD, Polysciences) after a 30 minute incubation of DNA and PEI at room temperature. Media was changed 18 hours after transfection. Forty-eight hours after transfection and following drug treatment, luciferase activity of both firefly and Renilla luciferase were measured using the Promega Dual-Glo Lucifease System with the SpectraMaxL (Molecular Devices).

Transwell Migration

Transwell migration assays were performed as described previously [123], except nuclei were stained in Hoechst/PBS (1:2000) for 20 minutes and imaged using a Nikon Eclipse TE2000-S equipped with a Sutter Instruments SmartShutter System and a QiClick QImaging camera. Migrated cells were counted with the assistance of the Nikon Elements Basic Research Software analysis tools.

Scratch Wound Migration Assay

Cells were grown to confluence in a 12-well dish and serum starved with or without TFP overnight under standard tissue culture conditions. A scratch wound was made in each well the following morning and cells were washed twice with 1X PBS and supplemented with complete media containing drugs or vehicle. Cells were allowed to migrate over eight hours, with bright field images being taken at time 0 and time 8 hours. Area for time 0 and time 8 hour were calculated using the Nikon Elements Basic Research Software analysis tools and percent change was calculated.

2-D dot migration assay

A collagen-cell mixture was dotted in a 96-well dish in a similar fashion to the 3-D invasion assay. Following collagen solidification, cell-matrix dots were overlaid with complete media. Cells were allowed to migrate up to 8 hours. Cells were then stained in Hoechst/PBS (1:2000) and images were captured using the previously described microscope and camera system. Migration was then quantified by counting nuclei using the Nikon Elements Basic Research Software analysis tools.

Gelatin zymography

Gelatin zymography was performed as described [239]. After electrophoresis, the gels were incubated in Triton X-100 to replace SDS followed by incubation in a Tris-based buffer overnight at 37^{o}C. Staining was accomplished using Coomassie Brilliant Blue and cleared areas were indicative of gelatinolytic activity.

Immunoblotting and Immunofluorescent staining

Immunoblotting was done according to previously published methods and developed on a BioRad ChemiDoc [72]. Immunofluorescent staining began by fixing treated cells in 4% paraformaldehyde in PBS at 4^{o}C, followed by permeabilization in 0.2% Triton X-100 at room temperature for 10 minutes. Blocking solution was composed of 3% bovine serum albumin/5% normal goat serum in PBS. After one hour blocking at room temperature, cells were exposed to anti-p-β-catenin^{Ser552} antibody (Cell Signaling Technology), visualized using the complimentary secondary fluorescent antibody (anti-rabbit Alexa Fluor 568), counterstained with Hoechst, and imaged on the Nikon microscope previously described.

Knockdown of DRD2

HT1080 cells were transiently transfected with aiRNA directed against DRD2 (Boston Biomedical, Inc.). Briefly, aiRNA and RNAiMax (Life Technologies) were incubated together at room temperature in serum free DMEM. Transfection mixture was added to HT1080 cells and incubated overnight under standard tissue culture conditions. Four separate aiRNA were tested

and the most efficient aiRNAs were identified by real-time PCR and chosen to complete downstream experiments.

Real-Time PCR

Cellular RNA was isolated from the target cells with the Qiagen RNeasy kit. cDNA was generated using random hexamers and the iScript reverse transcriptase (BioRad). The resultant cDNA was used for real-time PCR to detect DRD2 transcript levels. cDNA was subject to real-time PCR using primers generated specifically identifying DRD2 (F: 5'-CGGACAGACCCCACTACAA -3', R: 5'- CCTGCTGAATTTCCACTCACC -3') using the BioRad MyiQ single-color real-time PCR thermocycler. Hypoxanthine-guanine phosphoribosyltransferase (HPRT) was used as a normalization control. Results were analyzed using the BioRad software, MyiQ 2.0.

Statistical Analysis

Data is expressed as the standard error of the mean, as each experiment was repeated three times. Student's T-test was used to determine significant differences; any $P<0.05$ was considered significant.

REFERENCES

1. Edwards, B.K., et al., *Annual Report to the Nation on the status of cancer, 1975-2010, featuring prevalence of comorbidity and impact on survival among persons with lung, colorectal, breast, or prostate cancer.* Cancer, 2014. 120(9): p. 1290-314.
2. Kraljevic Pavelic, S., et al., *Metastasis: new perspectives on an old problem.* Mol Cancer, 2011. 10: p. 22.
3. Talmadge, J.E. and I.J. Fidler, *AACR centennial series: the biology of cancer metastasis: historical perspective.* Cancer Res, 2010. 70(14): p. 5649-69.
4. Weber, G.F., *Why does cancer therapy lack effective anti-metastasis drugs?* Cancer Lett, 2013. 328(2): p. 207-11.
5. Hanahan, D. and R.A. Weinberg, *Hallmarks of cancer: the next generation.* Cell, 2011. 144(5): p. 646-74.
6. Wan, L., K. Pantel, and Y. Kang, *Tumor metastasis: moving new biological insights into the clinic.* Nat Med, 2013. 19(11): p. 1450-64.
7. Tarin, D., et al., *Mechanisms of human tumor metastasis studied in patients with peritoneovenous shunts.* Cancer Res, 1984. 44(8): p. 3584-92.
8. Evensen, N.A., et al., *Development of a high-throughput three-dimensional invasion assay for anti-cancer drug discovery.* PLoS One, 2013. 8(12): p. e82811.
9. Zarrabi, K., et al., *Inhibition of matrix metalloproteinase 14 (MMP-14)-mediated cancer cell migration.* J Biol Chem, 2011. 286(38): p. 33167-77.
10. Dufour, A., et al., *Small-molecule anticancer compounds selectively target the hemopexin domain of matrix metalloproteinase-9.* Cancer Res, 2011. 71(14): p. 4977-88.
11. Dufour, A., et al., *Role of matrix metalloproteinase-9 dimers in cell migration: design of inhibitory peptides.* J Biol Chem, 2010. 285(46): p. 35944-56.
12. Gersh, I. and H.R. Catchpole, *The organization of ground substance and basement membrane and its significance in tissue injury, disease and growth.* American Journal of Anatomy, 1949. 85(3): p. 457-521.
13. Gross, J. and C.M. Lapiere, *Collagenolytic activity in amphibian tissues: a tissue culture assay.* Proc Natl Acad Sci U S A, 1962. 48: p. 1014-22.
14. Woessner, J.F., Jr., *Catabolism of collagen and non-collagen protein in the rat uterus during post-partum involution.* Biochem J, 1962. 83: p. 304-14.
15. Birkedal-Hansen, H., *From tadpole collagenase to a family of matrix metalloproteinases.* J Oral Pathol, 1988. 17(9-10): p. 445-51.
16. Grillo, H.C. and J. Gross, *Collagenolytic activity during mammalian wound repair.* Developmental Biology, 1967. 15(4): p. 300-317.
17. Grillo, H.C., et al., *Collagenolytic activity in regenerating forelimbs of the adult newt (Triturus viridescens).* Developmental Biology, 1968. 17(5): p. 571-583.
18. Fullmer, H.M. and W. Gibson, *Collagenolytic activity in gingivae of man.* Nature, 1966. 209(5024): p. 728-9.
19. Fullmer, H.M. and G.S. Lazarus, *Collagenase in bone of man.* J Histochem Cytochem, 1969. 17(12): p. 793-8.
20. Jeffrey, J.J. and J. Gross, *Collagenase from rat uterus. Isolation and partial characterization.* Biochemistry, 1970. 9(2): p. 268-73.
21. Lazarus, G.S., et al., *Human granulocyte collagenase.* Science, 1968. 159(3822): p. 1483-5.
22. Abramson, M., *Collagenolytic activity in middle ear cholesteatoma.* Ann Otol Rhinol Laryngol, 1969. 78(1): p. 112-24.
23. Abramson, M. and C.-C. Huang, *Localization of collagenase in human middle ear cholesteatoma.* The Laryngoscope, 1977. 87(5): p. 771-791.
24. Liotta, L.A., et al., *Preferential digestion of basement membrane collagen by an enzyme derived from a metastatic murine tumor.* Proc Natl Acad Sci U S A, 1979. 76(5): p. 2268-72.

25. Salo, T., L.A. Liotta, and K. Tryggvason, *Purification and characterization of a murine basement membrane collagen-degrading enzyme secreted by metastatic tumor cells.* J Biol Chem, 1983. 258(5): p. 3058-63.
26. Rawlings, N.D., A.J. Barrett, and A. Bateman, *MEROPS: the database of proteolytic enzymes, their substrates and inhibitors.* Nucleic Acids Res, 2012. 40(Database issue): p. D343-50.
27. Rawlings, N.D., et al., *MEROPS: the database of proteolytic enzymes, their substrates and inhibitors.* Nucleic Acids Res, 2014. 42(Database issue): p. D503-9.
28. Bode, W., F.-X. Gomis-Rüth, and W. Stöckler, *Astacins, serralysins, snake venom and matrix metalloproteinases exhibit identical zinc-binding environments (HEXXHXXGXXH and Met-turn) and topologies and should be grouped into a common family, the 'metzincins'.* FEBS Letters, 1993. 331(1–2): p. 134-140.
29. Rawlings, N.D. and A.J. Barrett, *Evolutionary families of peptidases.* Biochem J, 1993. 290 (Pt 1): p. 205-18.
30. Cerdà-Costa, N. and F. Xavier Gomis-Rüth, *Architecture and function of metallopeptidase catalytic domains.* Protein Science, 2014. 23(2): p. 123-144.
31. Nagase, H., R. Visse, and G. Murphy, *Structure and function of matrix metalloproteinases and TIMPs.* Cardiovascular Research, 2006. 69(3): p. 562-573.
32. Hua, Y. and S. Nair, *Proteases in cardiometabolic diseases: Pathophysiology, molecular mechanisms and clinical applications.* Biochimica et Biophysica Acta (BBA) - Molecular Basis of Disease, 2014(0).
33. Tallant, C., A. Marrero, and F.X. Gomis-Rüth, *Matrix metalloproteinases: Fold and function of their catalytic domains.* Biochimica et Biophysica Acta (BBA) - Molecular Cell Research, 2010. 1803(1): p. 20-28.
34. Evans, B.R., et al., *Mutation of membrane type-1 metalloproteinase, MT1-MMP, causes the multicentric osteolysis and arthritis disease Winchester syndrome.* Am J Hum Genet, 2012. 91(3): p. 572-6.
35. Pei, D., T. Kang, and H. Qi, *Cysteine Array Matrix Metalloproteinase (CA-MMP)/MMP-23 Is a Type II Transmembrane Matrix Metalloproteinase Regulated by a Single Cleavage for Both Secretion and Activation.* Journal of Biological Chemistry, 2000. 275(43): p. 33988-33997.
36. Walter, P. and A.E. Johnson, *Signal Sequence Recognition and Protein Targeting to the Endoplasmic Reticulum Membrane.* Annual Review of Cell Biology, 1994. 10(1): p. 87-119.
37. Park, A.J., et al., *Mutational analysis of the transin (rat stromelysin) autoinhibitor region demonstrates a role for residues surrounding the "cysteine switch".* J Biol Chem, 1991. 266(3): p. 1584-90.
38. Vartak, D.G. and R.A. Gemeinhart, *Matrix metalloproteases: underutilized targets for drug delivery.* J Drug Target, 2007. 15(1): p. 1-20.
39. Sanchez-Lopez, R., et al., *Structure-function relationships in the collagenase family member transin.* J Biol Chem, 1988. 263(24): p. 11892-9.
40. Windsor, L.J., et al., *An internal cysteine plays a role in the maintenance of the latency of human fibroblast collagenase.* Biochemistry, 1991. 30(3): p. 641-7.
41. Chen, L.C., M.E. Noelken, and H. Nagase, *Disruption of the cysteine-75 and zinc ion coordination is not sufficient to activate the precursor of human matrix metalloproteinase 3 (stromelysin 1).* Biochemistry, 1993. 32(39): p. 10289-10295.
42. Van Wart, H.E. and H. Birkedal-Hansen, *The cysteine switch: a principle of regulation of metalloproteinase activity with potential applicability to the entire matrix metalloproteinase gene family.* Proc Natl Acad Sci U S A, 1990. 87(14): p. 5578-82.
43. Springman, E.B., et al., *Multiple modes of activation of latent human fibroblast collagenase: evidence for the role of a Cys73 active-site zinc complex in latency and a "cysteine switch" mechanism for activation.* Proc Natl Acad Sci U S A, 1990. 87(1): p. 364-8.
44. Blaser, J., et al., *Mercurial activation of human polymorphonuclear leucocyte procollagenase.* Eur J Biochem, 1991. 202(3): p. 1223-30.

45. Verma, R.P. and C. Hansch, *Matrix metalloproteinases (MMPs): chemical-biological functions and (Q)SARs.* Bioorg Med Chem, 2007. 15(6): p. 2223-68.
46. Maskos, K., *Crystal structures of MMPs in complex with physiological and pharmacological inhibitors.* Biochimie, 2005. 87(3–4): p. 249-263.
47. Iyer, S., et al., *Crystal Structure of an Active Form of Human MMP-1*. Journal of Molecular Biology, 2006. 362(1): p. 78-88.
48. Butler, G.S., E.M. Tam, and C.M. Overall, *The Canonical Methionine 392 of Matrix Metalloproteinase 2 (Gelatinase A) Is Not Required for Catalytic Efficiency or Structural Integrity: PROBING THE ROLE OF THE METHIONINE-TURN IN THE METZINCIN METALLOPROTEASE SUPERFAMILY*. Journal of Biological Chemistry, 2004. 279(15): p. 15615-15620.
49. Tsukada, H. and T. Pourmotabbed, *Unexpected crucial role of residue 272 in substrate specificity of fibroblast collagenase*. J Biol Chem, 2002. 277(30): p. 27378-84.
50. Fasciglione, G.F., et al., *The collagenolytic action of MMP-1 is regulated by the interaction between the catalytic domain and the hinge region.* J Biol Inorg Chem, 2012. 17(4): p. 663-72.
51. Knäuper, V., et al., *Analysis of the contribution of the hinge region of human neutrophil collagenase (HNC, MMP-8) to stability and collagenolytic activity by alanine scanning mutagenesis.* FEBS Letters, 1997. 405(1): p. 60-64.
52. Overall, C.M., *Molecular determinants of metalloproteinase substrate specificity: matrix metalloproteinase substrate binding domains, modules, and exosites.* Mol Biotechnol, 2002. 22(1): p. 51-86.
53. Li, J., et al., *Structure of full-length porcine synovial collagenase reveals a C-terminal domain containing a calcium-linked, four-bladed β-propeller*. Structure, 1995. 3(6): p. 541-549.
54. Libson, A.M., et al., *Crystal structure of the haemopexin-like C-terminal domain of gelatinase A.* Nat Struct Mol Biol, 1995. 2(11): p. 938-942.
55. Wallon, U.M. and C.M. Overall, *The Hemopexin-like Domain (C Domain) of Human Gelatinase A (Matrix Metalloproteinase-2) Requires Ca2+ for Fibronectin and Heparin Binding: BINDING PROPERTIES OF RECOMBINANT GELATINASE A C DOMAIN TO EXTRACELLULAR MATRIX AND BASEMENT MEMBRANE COMPONENTS.* Journal of Biological Chemistry, 1997. 272(11): p. 7473-7481.
56. Murphy, G., et al., *The role of the C-terminal domain in collagenase and stromelysin specificity.* J Biol Chem, 1992. 267(14): p. 9612-8.
57. Arnold, L.H., et al., *The Interface between Catalytic and Hemopexin Domains in Matrix Metalloproteinase-1 Conceals a Collagen Binding Exosite.* Journal of Biological Chemistry, 2011. 286(52): p. 45073-45082.
58. Dufour, A., et al., *Role of Matrix Metalloproteinase-9 Dimers in Cell Migration: DESIGN OF INHIBITORY PEPTIDES.* Journal of Biological Chemistry, 2010. 285(46): p. 35944-35956.
59. Dufour, A., et al., *Small-Molecule Anticancer Compounds Selectively Target the Hemopexin Domain of Matrix Metalloproteinase-9.* Cancer Research, 2011. 71(14): p. 4977-4988.
60. Zarrabi, K., et al., *Inhibition of Matrix Metalloproteinase 14 (MMP-14)-mediated Cancer Cell Migration.* Journal of Biological Chemistry, 2011. 286(38): p. 33167-33177.
61. Remacle, A.G., et al., *Novel MT1-MMP small-molecule inhibitors based on insights into hemopexin domain function in tumor growth.* Cancer Res, 2012. 72(9): p. 2339-49.
62. Sato, H., et al., *A matrix metalloproteinase expressed on the surface of invasive tumour cells.* Nature, 1994. 370(6484): p. 61-5.
63. Takino, T., et al., *Identification of the Second Membrane-type Matrix Metalloproteinase (MT-MMP-2) Gene from a Human Placenta cDNA Library: MT-MMPs FORM A UNIQUE MEMBRANE-TYPE SUBCLASS IN THE MMP FAMILY*. Journal of Biological Chemistry, 1995. 270(39): p. 23013-23020.

64. Will, H. and B. Hinzmann, *cDNA sequence and mRNA tissue distribution of a novel human matrix metalloproteinase with a potential transmembrane segment.* Eur J Biochem, 1995. 231(3): p. 602-8.
65. Puente, X.S., et al., *Molecular Cloning of a Novel Membrane-type Matrix Metalloproteinase from a Human Breast Carcinoma.* Cancer Research, 1996. 56(5): p. 944-949.
66. Llano, E., et al., *Identification and Characterization of Human MT5-MMP, a New Membrane-bound Activator of Progelatinase A Overexpressed in Brain Tumors.* Cancer Research, 1999. 59(11): p. 2570-2576.
67. Sohail, A., et al., *MT4-(MMP17) and MT6-MMP (MMP25), A unique set of membrane-anchored matrix metalloproteinases: properties and expression in cancer.* Cancer Metastasis Rev, 2008. 27(2): p. 289-302.
68. Itoh, Y., et al., *Membrane Type 4 Matrix Metalloproteinase (MT4-MMP, MMP-17) Is a Glycosylphosphatidylinositol-anchored Proteinase.* Journal of Biological Chemistry, 1999. 274(48): p. 34260-34266.
69. Velasco, G., et al., *Human MT6-Matrix Metalloproteinase: Identification, Progelatinase A Activation, and Expression in Brain Tumors.* Cancer Research, 2000. 60(4): p. 877-882.
70. Radichev, I.A., et al., *Biochemical Characterization of the Cellular Glycosylphosphatidylinositol-linked Membrane Type-6 Matrix Metalloproteinase.* Journal of Biological Chemistry, 2010. 285(21): p. 16076-16086.
71. Pei, D. and S.J. Weiss, *Furin-dependent intracellular activation of the human stromelysin-3 zymogen.* Nature, 1995. 375(6528): p. 244-7.
72. Cao, J., et al., *Membrane Type Matrix Metalloproteinase 1 Activates Pro-gelatinase A without Furin Cleavage of the N-terminal Domain.* Journal of Biological Chemistry, 1996. 271(47): p. 30174-30180.
73. Kang, T., H. Nagase, and D. Pei, *Activation of Membrane-type Matrix Metalloproteinase 3 Zymogen by the Proprotein Convertase Furin in the trans-Golgi Network.* Cancer Research, 2002. 62(3): p. 675-681.
74. Wang, X. and D. Pei, *Shedding of Membrane Type Matrix Metalloproteinase 5 by a Furin-type Convertase: A POTENTIAL MECHANISM FOR DOWN-REGULATION.* Journal of Biological Chemistry, 2001. 276(38): p. 35953-35960.
75. Shiryaev, S.A., et al., *Matrix metalloproteinase proteolysis of the myelin basic protein isoforms is a source of immunogenic peptides in autoimmune multiple sclerosis.* PLoS One, 2009. 4(3): p. e4952.
76. Illman, S.A., et al., *The mouse matrix metalloproteinase, epilysin (MMP-28), is alternatively spliced and processed by a furin-like proprotein convertase.* Biochem J, 2003. 375(Pt 1): p. 191-7.
77. Cao, J., et al., *Furin directly cleaves proMMP-2 in the trans-Golgi network resulting in a nonfunctioning proteinase.* J Biol Chem, 2005. 280(12): p. 10974-80.
78. Matthews, B.W., *Structural basis of the action of thermolysin and related zinc peptidases.* Accounts of Chemical Research, 1988. 21(9): p. 333-340.
79. Mohan, R., et al., *Gelatinase B/lacZ Transgenic Mice, a Model for Mapping Gelatinase B Expression during Developmental and Injury-related Tissue Remodeling.* Journal of Biological Chemistry, 1998. 273(40): p. 25903-25914.
80. Sternlicht, M.D. and Z. Werb, *How matrix metalloproteinases regulate cell behavior.* Annu Rev Cell Dev Biol, 2001. 17: p. 463-516.
81. Yan, C. and D.D. Boyd, *Regulation of matrix metalloproteinase gene expression.* Journal of Cellular Physiology, 2007. 211(1): p. 19-26.
82. Fanjul-Fernández, M., et al., *Matrix metalloproteinases: Evolution, gene regulation and functional analysis in mouse models.* Biochimica et Biophysica Acta (BBA) - Molecular Cell Research, 2010. 1803(1): p. 3-19.

83. Zucker, S., et al., *Tissue Inhibitor of Metalloproteinase-2 (TIMP-2) Binds to the Catalytic Domain of the Cell Surface Receptor, Membrane Type 1-Matrix Metalloproteinase 1 (MT1-MMP).* Journal of Biological Chemistry, 1998. 273(2): p. 1216-1222.
84. Cao, J., et al., *The Propeptide Domain of Membrane Type 1-Matrix Metalloproteinase Acts as an Intramolecular Chaperone when Expressed in transwith the Mature Sequence in COS-1 Cells.* Journal of Biological Chemistry, 2000. 275(38): p. 29648-29653.
85. Welgus, H.G., et al., *A specific inhibitor of vertebrate collagenase produced by human skin fibroblasts.* J Biol Chem, 1979. 254(6): p. 1938-43.
86. Brew, K., D. Dinakarpandian, and H. Nagase, *Tissue inhibitors of metalloproteinases: evolution, structure and function.* Biochimica et Biophysica Acta (BBA) - Protein Structure and Molecular Enzymology, 2000. 1477(1–2): p. 267-283.
87. Piccard, H., P.E. Van den Steen, and G. Opdenakker, *Hemopexin domains as multifunctional liganding modules in matrix metalloproteinases and other proteins.* Journal of Leukocyte Biology, 2007. 81(4): p. 870-892.
88. Williamson, R.A., et al., *Disulphide bond assignment in human tissue inhibitor of metalloproteinases (TIMP).* Biochem J, 1990. 268(2): p. 267-74.
89. Sottrup-Jensen, L. and H. Birkedal-Hansen, *Human fibroblast collagenase-alpha-macroglobulin interactions. Localization of cleavage sites in the bait regions of five mammalian alpha-macroglobulins.* J Biol Chem, 1989. 264(1): p. 393-401.
90. Mott, J.D., et al., *Post-translational Proteolytic Processing of Procollagen C-terminal Proteinase Enhancer Releases a Metalloproteinase Inhibitor.* Journal of Biological Chemistry, 2000. 275(2): p. 1384-1390.
91. Takahara, K., et al., *Type I procollagen COOH-terminal proteinase enhancer protein: identification, primary structure, and chromosomal localization of the cognate human gene (PCOLCE).* Journal of Biological Chemistry, 1994. 269(42): p. 26280-26285.
92. Weeks, J.G., J. Halme, and J.F. Woessner, Jr., *Extraction of collagenase from the involuting rat uterus.* Biochim Biophys Acta, 1976. 445(1): p. 205-14.
93. Roswit, W.T., J. Halme, and J.J. Jeffrey, *Purification and properties of rat uterine procollagenase.* Archives of Biochemistry and Biophysics, 1983. 225(1): p. 285-295.
94. Shipley, J.M., et al., *Metalloelastase is required for macrophage-mediated proteolysis and matrix invasion in mice.* Proc Natl Acad Sci U S A, 1996. 93(9): p. 3942-6.
95. Itoh, T., et al., *Unaltered secretion of beta-amyloid precursor protein in gelatinase A (matrix metalloproteinase 2)-deficient mice.* J Biol Chem, 1997. 272(36): p. 22389-92.
96. Vu, T.H., et al., *MMP-9/gelatinase B is a key regulator of growth plate angiogenesis and apoptosis of hypertrophic chondrocytes.* Cell, 1998. 93(3): p. 411-22.
97. Holmbeck, K., et al., *MT1-MMP-deficient mice develop dwarfism, osteopenia, arthritis, and connective tissue disease due to inadequate collagen turnover.* Cell, 1999. 99(1): p. 81-92.
98. Urbanski, S.J., et al., *Expression of metalloproteinases and their inhibitors in primary pulmonary carcinomas.* Br J Cancer, 1992. 66(6): p. 1188-94.
99. Davies, B., et al., *Activity of type IV collagenases in benign and malignant breast disease.* Br J Cancer, 1993. 67(5): p. 1126-31.
100. Brown, P.D., et al., *Association between expression of activated 72-kilodalton gelatinase and tumor spread in non-small-cell lung carcinoma.* J Natl Cancer Inst, 1993. 85(7): p. 574-8.
101. Davies, B., et al., *Levels of matrix metalloproteases in bladder cancer correlate with tumor grade and invasion.* Cancer Res, 1993. 53(22): p. 5365-9.
102. Zeng, Z.S., et al., *Prediction of colorectal cancer relapse and survival via tissue RNA levels of matrix metalloproteinase-9.* J Clin Oncol, 1996. 14(12): p. 3133-40.
103. Wilson, C.L., et al., *Intestinal tumorigenesis is suppressed in mice lacking the metalloproteinase matrilysin.* Proc Natl Acad Sci U S A, 1997. 94(4): p. 1402-7.
104. Liotta, L.A., et al., *Metastatic potential correlates with enzymatic degradation of basement membrane collagen.* Nature, 1980. 284(5751): p. 67-8.

105. Basset, P., et al., *A novel metalloproteinase gene specifically expressed in stromal cells of breast carcinomas.* Nature, 1990. 348(6303): p. 699-704.
106. Masson, R., et al., *In vivo evidence that the stromelysin-3 metalloproteinase contributes in a paracrine manner to epithelial cell malignancy.* J Cell Biol, 1998. 140(6): p. 1535-41.
107. Stetler-Stevenson, W.G., *Matrix metalloproteinases in angiogenesis: a moving target for therapeutic intervention.* J Clin Invest, 1999. 103(9): p. 1237-41.
108. Itoh, T., et al., *Reduced angiogenesis and tumor progression in gelatinase A-deficient mice.* Cancer Res, 1998. 58(5): p. 1048-51.
109. Schultz, R.M., et al., *Inhibition by Human Recombinant Tissue Inhibitor of Metalloproteinases of Human Amnion Invasion and Lung Colonization by Murine B16-F10 Melanoma Cells.* Cancer Research, 1988. 48(19): p. 5539-5545.
110. Khokha, R., et al., *Up-regulation of TIMP-1 expression in B16-F10 melanoma cells suppresses their metastatic ability in chick embryo.* Clinical & Experimental Metastasis, 1992. 10(6): p. 365-370.
111. Chambers, A.F. and L.M. Matrisian, *Changing Views of the Role of Matrix Metalloproteinases in Metastasis.* Journal of the National Cancer Institute, 1997. 89(17): p. 1260-1270.
112. Ganea, E., et al., *Matrix metalloproteinases: useful and deleterious.* Biochem Soc Trans, 2007. 35(Pt 4): p. 689-91.
113. Whittaker, M., et al., *Design and therapeutic application of matrix metalloproteinase inhibitors.* Chem Rev, 1999. 99(9): p. 2735-76.
114. Davies, B., et al., *A synthetic matrix metalloproteinase inhibitor decreases tumor burden and prolongs survival of mice bearing human ovarian carcinoma xenografts.* Cancer Res, 1993. 53(9): p. 2087-91.
115. Chirivi, R.G., et al., *Inhibition of the metastatic spread and growth of B16-BL6 murine melanoma by a synthetic matrix metalloproteinase inhibitor.* Int J Cancer, 1994. 58(3): p. 460-4.
116. Wang, X., et al., *Matrix metalloproteinase inhibitor BB-94 (batimastat) inhibits human colon tumor growth and spread in a patient-like orthotopic model in nude mice.* Cancer Res, 1994. 54(17): p. 4726-8.
117. Taraboletti, G., et al., *Inhibition of angiogenesis and murine hemangioma growth by batimastat, a synthetic inhibitor of matrix metalloproteinases.* J Natl Cancer Inst, 1995. 87(4): p. 293-8.
118. Alcantara, M.B. and C.R. Dass, *Pigment epithelium-derived factor as a natural matrix metalloproteinase inhibitor: a comparison with classical matrix metalloproteinase inhibitors used for cancer treatment.* Journal of Pharmacy and Pharmacology, 2014. 66(7): p. 895-902.
119. Pavlaki, M. and S. Zucker, *Matrix metalloproteinase inhibitors (MMPIs): The beginning of phase I or the termination of phase III clinical trials.* Cancer and Metastasis Reviews, 2003. 22(2-3): p. 177-203.
120. Golub, L.M., et al., *Tetracyclines inhibit connective tissue breakdown by multiple non-antimicrobial mechanisms.* Adv Dent Res, 1998. 12(2): p. 12-26.
121. Pasternak, B. and P. Aspenberg, *Metalloproteinases and their inhibitors-diagnostic and therapeutic opportunities in orthopedics.* Acta Orthop, 2009. 80(6): p. 693-703.
122. Zucker, S. and J. Cao, *Selective matrix metalloproteinase (MMP) inhibitors in cancer therapy: ready for prime time?* Cancer Biol Ther, 2009. 8(24): p. 2371-3.
123. Dufour, A., et al., *Role of the hemopexin domain of matrix metalloproteinases in cell migration.* J Cell Physiol, 2008. 217(3): p. 643-51.
124. Edwards, B.K., et al., *Annual report to the nation on the status of cancer, 1975-2006, featuring colorectal cancer trends and impact of interventions (risk factors, screening, and treatment) to reduce future rates.* Cancer, 2010. 116(3): p. 544-573.
125. Sato, H., et al., *A matrix metalloproteinase expressed on the surface of invasive tumour cells.* Nature, 1994. 370(6484): p. 61-65.
126. Itoh, Y., *MT1-MMP: A key regulator of cell migration in tissue.* IUBMB Life, 2006. 58(10): p. 589-596.

127. Zöller, M., *CD44: can a cancer-initiating cell profit from an abundantly expressed molecule?* Nat Rev Cancer, 2011. 11(4): p. 254-267.
128. Günthert, U., et al., *A new variant of glycoprotein CD44 confers metastatic potential to rat carcinoma cells.* Cell, 1991. 65(1): p. 13-24.
129. Mori, H., et al., *CD44 directs membrane-type 1 matrix metalloproteinase to lamellipodia by associating with its hemopexin-like domain.* EMBO J, 2002. 21(15): p. 3949-3959.
130. Stamenkovic, I. and Q. Yu, *Shedding light on proteolytic cleavage of CD44: the responsible sheddase and functional significance of shedding*. J Invest Dermatol, 2009. 129(6): p. 1321-4.
131. Strongin, A.Y., *Proteolytic and non-proteolytic roles of membrane type-1 matrix metalloproteinase in malignancy.* Biochim Biophys Acta, 2010. 1803(1): p. 133-41.
132. Cao, J., et al., *The propeptide domain of membrane type 1 matrix metalloproteinase is required for binding of tissue inhibitor of metalloproteinases and for activation of pro-gelatinase A.* J Biol Chem, 1998. 273(52): p. 34745-52.
133. Pavlaki, M., et al., *A Conserved Sequence within the Propeptide Domain of Membrane Type 1 Matrix Metalloproteinase Is Critical for Function as an Intramolecular Chaperone.* Journal of Biological Chemistry, 2002. 277(4): p. 2740-2749.
134. English, W.R., et al., *Characterization of the Role of the "MT-loop": AN EIGHT-AMINO ACID INSERTION SPECIFIC TO PROGELATINASE A (MMP2) ACTIVATING MEMBRANE-TYPE MATRIX METALLOPROTEINASES.* Journal of Biological Chemistry, 2001. 276(45): p. 42018-42026.
135. Lang, R., et al., *Crystal Structure of the Catalytic Domain of MMP-16/MT3-MMP: Characterization of MT-MMP Specific Features.* Journal of Molecular Biology, 2004. 336(1): p. 213-225.
136. Woskowicz, A.M., et al., *MT-LOOP-dependent Localization of Membrane Type I Matrix Metalloproteinase (MT1-MMP) to the Cell Adhesion Complexes Promotes Cancer Cell Invasion.* Journal of Biological Chemistry, 2013. 288(49): p. 35126-35137.
137. Lehti, K., et al., *Regulation of membrane-type-1 matrix metalloproteinase activity by its cytoplasmic domain.* J Biol Chem, 2000. 275(20): p. 15006-13.
138. Gingras, D., et al., *Activation of the extracellular signal-regulated protein kinase (ERK) cascade by membrane-type-1 matrix metalloproteinase (MT1-MMP).* FEBS Lett, 2001. 507(2): p. 231-6.
139. Jiang, A., et al., *Regulation of membrane-type matrix metalloproteinase 1 activity by dynamin-mediated endocytosis.* Proc Natl Acad Sci U S A, 2001. 98(24): p. 13693-8.
140. Anilkumar, N., et al., *Palmitoylation at Cys574 is essential for MT1-MMP to promote cell migration.* The FASEB Journal, 2005.
141. Kim, S., et al., *Posttranslational regulation of membrane type 1-matrix metalloproteinase (MT1-MMP) in mouse PTEN null prostate cancer cells: Enhanced surface expression and differential O-glycosylation of MT1-MMP.* Biochim Biophys Acta, 2010. 1803(11): p. 1287-97.
142. Wu, Y.I., et al., *Glycosylation broadens the substrate profile of membrane type 1 matrix metalloproteinase.* J Biol Chem, 2004. 279(9): p. 8278-89.
143. Remacle, A.G., et al., *O-glycosylation regulates autolysis of cellular membrane type-1 matrix metalloproteinase (MT1-MMP).* J Biol Chem, 2006. 281(25): p. 16897-905.
144. Ludwig, T., et al., *The cytoplasmic tail dileucine motif LL572 determines the glycosylation pattern of membrane-type 1 matrix metalloproteinase.* J Biol Chem, 2008. 283(51): p. 35410-8.
145. Seiki, M., *Membrane-type 1 matrix metalloproteinase: a key enzyme for tumor invasion.* Cancer Letters, 2003. 194(1): p. 1-11.
146. Ohuchi, E., et al., *Membrane Type 1 Matrix Metalloproteinase Digests Interstitial Collagens and Other Extracellular Matrix Macromolecules.* Journal of Biological Chemistry, 1997. 272(4): p. 2446-2451.
147. Barbolina, M.V. and M.S. Stack, *Membrane type 1-matrix metalloproteinase: substrate diversity in pericellular proteolysis.* Semin Cell Dev Biol, 2008. 19(1): p. 24-33.

148. Koshikawa, N., et al., *Role of Cell Surface Metalloprotease Mt1-Mmp in Epithelial Cell Migration over Laminin-5.* The Journal of Cell Biology, 2000. 148(3): p. 615-624.
149. Endo, K., et al., *Cleavage of syndecan-1 by membrane type matrix metalloproteinase-1 stimulates cell migration.* J Biol Chem, 2003. 278(42): p. 40764-70.
150. Kajita, M., et al., *Membrane-type 1 matrix metalloproteinase cleaves CD44 and promotes cell migration.* J Cell Biol, 2001. 153(5): p. 893-904.
151. Covington, M.D., R.C. Burghardt, and A.R. Parrish, *Ischemia-induced cleavage of cadherins in NRK cells requires MT1-MMP (MMP-14).* Am J Physiol Renal Physiol, 2006. 290(1): p. F43-51.
152. Mu, D., et al., *The integrin alpha(v)beta8 mediates epithelial homeostasis through MT1-MMP-dependent activation of TGF-beta1.* J Cell Biol, 2002. 157(3): p. 493-507.
153. Karsdal, M.A., et al., *Matrix metalloproteinase-dependent activation of latent transforming growth factor-beta controls the conversion of osteoblasts into osteocytes by blocking osteoblast apoptosis.* J Biol Chem, 2002. 277(46): p. 44061-7.
154. McQuibban, G.A., et al., *Matrix metalloproteinase processing of monocyte chemoattractant proteins generates CC chemokine receptor antagonists with anti-inflammatory properties in vivo.* Blood, 2002. 100(4): p. 1160-7.
155. Csoka, A.B. and R. Stern, *Hypotheses on the evolution of hyaluronan: a highly ironic acid.* Glycobiology, 2013. 23(4): p. 398-411.
156. Reitinger, S. and G. Lepperdinger, *Hyaluronan, a ready choice to fuel regeneration: a mini-review.* Gerontology, 2013. 59(1): p. 71-6.
157. Sneath, R.J. and D.C. Mangham, *The normal structure and function of CD44 and its role in neoplasia.* Molecular Pathology, 1998. 51(4): p. 191-200.
158. Thomas, L., et al., *CD44H regulates tumor cell migration on hyaluronate-coated substrate.* J Cell Biol, 1992. 118(4): p. 971-7.
159. Goldstein, L.A., et al., *A human lymphocyte homing receptor, the Hermes antigen, is related to cartilage proteoglycan core and link proteins.* Cell, 1989. 56(6): p. 1063-1072.
160. Lesley, J. and R. Hyman, *CD44 structure and function.* Front Biosci, 1998. 3: p. d616-30.
161. He, Q., et al., *Molecular isoforms of murine CD44 and evidence that the membrane proximal domain is not critical for hyaluronate recognition.* J Cell Biol, 1992. 119(6): p. 1711-9.
162. Misra, S., et al., *Hyaluronan-CD44 interactions as potential targets for cancer therapy.* FEBS J, 2011. 278(9): p. 1429-43.
163. Yu, Q. and B.P. Toole, *A New Alternatively Spliced Exon between v9 and v10 Provides a Molecular Basis for Synthesis of Soluble CD44.* Journal of Biological Chemistry, 1996. 271(34): p. 20603-20607.
164. Williams, K., et al., *CD44 integrates signaling in normal stem cell, cancer stem cell and (pre)metastatic niches.* Experimental Biology and Medicine, 2013. 238(3): p. 324-338.
165. Perschl, A., et al., *Transmembrane domain of CD44 is required for its detergent insolubility in fibroblasts.* J Cell Sci, 1995. 108 (Pt 3): p. 1033-41.
166. Lesley, J., et al., *Requirements for hyaluronic acid binding by CD44: a role for the cytoplasmic domain and activation by antibody.* J Exp Med, 1992. 175(1): p. 257-66.
167. Perschl, A., et al., *Role of CD44 cytoplasmic domain in hyaluronan binding.* Eur J Immunol, 1995. 25(2): p. 495-501.
168. von Andrian, U.H., et al., *A central role for microvillous receptor presentation in leukocyte adhesion under flow.* Cell, 1995. 82(6): p. 989-99.
169. Lewis, C.A., P.A. Townsend, and C.M. Isacke, *Ca(2+)/calmodulin-dependent protein kinase mediates the phosphorylation of CD44 required for cell migration on hyaluronan.* Biochem J, 2001. 357(Pt 3): p. 843-50.
170. Thorne, R.F., J.W. Legg, and C.M. Isacke, *The role of the CD44 transmembrane and cytoplasmic domains in co-ordinating adhesive and signalling events.* Journal of Cell Science, 2004. 117(3): p. 373-380.

171. Lesley, J., et al., *Variant cell lines selected for alterations in the function of the hyaluronan receptor CD44 show differences in glycosylation.* J Exp Med, 1995. 182(2): p. 431-7.
172. English, N.M., J.F. Lesley, and R. Hyman, *Site-specific de-N-glycosylation of CD44 can activate hyaluronan binding, and CD44 activation states show distinct threshold densities for hyaluronan binding.* Cancer Res, 1998. 58(16): p. 3736-42.
173. Takahashi, K., et al., *Keratan sulfate modification of CD44 modulates adhesion to hyaluronate.* J Biol Chem, 1996. 271(16): p. 9490-6.
174. Esford, L.E., et al., *Analysis of CD44 interactions with hyaluronan in murine L cell fibroblasts deficient in glycosaminoglycan synthesis: a role for chondroitin sulfate.* J Cell Sci, 1998. 111 (Pt 7): p. 1021-9.
175. Greenfield, B., et al., *Characterization of the heparan sulfate and chondroitin sulfate assembly sites in CD44.* J Biol Chem, 1999. 274(4): p. 2511-7.
176. Bijlmakers, M.J. and M. Marsh, *The on-off story of protein palmitoylation.* Trends Cell Biol, 2003. 13(1): p. 32-42.
177. Thankamony, S.P. and W. Knudson, *Acylation of CD44 and its association with lipid rafts are required for receptor and hyaluronan endocytosis.* J Biol Chem, 2006. 281(45): p. 34601-9.
178. Bourguignon, L.Y., E.L. Kalomiris, and V.B. Lokeshwar, *Acylation of the lymphoma transmembrane glycoprotein, GP85, may be required for GP85-ankyrin interaction.* J Biol Chem, 1991. 266(18): p. 11761-5.
179. Lee, J.L., et al., *CD44 engagement promotes matrix-derived survival through the CD44-SRC-integrin axis in lipid rafts.* Mol Cell Biol, 2008. 28(18): p. 5710-23.
180. Babina, I.S., et al., *A novel mechanism of regulating breast cancer cell migration via palmitoylation-dependent alterations in the lipid raft affiliation of CD44.* Breast Cancer Res, 2014. 16(1): p. R19.
181. Tarone, G., et al., *A cell surface integral membrane glycoprotein of 85,000 mol wt (gp85) associated with triton X-100-insoluble cell skeleton.* J Cell Biol, 1984. 99(2): p. 512-9.
182. Jacobson, K., et al., *Redistribution of a major cell surface glycoprotein during cell movement.* J Cell Biol, 1984. 99(5): p. 1613-23.
183. Lacy, B.E. and C.B. Underhill, *The hyaluronate receptor is associated with actin filaments.* J Cell Biol, 1987. 105(3): p. 1395-404.
184. Sainio, M., et al., *Neurofibromatosis 2 tumor suppressor protein colocalizes with ezrin and CD44 and associates with actin-containing cytoskeleton.* J Cell Sci, 1997. 110 (Pt 18): p. 2249-60.
185. Günthert, U., et al., *A new variant of glycoprotein CD44 confers metastatic potential to rat carcinoma cells.* Cell, 1991. 65(1): p. 13-24.
186. Katoh, S., J.B. McCarthy, and P.W. Kincade, *Characterization of soluble CD44 in the circulation of mice. Levels are affected by immune activity and tumor growth.* The Journal of Immunology, 1994. 153(8): p. 3440-9.
187. Sy, M.S., Y.J. Guo, and I. Stamenkovic, *Inhibition of tumor growth in vivo with a soluble CD44-immunoglobulin fusion protein.* J Exp Med, 1992. 176(2): p. 623-7.
188. Guo, Y., et al., *Inhibition of human melanoma growth and metastasis in vivo by anti-CD44 monoclonal antibody.* Cancer Res, 1994. 54(6): p. 1561-5.
189. Bartolazzi, A., et al., *Interaction between CD44 and hyaluronate is directly implicated in the regulation of tumor development.* J Exp Med, 1994. 180(1): p. 53-66.
190. Iida, N. and L.Y. Bourguignon, *New CD44 splice variants associated with human breast cancers.* J Cell Physiol, 1995. 162(1): p. 127-33.
191. Gross, N., K. Balmas, and C. Beretta Brognara, *Role of CD44H carbohydrate structure in neuroblastoma adhesive properties.* Med Pediatr Oncol, 2001. 36(1): p. 139-41.
192. Heider, K.H., et al., *A human homologue of the rat metastasis-associated variant of CD44 is expressed in colorectal carcinomas and adenomatous polyps.* J Cell Biol, 1993. 120(1): p. 227-33.

193. Guo, Y.J., et al., *Potential use of soluble CD44 in serum as indicator of tumor burden and metastasis in patients with gastric or colon cancer*. Cancer Res, 1994. 54(2): p. 422-6.
194. Bazil, V. and J.L. Strominger, *Metalloprotease and serine protease are involved in cleavage of CD43, CD44, and CD16 from stimulated human granulocytes. Induction of cleavage of L-selectin via CD16.* J Immunol, 1994. 152(3): p. 1314-22.
195. Cichy, J. and E. Pure, *The liberation of CD44*. J Cell Biol, 2003. 161(5): p. 839-43.
196. Okamoto, I., et al., *CD44 cleavage induced by a membrane-associated metalloprotease plays a critical role in tumor cell migration.* Oncogene, 1999. 18(7): p. 1435-46.
197. Banerji, S., et al., *Characterization of a Functional Hyaluronan-Binding Domain from the Human CD44 Molecule Expressed inEscherichia coli.* Protein Expression and Purification, 1998. 14(3): p. 371-381.
198. Ponta, H., L. Sherman, and P.A. Herrlich, *CD44: from adhesion molecules to signalling regulators.* Nat Rev Mol Cell Biol, 2003. 4(1): p. 33-45.
199. Blakeley, B.D., A.M. Chapman, and B.R. McNaughton, *Split-superpositive GFP reassembly is a fast, efficient, and robust method for detecting protein-protein interactions in vivo.* Molecular BioSystems, 2012. 8(8): p. 2036-2040.
200. Uekita, T., et al., *Cytoplasmic tail-dependent internalization of membrane-type 1 matrix metalloproteinase is important for its invasion-promoting activity*. J Cell Biol, 2001. 155(7): p. 1345-56.
201. Klemke, R.L., et al., *Regulation of cell motility by mitogen-activated protein kinase*. J Cell Biol, 1997. 137(2): p. 481-92.
202. Huang, C., K. Jacobson, and M.D. Schaller, *MAP kinases and cell migration.* Journal of Cell Science, 2004. 117(20): p. 4619-4628.
203. Schlegel, J., et al., *Amplification and differential expression of members of the erbB-gene family in human glioblastoma.* J Neurooncol, 1994. 22(3): p. 201-7.
204. Morishige, M., et al., *GEP100 links epidermal growth factor receptor signalling to Arf6 activation to induce breast cancer invasion.* Nat Cell Biol, 2008. 10(1): p. 85-92.
205. Fruehauf, J., *EGFR function and detection in cancer therapy.* J Exp Ther Oncol, 2006. 5(3): p. 231-46.
206. Tarcic, G., et al., *EGR1 and the ERK-ERF axis drive mammary cell migration in response to EGF*. The FASEB Journal, 2012. 26(4): p. 1582-1592.
207. Liu, Z.-X., et al., *Hepatocyte Growth Factor Induces ERK-dependent Paxillin Phosphorylation and Regulates Paxillin-Focal Adhesion Kinase Association.* Journal of Biological Chemistry, 2002. 277(12): p. 10452-10458.
208. Hunger-Glaser, I., et al., *Bombesin, Lysophosphatidic Acid, and Epidermal Growth Factor Rapidly Stimulate Focal Adhesion Kinase Phosphorylation at Ser-910: REQUIREMENT FOR ERK ACTIVATION*. Journal of Biological Chemistry, 2003. 278(25): p. 22631-22643.
209. Han, M.Y., et al., *Extracellular signal-regulated kinase/mitogen-activated protein kinase regulates actin organization and cell motility by phosphorylating the actin cross-linking protein EPLIN*. Mol Cell Biol, 2007. 27(23): p. 8190-204.
210. Steffensen, B., U.M. Wallon, and C.M. Overall, *Extracellular matrix binding properties of recombinant fibronectin type II-like modules of human 72-kDa gelatinase/type IV collagenase. High affinity binding to native type I collagen but not native type IV collagen.* J Biol Chem, 1995. 270(19): p. 11555-66.
211. Collier, I.E., et al., *Alanine scanning mutagenesis and functional analysis of the fibronectin-like collagen-binding domain from human 92-kDa type IV collagenase.* J Biol Chem, 1992. 267(10): p. 6776-81.
212. Mattu, T.S., et al., *O-Glycan Analysis of Natural Human Neutrophil Gelatinase B Using a Combination of Normal Phase- HPLC and Online Tandem Mass Spectrometry: Implications for the Domain Organization of the Enzyme†.* Biochemistry, 2000. 39(51): p. 15695-15704.

213. Van den Steen, P.E., et al., *The Hemopexin and O-Glycosylated Domains Tune Gelatinase B/MMP-9 Bioavailability via Inhibition and Binding to Cargo Receptors.* Journal of Biological Chemistry, 2006. 281(27): p. 18626-18637.
214. Vandooren, J., et al., *Gelatin degradation assay reveals MMP-9 inhibitors and function of O-glycosylated domain.* World J Biol Chem, 2011. 2(1): p. 14-24.
215. Rosenblum, G., et al., *Insights into the Structure and Domain Flexibility of Full-Length Pro-Matrix Metalloproteinase-9/Gelatinase B.* Structure, 2007. 15(10): p. 1227-1236.
216. Rosenblum, G., et al., *Direct visualization of protease action on collagen triple helical structure.* PLoS One, 2010. 5(6): p. e11043.
217. Kotra, L.P., et al., *N-Glycosylation pattern of the zymogenic form of human matrix metalloproteinase-9.* Bioorg Chem, 2002. 30(5): p. 356-70.
218. Vandooren, J., P.E. Van den Steen, and G. Opdenakker, *Biochemistry and molecular biology of gelatinase B or matrix metalloproteinase-9 (MMP-9): the next decade.* Crit Rev Biochem Mol Biol, 2013. 48(3): p. 222-72.
219. Yu, Q. and I. Stamenkovic, *Cell surface-localized matrix metalloproteinase-9 proteolytically activates TGF-beta and promotes tumor invasion and angiogenesis.* Genes Dev, 2000. 14(2): p. 163-76.
220. Van den Steen, P.E., et al., *Neutrophil gelatinase B potentiates interleukin-8 tenfold by aminoterminal processing, whereas it degrades CTAP-III, PF-4, and GRO-alpha and leaves RANTES and MCP-2 intact.* Blood, 2000. 96(8): p. 2673-81.
221. Brown, J.M., *Tumor Hypoxia in Cancer Therapy*, in *Methods in Enzymology*, S. Helmut and B. Bernhard, Editors. 2007, Academic Press. p. 295-321.
222. Yan, L., et al., *The High Molecular Weight Urinary Matrix Metalloproteinase (MMP) Activity Is a Complex of Gelatinase B/MMP-9 and Neutrophil Gelatinase-associated Lipocalin (NGAL): MODULATION OF MMP-9 ACTIVITY BY NGAL.* Journal of Biological Chemistry, 2001. 276(40): p. 37258-37265.
223. Bodden, M.K., et al., *Human TIMP-1 binds to pro-M(r) 92K GL (gelatinase B, MMP-9) through the "second disulfide knot".* Ann N Y Acad Sci, 1994. 732: p. 403-7.
224. Roderfeld, M., et al., *Latent MMP-9 is bound to TIMP-1 before secretion.* Biol Chem, 2007. 388(11): p. 1227-34.
225. Sciaky, N., et al., *Golgi Tubule Traffic and the Effects of Brefeldin A Visualized in Living Cells.* The Journal of Cell Biology, 1997. 139(5): p. 1137-1155.
226. Cha, H., et al., *Structural basis of the adaptive molecular recognition by MMP9.* J Mol Biol, 2002. 320(5): p. 1065-79.
227. Olson, M.W., et al., *Characterization of the monomeric and dimeric forms of latent and active matrix metalloproteinase-9. Differential rates for activation by stromelysin 1.* J Biol Chem, 2000. 275(4): p. 2661-8.
228. Goldberg, G.I., et al., *Interaction of 92-kDa type IV collagenase with the tissue inhibitor of metalloproteinases prevents dimerization, complex formation with interstitial collagenase, and activation of the proenzyme with stromelysin.* J Biol Chem, 1992. 267(7): p. 4583-91.
229. Takatsuki, A., K. Arima, and G. Tamura, *Tunicamycin, a new antibiotic. I. Isolation and characterization of tunicamycin.* J Antibiot (Tokyo), 1971. 24(4): p. 215-23.
230. Takatsuki, A. and G. Tamura, *Tunicamycin, a new antibiotic. II. Some biological properties of the antiviral activity of tunicamycin.* J Antibiot (Tokyo), 1971. 24(4): p. 224-31.
231. Takatsuki, A. and G. Tamura, *Tunicamycin, a new antibiotic. 3. Reversal of the antiviral activity of tunicamycin by aminosugars and their derivatives.* J Antibiot (Tokyo), 1971. 24(4): p. 232-8.
232. Tanaka, S., T. Uehara, and Y. Nomura, *Up-regulation of Protein-disulfide Isomerase in Response to Hypoxia/Brain Ischemia and Its Protective Effect against Apoptotic Cell Death.* Journal of Biological Chemistry, 2000. 275(14): p. 10388-10393.

233. Tian, F., et al., *Protein disulfide isomerase increases in myocardial endothelial cells in mice exposed to chronic hypoxia: a stimulatory role in angiogenesis.* American Journal of Physiology - Heart and Circulatory Physiology, 2009. 297(3): p. H1078-H1086.
234. Hanania, R., et al., *Classically Activated Macrophages Use Stable Microtubules for Matrix Metalloproteinase-9 (MMP-9) Secretion.* Journal of Biological Chemistry, 2012. 287(11): p. 8468-8483.
235. Khan, M.M., et al., *Protein disulfide isomerase-mediated disulfide bonds regulate the gelatinolytic activity and secretion of matrix metalloproteinase-9.* Exp Cell Res, 2012. 318(8): p. 904-14.
236. Deryugina, E.I. and J.P. Quigley, *Matrix metalloproteinases and tumor metastasis.* Cancer Metastasis Rev, 2006. 25(1): p. 9-34.
237. Collier, I.E., et al., *Diffusion of MMPs on the surface of collagen fibrils: the mobile cell surface-collagen substratum interface.* PLoS One, 2011. 6(9): p. e24029.
238. Lu, X. and Y. Kang, *Hypoxia and hypoxia-inducible factors: master regulators of metastasis.* Clin Cancer Res, 2010. 16(24): p. 5928-35.
239. Zucker, S., et al., *Thrombin Induces the Activation of Progelatinase A in Vascular Endothelial Cells: PHYSIOLOGIC REGULATION OF ANGIOGENESIS.* Journal of Biological Chemistry, 1995. 270(40): p. 23730-23738.
240. Sams-Dodd, F., *Is poor research the cause of the declining productivity of the pharmaceutical industry? An industry in need of a paradigm shift.* Drug Discov Today, 2013. 18(5-6): p. 211-7.
241. Swinney, D.C. and J. Anthony, *How were new medicines discovered?* Nat Rev Drug Discov, 2011. 10(7): p. 507-19.
242. Pammolli, F., L. Magazzini, and M. Riccaboni, *The productivity crisis in pharmaceutical R&D.* Nat Rev Drug Discov, 2011. 10(6): p. 428-38.
243. Redig, A.J. and S.S. McAllister, *Breast cancer as a systemic disease: a view of metastasis.* Journal of Internal Medicine, 2013. 274(2): p. 113-126.
244. Norton, L. and J. Massague, *Is cancer a disease of self-seeding?* Nat Med, 2006. 12(8): p. 875-878.
245. Hanahan, D. and Robert A. Weinberg, *Hallmarks of Cancer: The Next Generation.* Cell, 2011. 144(5): p. 646-674.
246. Comen, E. and L. Norton, *Self-seeding in cancer.* Recent Results Cancer Res, 2012. 195: p. 13-23.
247. Moffat, J.G., J. Rudolph, and D. Bailey, *Phenotypic screening in cancer drug discovery - past, present and future.* Nat Rev Drug Discov, 2014. 13(8): p. 588-602.
248. Horning, J.L., et al., *3-D Tumor Model for In Vitro Evaluation of Anticancer Drugs.* Molecular Pharmaceutics, 2008. 5(5): p. 849-862.
249. Gupta, S.C., et al., *Cancer drug discovery by repurposing: teaching new tricks to old dogs.* Trends Pharmacol Sci, 2013. 34(9): p. 508-17.
250. Li, Y.Y. and S.J. Jones, *Drug repositioning for personalized medicine.* Genome Med, 2012. 4(3): p. 27.
251. Gelijns, A.C., N. Rosenberg, and A.J. Moskowitz, *Capturing the unexpected benefits of medical research.* N Engl J Med, 1998. 339(10): p. 693-8.
252. Thayer, A.M., *Drug Repurposing*, in *Chemical & Engineering News*. 2012. p. 15-25.
253. Aubé, J., *Drug Repurposing and the Medicinal Chemist.* ACS Medicinal Chemistry Letters, 2012. 3(6): p. 442-444.
254. Collins, F.S., *Mining for therapeutic gold.* Nat Rev Drug Discov, 2011. 10(6): p. 397-397.
255. Marques, L.O., M.S. Lima, and B.G. Soares, *Trifluoperazine for schizophrenia.* Cochrane Database Syst Rev, 2004(1): p. CD003545.
256. Peng, C.C., et al., *Cytotoxicity of ferulic Acid on T24 cell line differentiated by different microenvironments.* Biomed Res Int, 2013. 2013: p. 579859.

257. Friedl, P. and S. Alexander, *Cancer invasion and the microenvironment: plasticity and reciprocity.* Cell, 2011. 147(5): p. 992-1009.
258. Tonini, T., F. Rossi, and P.P. Claudio, *Molecular basis of angiogenesis and cancer.* Oncogene, 2003. 22(42): p. 6549-6556.
259. Ferrara, N., *Vascular Endothelial Growth Factor: Basic Science and Clinical Progress.* Endocrine Reviews, 2004. 25(4): p. 581-611.
260. Ribatti, D., et al., *Chorioallantoic membrane capillary bed: A useful target for studying angiogenesis and anti-angiogenesis in vivo.* The Anatomical Record, 2001. 264(4): p. 317-324.
261. LeBleu, V.S., B. MacDonald, and R. Kalluri, *Structure and Function of Basement Membranes.* Experimental Biology and Medicine, 2007. 232(9): p. 1121-1129.
262. Huang, D.W., B.T. Sherman, and R.A. Lempicki, *Systematic and integrative analysis of large gene lists using DAVID bioinformatics resources.* Nat. Protocols, 2008. 4(1): p. 44-57.
263. Huang da, W., B.T. Sherman, and R.A. Lempicki, *Bioinformatics enrichment tools: paths toward the comprehensive functional analysis of large gene lists.* Nucleic Acids Res, 2009. 37(1): p. 1-13.
264. McCubrey, J.A., et al., *Multifaceted roles of GSK-3 and Wnt/beta-catenin in hematopoiesis and leukemogenesis: opportunities for therapeutic intervention.* Leukemia, 2014. 28(1): p. 15-33.
265. Fang, D., et al., *Phosphorylation of β-Catenin by AKT Promotes β-Catenin Transcriptional Activity.* Journal of Biological Chemistry, 2007. 282(15): p. 11221-11229.
266. Zhang, X., J.P. Gaspard, and D.C. Chung, *Regulation of vascular endothelial growth factor by the Wnt and K-ras pathways in colonic neoplasia.* Cancer Res, 2001. 61(16): p. 6050-4.
267. Sullivan, G.F., et al., *Augmentation of apoptosis by the combination of bleomycin with trifluoperazine in the presence of mutant p53.* Journal of Experimental Therapeutics and Oncology, 2002. 2(1): p. 19-26.
268. Zhelev, Z., et al., *Phenothiazines suppress proliferation and induce apoptosis in cultured leukemic cells without any influence on the viability of normal lymphocytes.* Cancer Chemotherapy and Pharmacology, 2004. 53(3): p. 267-275.
269. Polischouk, A.G., et al., *The antipsychotic drug trifluoperazine inhibits DNA repair and sensitizes non–small cell lung carcinoma cells to DNA double-strand break–induced cell death.* Molecular Cancer Therapeutics, 2007. 6(8): p. 2303-2309.
270. Sangodkar, J., et al., *Targeting the FOXO1/KLF6 axis regulates EGFR signaling and treatment response.* The Journal of Clinical Investigation, 2012. 122(7): p. 2637-2651.
271. Zacharski, L.R., et al., *Chronic calcium antagonist use in carcinoma of the lung and colon: a retrospective cohort observational study.* Cancer Invest, 1990. 8(5): p. 451-8.
272. Beaulieu, J.-M. and R.R. Gainetdinov, *The Physiology, Signaling, and Pharmacology of Dopamine Receptors.* Pharmacological Reviews, 2011. 63(1): p. 182-217.
273. Basu, B., et al., *D1 and D2 dopamine receptor-mediated inhibition of activated normal T cell proliferation is lost in jurkat T leukemic cells.* J Biol Chem, 2010. 285(35): p. 27026-32.
274. Arvigo, M., et al., *Somatostatin and dopamine receptor interaction in prostate and lung cancer cell lines.* Journal of Endocrinology, 2010. 207(3): p. 309-317.
275. Yeh, C.-T., et al., *Trifluoperazine, an Antipsychotic Agent, Inhibits Cancer Stem Cell Growth and Overcomes Drug Resistance of Lung Cancer.* American Journal of Respiratory and Critical Care Medicine, 2012. 186(11): p. 1180-1188.
276. Tetsu, O. and F. McCormick, *[beta]-Catenin regulates expression of cyclin D1 in colon carcinoma cells.* Nature, 1999. 398(6726): p. 422-426.
277. Boon, E.M., et al., *Wnt signaling regulates expression of the receptor tyrosine kinase met in colorectal cancer.* Cancer Res, 2002. 62(18): p. 5126-8.
278. He, T.-C., et al., *Identification of c-MYC as a Target of the APC Pathway.* Science, 1998. 281(5382): p. 1509-1512.
279. Ai, Z., et al., *Wnt-1 regulation of connexin43 in cardiac myocytes.* J Clin Invest, 2000. 105(2): p. 161-71.

280. Clevers, H. and R. Nusse, *Wnt/β-Catenin Signaling and Disease*. Cell, 2012. 149(6): p. 1192-1205.
281. Takada, K., et al., *Targeted disruption of the BCL9/beta-catenin complex inhibits oncogenic Wnt signaling.* Sci Transl Med, 2012. 4(148): p. 148ra117.
282. Yaguchi, T., et al., *Immune Suppression and Resistance Mediated by Constitutive Activation of Wnt/β-Catenin Signaling in Human Melanoma Cells.* The Journal of Immunology, 2012. 189(5): p. 2110-2117.
283. Hsieh, C.H., et al., *Norcantharidin, Derivative of Cantharidin, for Cancer Stem Cells.* Evid Based Complement Alternat Med, 2013. 2013: p. 838651.
284. Sachlos, E., et al., *Identification of drugs including a dopamine receptor antagonist that selectively target cancer stem cells.* Cell, 2012. 149(6): p. 1284-97.
285. Barker, N. and H. Clevers, *Mining the Wnt pathway for cancer therapeutics.* Nat Rev Drug Discov, 2006. 5(12): p. 997-1014.
286. Takahashi-Yanaga, F. and M. Kahn, *Targeting Wnt Signaling: Can We Safely Eradicate Cancer Stem Cells?* Clinical Cancer Research, 2010. 16(12): p. 3153-3162.
287. Paul, S.M., et al., *How to improve R&D productivity: the pharmaceutical industry's grand challenge.* Nat Rev Drug Discov, 2010. 9(3): p. 203-214.
288. Nilubol, N., et al., *Four clinically utilized drugs were identified and validated for treatment of adrenocortical cancer using quantitative high-throughput screening.* J Transl Med, 2012. 10: p. 198.
289. Deryugina, E.I. and J.P. Quigley, *Chick embryo chorioallantoic membrane model systems to study and visualize human tumor cell metastasis.* Histochem Cell Biol, 2008. 130(6): p. 1119-30.
290. Ribatti, D., et al., *The gelatin sponge-chorioallantoic membrane assay.* Nat. Protocols, 2006. 1(1): p. 85-91.